公益財団法人　老年病研究所

業　績　集

第16集

2016

平成28年7月

ま え が き

公益財団法人老年病研究所業績集第16集2016年版をまとめることができました。ご覧いただけると幸いです。20論文中英語論文は６編ありました。

最近、某大学の教授が「10年間で共著も含めて20編の論文がなかった」という理由で任期が更新されず解雇になったというニュースがありました。多くの大学で、教員の任期制が採用されるようになっており、その評価には英語の論文が重視されているようです。

「The アジア大学ランキング2016」が最近発表されましたが、東京大学は2013年の調査開始以来３年連続１位でしたが、2016年の順位は７位に下がっていたということで話題になりました。そのランキングの評価基準は、「教育の質・学習環境」、「学生と教員の国際性」、「産学連携による収入」、「研究の質」、「論文被引用数」の５分野であり、更に分野ごとに詳細な審査項目があるとのことです。

公益財団法人継続のための評価基準がありますが、「業績」も重要な分野となっています。当研究所は人員や施設からみて小規模であり、研究のみに専念できる研究者はおりません。しかしながら、当研究所附属病院には、内科、神経内科、循環器内科、脳神経外科、整形外科、眼科、歯科、病理診断科などがあり、各々の角度から臨床的研究を推進しております。研究成果の発表（学会発表等）の項目を見ていただきますと、医師、薬剤師、看護師、リハビリスタッフなど多くの職員が学会などで発表しているのが分かります。日常の多忙な中で、問題意識を持って業務にあたり、その成果を発表する姿勢は「大学の附属病院」にも劣らないように思います。

今後も臨床的、基礎的研究をさらに遂行し、より多くの高齢者が健やかに暮らせるように、高齢者医療の発展、福祉の向上に貢献して行く所存です。ご支援、ご協力をよろしくお願いします。

平成28年７月

公益財団法人　老年病研究所

所長　岡本　幸市

目　　次

NEUROPATHOLOGY

Neuropathology 2015; 35, 462–468 doi:10.1111/neup.12209

Case Report

An autopsy case of familial amyotrophic lateral sclerosis with a *TARDBP* Q343R mutation

Koichi Okamoto,[1] Yukio Fujita,[2] Eri Hoshino,[2] Yuhji Tamura,[5] Toshio Fukuda,[3] Masato Hasegawa[6] and Masamitsu Takatama[4]

[1]Department of Neurology, Geriatrics Research Institute and Hospital, [2]Department of Neurology, Gunma University Graduate School of Medicine, [3]Department of Histopathology and Cytopathology, Gunma University Graduate School of Health Sciences, [4]Department of Internal Medicine, Geriatrics Research Institute and Hospital, Maebashi, [5]Department of Internal Medicine, Kiboukan Hospital, Takasaki and [6]Department of Neuropathology and Cell Biology, Tokyo Metropolitan Institute of Medical Science, Tokyo, Japan

We describe a Japanese autopsy case of familial amyotrophic lateral sclerosis (FALS) with a *TARDBP* Q343R mutation. This male patient developed dysarthria at the age of 52 years, and bulbar symptoms progressed, with weakness and atrophy in the extremities. His mental status was normal, but he became bedridden, received artificial respiratory support at 54 years of age, and gradually acquired a locked-in state and died at 58 years of age. Microscopically, marked diffuse myelin pallor was observed in the anterolateral columns of the spinal cord. The remaining anterior horn cells contained Bunina bodies and phosphorylation-dependent transactivation response DNA-binding protein of 43 kDa (pTDP-43)-positive neuronal cytoplasmic inclusions (NCIs). Glial cytoplasmic inclusions (GCIs) were also observed. The number of ubiquitin- and p62-positive inclusions was markedly lower than that of pTDP-43-positive inclusions. NCIs and many fine dot-like pTDP-43-positive granules in the neuropil were mainly seen in the temporal and motor cortices, and striatum. NCIs were rare in hippocampal granular cells. Immunoblotting of samples from the cerebral cortex using an anti-pTDP-43 antibody was slightly different from previous TDP-43 pathological subtypes.

Key words: amyotrophic lateral sclerosis, p62, pathology, *TARDBP* Q343R mutation, TDP-43.

INTRODUCTION

Amyotrophic lateral sclerosis (ALS) is a fatal and incurable adult-onset neurodegenerative disease.[1] Transactivation response DNA-binding protein of 43 kDa (TDP-43) has been identified as a major component of the pathological inclusions in most forms of frontotemporal lobar degeneration with ubiquitin-positive and tau-negative inclusions, as well as in ALS.[2–5] TDP-43 is an RNA-binding and DNA-binding multifunctional protein that is encoded by the TAR DNA-binding protein gene (*TARDBP*) located on chromosome 1. TDP-43 aggregates have been detected in neuronal and glial cells in ALS, in frontotemporal lobar degeneration (FTLD-TDP), and in several other diseases. FTLD-TDP and ALS are considered to form a spectrum of disorders that are linked by a common molecular pathology called TDP-43 proteinopathy.[6,7] Even though most *TARDBP* mutations have been reported in autosomal dominant ALS, reports of the FTLD-TDP type are very rare.[8,9] Moreover, autopsied cases with pathogenic *TARDBP* mutations are few,[10–18] and the contribution of any one mutation to a particular phenotype remains uncertain.

Tagawa *et al.*[10] reported an autopsy case of familial ALS (FALS); the clinical and pathological findings of that woman were indistinguishable from those of sporadic ALS (SALS). Moreover, Yokoseki *et al.*[11] described a missense *TARDBP* Q343R mutation in that family, including in our patient. We observed a patient from this family throughout the course of the illness, and autopsied him. Induced pluripotent stem (iPS) cells were also produced from patients with *TARDBP* mutations, including our patient.[19] Here, we report the neuropathological findings of this case and review the previous autopsy-confirmed FALS cases with several *TARDBP* mutations.

Correspondence: Koichi Okamoto, MD, PhD, Department of Neurology, Geriatrics Research Institute and Hospital, 3-26-8, Otomo-machi, Maebashi, Gunma 371-0847, Japan. Email: okumotok@roneanbyo.or.jp

Received 9 February 2015; revised and accepted 2 March 2015; published online 12 June 2015.

CLINICAL SUMMARY

A Japanese man developed dysarthria at the age of 52 years and noticed dysphagia within a few months. These symptoms progressed, and he visited our hospital 3 months after the onset of the condition. His past medical history was unremarkable. Several ALS cases were observed in his family; the clinical history and molecular genetics of this family were reported previously (Fig. 1).[10,11] The present patient also had a *TARDBP* Q343R mutation.[11]

On neurological examination, his tongue exhibited atrophy with fasciculation. Muscle weakness and atrophy were not observed in the neck and extremities. The jaw reflex and tendon reflexes on the extremities were hyperactive. Extrapyramidal signs, cognitive dysfunction, cerebellar ataxia and Babinski sign were absent. Ocular movements, sensation, and the autonomic nervous system were also normal. Motor and sensory nerve conduction studies were normal, but electromyography showed denervation in the upper and lower extremities. MRI of the brain and spinal cord was normal, and serum and CSF studies were unremarkable. Bulbar symptoms progressed, with weakness and atrophy in the extremities. The patient received a gastrostomy at 52 and laryngeal diversion at 53 years of age. His mental status was normal, but he became bedridden, received artificial respiratory support at age 54, and gradually became locked-in and died of bronchopneumonia at 58 years of age, 6 years and 5 months after the onset of the symptoms.

PATHOLOGICAL FINDINGS

Autopsy was performed in accordance with established procedures, and the samples were used in this study after obtaining informed consent from the patient's family. Autopsy was performed 2 h after death. The general autopsy findings showed bronchopneumonia and urinary calculi. Tissues were fixed with 4% paraformaldehyde in PBS (pH 7.4) and embedded in paraffin. Brain and spinal cord sections (5 μm in thickness) were stained with HE and KB stains.

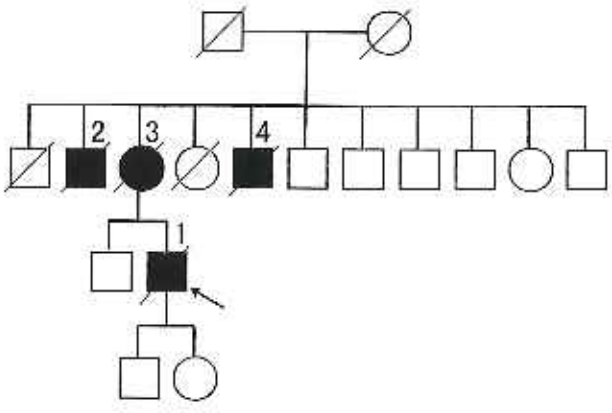

Fig. 1 Family pedigree. The closed symbols indicate patients with ALS, and the arrow indicates the present patient. This family was reported elsewhere.[10,11] Squares, males; circles, females.

The brain weighed 1100 g before fixation and showed no external abnormalities. Microscopically, diffuse myelin pallor was obvious in the anterolateral columns of the spinal cord (Fig. 2a). Neuronal loss and gliosis were marked in the anterior horns, and a few remaining anterior horn cells contained Bunina bodies (Fig. 2b). In the brain, spongy states were mainly observed in the second and third layers of the motor and temporal cortices, and gliosis was detected in those cortices. Focal degeneration was not observed in the CA1-subiculum transitional area.[20]

Immunohistochemical analysis

Deparaffinized sections of the brain, brain stem and spinal cord were incubated with 1% H_2O_2 in methanol for 30 min, to eliminate endogenous peroxidase activity in the tissue. The sections were blocked with normal serum and incubated overnight at 4°C with the following antibodies: polyclonal anti-phosphorylation-dependent TDP-43 (pTDP-43) antibody (generated in our laboratory[21]), polyclonal anti-pTDP-43 antibody (pS409/410) (Cosmo Bio, Tokyo, Japan), anti-phosphorylation-independent TDP-43 (TDP-43) antibody (Proteintech, Chicago, USA), polyclonal anti-ubiquitin antibody (Dako, Glostrup, Denmark), polyclonal anti-trans Golgi network (TGN-46) antibody (generated in our laboratory[22]), monoclonal GFAP antibody (Dako), guinea pig polyclonal anti-N-terminal of p62 (Progen Biotechnik, Heidelberg, Germany), monoclonal anti-phosphorylated tau antibody (AT8) (Innogenetics, Ghent, Belgium), monoclonal anti-beta-amyloid 17–24 (4G8) antibody (Covance, New Jersey, USA), and polyclonal anti-alpha-synuclein (phospho S129) antibody (Abcam, Cambridge, UK). For enhancement, samples were autoclaved for 5 min before reaction with the antibodies, with the exception of the anti-ubiquitin antibody. Sections were blocked using an endogenous avidin–biotin blocking kit (Nichirei, Tokyo, Japan) at room temperature, labeled with the primary antibodies at 4°C overnight, washed in PBS for 30 min, and incubated with Histofine simple stain MAX-PO® (Nichirei) or Vector® VIP (Vector, Burlingame, CA, USA) for p62 and TGN-46. Double immunostaining was performed; according to the above-mentioned methods, deparaffinized sections of the spinal cord were labeled with anti-pTDP-43 antibody at 4°C overnight, washed in PBS for 30 min, and incubated with Histofine simple stain MAX-PO®, washed in glycine-HCl buffer for 2 h, then anti-TGN-46 antibody at 4°C overnight, washed in PBS for 30 min, and incubated with VIP.

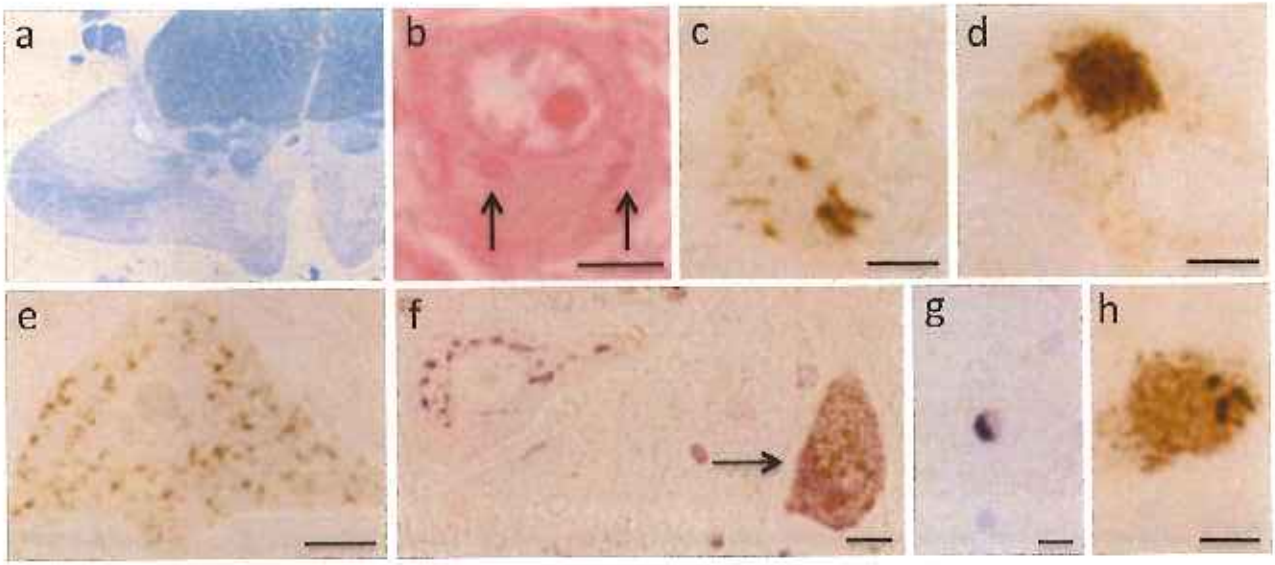

Fig. 2 (a) Thoracic spinal cord segment showing marked myelin pallor in the anterolateral columns. (b–c) Spinal cord anterior horn cells showing Bunina bodies (arrows) (b); skein-like inclusions (c); round inclusion (d); and fine granular neuronal cytoplasmic inclusions (NCIs) (e). (f) A left upper neuron showing a normal-looking Golgi apparatus, with the arrow indicating a neuron with Golgi fragmentation and fine granular NCIs. (g) Glial cytoplasmic inclusion in the white matter of the spinal cord. (h) NCI observed in the dorsal root ganglion. (a) Klüver–Barrera; (b) hematoxylin–eosin, and (c–e, h) pTDP-43 immunostaining; (f) pTDP-43 and TGN-46 double immunostaining; and (g) p62 immunostaining. Scale bars: 20 μm.

The two antibodies against pTDP-43 showed almost similar immunoreactivity. In the spinal cord, pTDP-43-positive neuronal inclusions (NCIs) and glial cytoplasmic inclusions (GCIs) were found. Skein-like inclusions (Fig. 2c) and round inclusions (Fig. 2d) were observed. The majority of the remaining anterior horn cells contained many fine pTDP-43-positive granules (Fig. 2e), and these neurons with NCIs showed fragmentation of the Golgi apparatus (Fig. 2f). The number of ubiquitin-positive and p62-positive inclusions was markedly lower than that of pTDP-43-positive inclusions, and skein-like and round inclusions and some GCIs were positive for ubiquitin and p62 (Fig. 2g); however, neuronal fine pTDP-43-positive granules were negative for ubiquitin and p62. pTDP-43-positive NCIs were also found in the dorsal root ganglia (Fig. 2h), brain stem, cerebrum and basal ganglia. GCIs were also present, mainly in the white matter of the brain stem, cerebrum and basal ganglia.

Many NCIs and fine dot-like pTDP-43-positive granules in the neuropil were observed mainly in the temporal (Fig. 3a) and motor cortices, as well as in the striatum. Some fine dot-like pTDP-43-positive granules were arranged linearly. However, NCIs were rare in hippocampal granular cells. The number of ubiquitin-positive and p62-positive NCIs and GCIs was markedly lower than that of pTDP-43-positive structures, and fine dot-like pTDP-43 granules were negative for ubiquitin and p62 (Fig. 3b).

Lewy pathology was observed in the pons, medulla oblongata and olfactory bulb; however, it was not detected in the midbrain and cerebrum. Neurofibrillary tangles were only observed in the parahippocampal gyrus, but amyloid plaques were absent.

Immunoblot analysis of phosphorylated TDP-43 (pS409/410)

Sarkosyl-insoluble TDP-43 of this case (cerebellum, thoracic cord, frontal lobe and temporal lobe) were analyzed by immunoblotting and compared with other FTLD-TDP cases (types A, B and C) from Shizuoka Institute of Epilepsy and Neurological Disorders (Shizuoka, Japan), and Tokyo Metropolitan Institute of Gerontology (Tokyo, Japan). Brain tissues (0.5 g) were homogenized and incubated in 10 mL of buffer containing 10 mmol/L Tris-HCl (pH 7.5), 0.8 mol/L NaCl, 10% sucrose, 1 mmol/L EGTA, 2% Sarkosyl for 30 min at 37°C. After centrifugation at 20 000 × *g* for 10 min at 25°C, the supernatants were ultracentrifuged at 100 000 × *g* for 20 min at 25°C. The pellets were solubilized in SDS-sample buffer and subjected to 12% polyacrylamide gel SDS–PAGE, transferred to poly(vinylidene difluoride) membrane and incubated overnight with the anti-pTDP-43 (pS409/410) antibody.[5] The labeling was developed with diaminobenzidine and nickel chloride. In the temporal lobe, phosphorylated full-length TDP-43 at ~45 kDa and C-terminal fragments (CTFs) with some major and minor bands at 19–27 kDa were detected (Fig. 4, lane 4). The banding pattern of CTFs (major doublet bands at 26 kDa and a single band at 24 kDa) is similar to that of ALS (type B), but different from those of types A–C

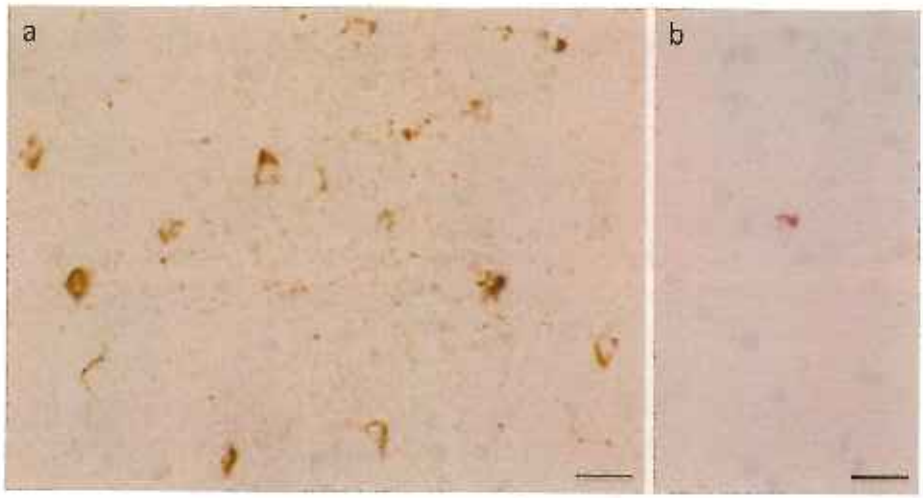

Fig. 3 (a) Temporal tip cortex. Many small neurons contain fine granular neuronal cytoplasmic inclusions (NCIs), and many fine dot-like granules are observed in the neuropil, some of which are linearly arranged. (b) Adjacent area of (a). The majority of the NCIs and fine granules in the neuropil are negative for p62. (a) pTDP-43 immunostaining; (b) p62 immunostaining. Scale bars: 20 μm.

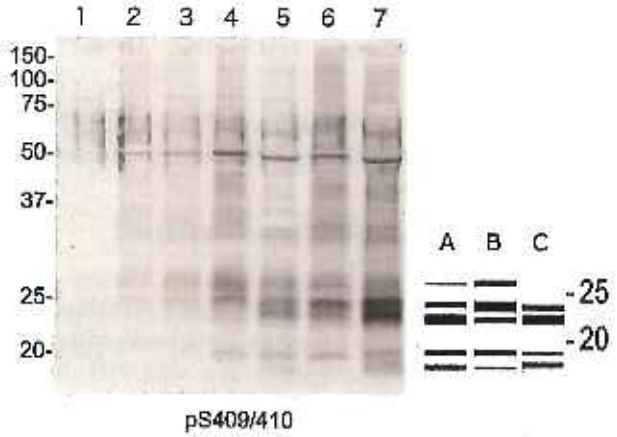

Fig. 4 Immunoblot analysis of sarkosyl-insoluble fractions of samples from the cerebellum, thoracic cord, frontal lobe and temporal lobe using a phosphorylation-dependent anti-TDP-43 antibody that is specific for pS409/410. In the temporal lobe, the pS409/410 antibody detected phosphorylated full-length TDP-43 at ~45 kDa and C-terminal fragments (CTFs) with some major and minor bands at 19–27 kDa (lane 4). The banding pattern of CTFs (major doublet bands at 26 kDa and a single band at 24 kDa) is similar to that of ALS Type B, but different from those of Types A, C (lanes 5–7). The same pS409/410-positive bands were also detected in the thoracic cord (lane 2) and frontal cortex (lane 3), but not in the cerebellum (lane 1). Lane 1, cerebellum; lane 2, thoracic cord; lane 3, frontal cortex; lane 4, temporal cortex; lane 5, Type A; lane 6, Type B; lane 7, Type C. Schema of Types A–C are shown in the right corner.

(Fig. 4, lanes 5–7). The same pS409/410-positive bands were detected in the thoracic cord (Fig. 4, lane 2) and frontal cortex (Fig. 4, lane 3) but not in the cerebellum (Fig. 4, lane 1).

DISCUSSION

Although most ALS cases are sporadic, approximately 10% of cases are familial, among which 20% carry Cu/Zn superoxide dismutase (*SOD1*) gene mutations and about 2%–5% have *TARDBP* gene mutations.[1] More than 30 mutations of the *TARDBP* gene have been identified; however, only a few cases with neuropathological findings are available, as shown in Table 1, including our case.[10–18] In the familial ALS with an M337V mutation reported by Tamaoka *et al.*,[15] the aunt of the proband was autopsied.[16] Although the case of Tamaoka *et al.*[15] and our families showed bulbar-onset-type ALS, the sites of the onset were variable, and most cases exhibited both upper motor neuron (UMN) and lower motor neuron (LMN) signs during the course of the disease. The cases exhibited several common neuropathological features: degeneration of both the UMN and LMN systems, presence of Bunina bodies, and widespread TDP-43-positive NCIs and GCIs.[10–18] However, precise descriptions of pTDP-43 in the brain were scarce among those cases. Our case showed the above-mentioned pathology, which was quite similar to that of SALS. Bunina bodies,[23] which are small eosinophilic intraneuronal inclusions present in the remaining lower motor neurons, are generally considered to be a specific pathological hallmark of SALS; these bodies were observed frequently in the reported cases with *TARDBP* gene mutations.

However, there are somewhat different findings in our case. First, the number of ubiquitin- and p62-positive inclusions was markedly lower than that of pTDP-43-positive inclusions. p62 is one of the components of ubiquitin-containing inclusions, and p62 immunoreactivity

Table 1 Clinicopathological data of autopsied ALS patients with *TARDBP* mutations

TARDBP mutations [References]	Age at onset	Sex	Duration (years)	Respirator	Initial symptoms	Cognitive dysfunction	Other	Bunina bodies	Widespread
G294A[13]	64y	M	6	–	Wasting of muscles	–		ND	–
G298S[32]	52	F	4	–	Right leg	–		+	+
G298S[32]	41	M	2	–	Left hand	–		+	+
A315T[34]	83	ND	3	–	Right leg	–		–	+
A315E[37]	63	F	6	–	Right leg	–		+	–
A315E[37]	57	F	4	–	Resting tremor	ND	Parkinsonism	+	–
M337V[35,36]	57	F	9	–	Dysarthria	–		+	ND
Q343R[10,11]	75	F	2	–	Dysarthria	–		+	+
Q343R This case	52	M	8	4 years	Dysarthria	–	Locked-in	+	+
N352S[12]	74	M	4	–	Hand	–		+	Less

ND, no data.

is observed in ubiquitin-containing intraneuronal or intraglial inclusions, including skein-like or round inclusions and inclusions in FTLD-TDP.[24] Similar discrepancies were observed in this case's mother's brain, namely, TDP-43-immunoreactive NCIs and GCIs were observed in various regions of the CNS;[31] however, small neurons in the putamen rarely contained ubiquitin-positive NCIs.[10] In general, it is said that TDP-43 consistently colocalizes with ubiquitinated inclusions in ALS or FTLD-TDP;[25] however, it has been reported that the percentage of spinal motor neurons with cytoplasmic TDP-43 immunoreactivity is higher than that of ubiquitin-immunoreactive ones.[26] In our experience, similar discrepancies between pTDP-43 and ubiquitin or p62 immunoreactivity were frequently observed in the brains of patients with widespread types of SALS (data not shown). Similar observations were described, and dash-like pTDP-43 aggregates reportedly merged into more compact net-like aggregates that were p62- and ubiquitin-positive.[27] The fine granular pTDP-43-positive inclusions without ubiquitin and p62 immunoreactivity may represent an earlier dysfunction in the cascade of the events that lead to neuronal degeneration.[26,27] Fine dot-like pTDP-43 granules may be present in the neuronal processes and may be earlier stages of pTDP-43 aggregation.[27]

Second, this was the first autopsy case that became totally locked-in after 4 years of artificial respiratory support. It has been reported that widespread multisystem degeneration can occur in patients with sporadic ALS who have survived for long periods with artificial respiratory support, who often clinically exhibit a totally locked-in state.[28] However, there was no significant difference in the distribution pattern of NCIs between SALS cases with or without artificial respiratory support.[29] In general, pTDP-43 aggregates in FTLD-TDP are observed frequently in neurons of the hippocampal granular cell layers and frontal and temporal cortices, and these aggregates are ubiquitinated.[2–5] The topographic patterns of the present case were similar to those of his mother.[10,11] NCIs were mainly present in the motor, parietal and temporal cortices and in the caudate and putamen; however, a few NCIs were observed in the frontal and entorhinal cortices and in the hippocampus.[11] Our case was severely affected in the same regions, probably because of the prolonged course of artificial respiratory support. Thus, the distribution patterns in this family were different from those of the usual FTLD-TDP. The case described by Honma *et al.*[18] exhibited a widespread distribution of NCIs and GCIs; however, the brain (including the frontal and temporal cortices and the limbic system) was preserved.

Third, the FTLD-TDP pathology is divided into four subtypes: Type A, many NCIs and many short dystrophic

neurites (DNs); Type B, moderate NCIs and few DNs; Type C, many long DNs and few NCIs; and Type D, many short DNs and many lentiform neuronal intranuclear inclusions (NIIs).[30] The majority of ALS cases are Type B. Although this case was similar to Type B, there were many fine dot-like granules in the neuropil of the severely affected cortices and putamen. These fine dot-like granules were also observed in our FTLD-TDP cases, but their density was greater in this case (data not shown). The reasons for this finding are obscure, but a few possibilities come to mind, such as *TARDBP* gene mutation and well fixation.

Fourth, the banding patterns of abnormally phosphorylated C-terminal fragments (CTFs) of TDP-43 can be classified into at least three types, according to the FTLD-TDP histopathological subtypes[5,21,22] Immunoblotting of samples from the cerebral cortex using pS409/410 antibody showed that the banding pattern was similar but different from that of ALS with doublet bands at 26 kDa, a single band at 24 kDa, and a single band at 19 kDa. The different banding patterns observed in TDP-43 proteinopathies may represent different conformations of abnormal TDP-43 or their aggregates.[31] In this case, the morphology of pTDP-43 structures was somewhat different from the TDP-43 subtypes; therefore, it is reasonable to think that differences can be detected via biochemical characterization using the banding pattern of CTFs. Additional studies are needed to clarify these results.

Lewy pathology and NFTs were observed, albeit to a mild degree. We suppose that they occurred coincidentally because of the aging process.

ACKNOWLEDGMENTS

We are very grateful to Drs A. Yokoseki and O. Onodera, Department of Neurology, Clinical Neuroscience Branch, Brain Research Institute (A.Y.), and Department of Molecular Neuroscience, Resource Branch for Brain Disease, Brain Research Institute (O.O.), Niigata University, for *TARDBP* analysis. This work was supported by grants from the Ministry of Health, Labour and Welfare of Japan. The authors express their appreciation to Ms Kunie Watanabe for her excellent technical assistance.

REFERENCES

1. Wijesekera LC, Leigh PN. Amyotrophic lateral sclerosis. *Orphanet J Rare Dis* 2009; **4**: 3–22.
2. Arai T, Hasegawa M, Akiyama H *et al.* TDP-43 is a component of ubiquitin-positive tau-negative inclusions in frontotemporal lobar degeneration and amyotrophic lateral sclerosis. *Biochem Biophys Res Commun* 2006; **351**: 602–611.
3. Neumann M, Sampathu DM, Kwong LK *et al.* Ubiquitinated TDP-43 in frontotemporal lobar degeneration and amyotrophic lateral sclerosis. *Science* 2006; **314**: 130–133.
4. Okamoto K. Ubiquitin-positive tau-negative intraneuronal inclusions in dementia with motor neuron disease. *Neuropathology* 2010; **30**: 486–489.
5. Hasegawa M, Arai T, Nonaka T *et al.* Phosphorylated TDP-43 in frontotemporal lobar degeneration and amyotrophic lateral sclerosis. *Ann Neurol* 2008; **64**: 60–70.
6. Chen-Plotkin AS, Lee VM-Y, Trojanowski JQ. TAR DNA-binding protein 43 in neurodegenerative disease. *Nat Rev Neurol* 2010; **6**: 211–220.
7. Geser F, Lee VM-Y, Trojanowski JQ. Amyotrophic lateral sclerosis and frontotemporal lobar degeneration: a spectrum of TDP-43 proteinopathies. *Neuropathology* 2010; **30**: 103–112.
8. Benajiba L, Ber IL, Camuzat A *et al. TARDBP* mutations in motoneuron disease with frontotemporal lobar degeneration. *Ann Neurol* 2009; **65**: 470–474.
9. Borroni B, Bonvicini C, Alberici A *et al.* Mutation within *TARDBP* leads to frontotemporal dementia without motor neuron disease. *Hum Mutat* 2009; **30**: E974–E983.
10. Tagawa A, Tan C-F, Kikugawa K *et al.* Familial amyotrophic lateral sclerosis: a SOD1-unrelated Japanese family of bulbar type with Bunina bodies and ubiquitin-positive skein-like inclusions in lower motor neurons. *Acta Neuropathol* 2007; **113**: 205–211.
11. Yokoseki A, Shiga A, Tan C-F *et al.* TDP-43 mutation in familial amyotrophic lateral sclerosis. *Ann Neurol* 2008; **63**: 538–542.
12. Van Deerlin VM, Leverenz JB, Bekris LM *et al. TARDBP* mutations in amyotrophic lateral sclerosis with TDP-43 neuropathology: a genetic and histopathological analysis. *Lancet Neurol* 2008; **7**: 409–416.
13. Pamphlett R, Luquin N, McLean C, Jew SK, Adams L. TDP-43 neuropathology is similar in sporadic amyotrophic lateral sclerosis with or without TDP-43 mutations. *Neuropathol Appl Neurobiol* 2009; **35**: 222–225.
14. Cairns NJ, Perrin RJ, Schmidt RE *et al.* TDP-43 proteinopathy in familial motor neuron disease with *TARDBP* A315T mutation: a case report. *Neuropathol Appl Neurobiol* 2010; **36**: 673–679.
15. Tamaoka A, Arai M, Itokawa M *et al.* TDP-43 M337V mutation in familial amyotrophic lateral sclerosis in Japan. *Intern Med* 2010; **49**: 331–334.
16. Tsuchiya K, Shinani S, Nakabayashi H *et al.* Familial amyotrophic lateral sclerosis with onset in bulbar sign, benign clinical course, and Bunina bodies: a clinical, genetic, and pathological study of a Japanese family. *Acta Neuropathol* 2000; **100**: 603–607.

17. Fujita Y, Ikeda M, Yanagisawa T *et al.* Different clinical and neuropathologic phenotypes of familial ALS with A315E *TARDBP* mutation. *Neurology* 2011; **77**: 1427–1431.
18. Homma T, Nagaoka U, Kawata A *et al.* Neuropathological features of Japanese familial amyotrophic lateral sclerosis with p.N352S mutation in *TARDBP*. *Neuropathol Appl Neurobiol* 2014; **40**: 231–236.
19. Egawa N, Kitaoka S, Tsukita K *et al.* Drug screening for ALS using patient-specific induced pluripotent stem cells. *Sci Transl Med* 2012; **4**: 1–8.
20. Nakano I. Frontotemporal dementia with motor neuron disease (amyotrophic lateral sclerosis with dementia). *Neuropathology* 2000; **1**: 68–75.
21. Kadokura A, Yamazaki T, Kakuda S *et al.* Phosphorylation-dependent TDP-43 antibody detects intraneuronal dot-like structures showing morphological characters of granulovacuolar degeneration. *Neurosci Lett* 2009; **463**: 87–92.
22. Fujita Y, Mizuno Y, Takatama M, Okamoto K. Anterior horn cells with abnormal TDP-43 immunoreactivities show fragmentation of the Golgi apparatus in ALS. *J Neurol Sci* 2008; **269**: 30–34.
23. Okamoto K, Mizuno Y, Fujita Y. Bunina bodies in amyotrophic lateral sclerosis. *Neuropathology* 2008; **28**: 109–115.
24. Mizuno Y, Amari M, Takatama M *et al.* Immunoreactivities of p62, an ubiquitin-binding protein, in the spinal anterior horn cells of patients with amyotrophic lateral sclerosis. *J Neurol Sci* 2006; **249**: 13–18.
25. Mackawa S, Leigh PL, King A *et al.* TDP-43 is consistently co-localized with ubiquitinated inclusions in sporadic and Guam amyotrophic lateral sclerosis but not in familial amyotrophic lateral sclerosis with or without SOD1 mutations. *Neuropathology* 2009; **29**: 672–683.
26. Giordana MT, Piccinini M, Grifoni S *et al.* TDP-43 redistribution is an early event in the sporadic amyotrophic lateral sclerosis. *Brain Pathol* 2010; **20**: 351–360.
27. Braak H, Ludolph A, Thal DR *et al.* Amyotrophic lateral sclerosis: dash-like accumulation of phosphorylated TDP-43 in somatodendritic and axonal compartments of somatomotor neurons of the lower brainstem and spinal cord. *Acta Neuropathol* 2010; **120**: 67–74.
28. Nishihira Y, Tan C-F, Hoshi Y *et al.* Sporadic amyotrophic lateral sclerosis of long duration is associated with relatively mild TDP-43 pathology. *Acta Neuropathol* 2009; **117**: 45–53.
29. Nishihira Y, Tan C-F, Onodera O *et al.* Sporadic amyotrophic lateral sclerosis: two pathological patterns shown by analysis of distribution of TDP-43 immunoreactive neuronal and glial cytoplasmic inclusions. *Acta Neuropathol* 2008; **116**: 169–182.
30. Mackenzie IRA, Neumann M, Baborie A *et al.* A harmonized classification system for FTLD-TDP pathology. *Acta Neuropathol* 2011; **122**: 111–113.
31. Tsuji H, Arai T, Kametani F *et al.* Molecular analysis and biochemical classification of TDP-43 proteinopathy. *Brain* 2012; **135**: 3380–3391.
32. Arai T. Significance and limitation of pathological classification of TDP-43 proteinopathy. *Neuropathology* 2014; **34**: 578–588.

Okamoto et al., J Clin Case Rep 2015, 5:12
http://dx.doi.org/10.4172/2165-7920.1000654

Clinical Case Reports

Case Report Open Access

Bilateral Involvement in Three Patients with Hirayama Disease

Koichi Okamoto[1]*, Masakuni Amari[1], Haruhiko Shimada[2] and Masamitsu Takatama[3]

[1]Department of Neurology, Geriatrics Research Institute and Hospital, Maebashi, Gunma, Japan
[2]Department of Orthopedic Surgery, Geriatrics Research Institute and Hospital, Maebashi, Gunma, Japan
[3]Department of Internal Medicine, Geriatrics Research Institute and Hospital, Maebashi, Gunma, Japan

Abstract

We report three patients with Hirayama disease with bilateral involvement. Case 1 developed weakness and wasting of bilateral hands at the age of 15 years. Case 2 developed unilateral weakness and wasting of the hand at the age of 18 years, and gradually exhibited progression to the other side within 1 year. Case 3 was a female who developed weakness and wasting of one hand at the age of 17 years, and showed dysesthesia and weakness in the other side, with pyramidal tract signs 31 years after the onset of the disease; she was diagnosed with complication of cervical disc hernia. We notice that bilateral involvement represents a severe form of this disease. We also need to differentiate incidental complications when the patients show worsening after a long stationary period.

Keywords: Hirayama disease; Cervical disc hernia; MRI

Introduction

Hirayama disease is a benign focal amyotrophy of the distal upper limbs. This disease was first reported in 1959 as "juvenile muscular atrophy of the unilateral upper extremity" [1]. Since then, similar cases have been described under a variety of names not only in Japan, but also in other Asian countries, as well as in Europe and North America [2-4]. The disease is characterized by the insidious onset of unilateral or asymmetric atrophy of the hand and forearm, with sparing of the brachioradialis muscle. After a period of deterioration of 3-5 years, a stable stage is reached. The pathophysiology of this disease is considered to be dynamic cord compression during neck flexion [2-4]. A bilaterally symmetric form of the disease is reported rarely [5,6]. Recently, we experienced three patients with Hirayama disease and bilateral involvement, one of whom received anterior decompression and fusion for a cervical disc hernia 31 years after the initial onset of the condition.

Case Reports

Case 1

A Japanese 37-year-old male developed weakness and wasting of bilateral hands at the age of 15 years. He was diagnosed as having Hirayama disease at the local university hospital. The weakness and wasting of the hands ceased within a few years. He visited our hospital for consultation 22 years after the onset of the condition. His past medical history was unremarkable. He played volleyball during junior high school. On neurological examination, weakness and atrophies of the bilateral upper extremities were confined. Ulnar-side dominant weakness atrophies were apparent in the forearms and in the intrinsic hand muscles (Figure 1a). Handgrip power was 6.1 kg on the right side and 0 kg on the left side. Postural hand tremor was observed. Sensation was intact. Tendon reflexes on the upper and lower extremities were almost normal, and Babinski sign was absent. Routine laboratory data were mostly normal. Cervical T2-weighted Magnetic Resonance Imaging (MRI) in sagittal and axial planes disclosed cervical cord atrophy, with a maximum at the C6 level and a hyperintense signal in the parenchyma (Figure 2a and 2b).

Figure 1a: Muscular atrophies of bilateral forearms and intrinsic hand muscles in Case 1. The brachioradialis muscles were spared and showed oblique atrophies, and the little fingers were slightly flexed.

Figure 1b: In Case 3, bilateral weakness and atrophies were observed in the forearms and hands, predominantly at the right side, and 2-5 fingers exhibited a flexed position.

***Corresponding author:** Koichi Okamoto, 1Department of Neurology, Geriatrics Research Institute and Hospital, Maebashi, Gunma, Japan, Tel: +81-27-253-3311; Fax: +81-27-252-7575; E-mail: okamotok@ronenbyo.or.jp

Received October 20, 2015; **Accepted** December 02, 2015; **Published** December 09, 2015

Citation: Okamoto K, Amari M, Shimada H, Takatama M (2015) Bilateral Involvement in Three Patients with Hirayama Disease. J Clin Case Rep 5: 654. doi:10.4172/2165-7920.1000654

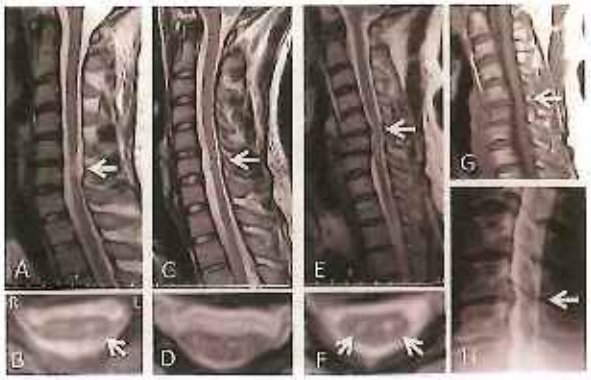

Figure 2: MRI findings of Case 1 (A, B), Case 2 (C, D), and Case 3 (E, F, G), and myelography findings of Case 3 (H). T2-weighted MRI showed localized cervical cord atrophy, with a maximum at C6–C7 (arrows) (A, C, E) and intramedullary hyperintensities (arrows) (A, E). Axial T2-weighted MRI disclosed hyperintense signals in the anterior horns (B, F). T1-weighted MRI (G) and myelography (H) disclosed a disc hernia at the C5/C6 level (arrows).

Case 2

A Japanese 22-year-old male developed weakness and wasting of the right hand at the age of 18 years and exhibited gradual progression of the condition. He noticed weakness and wasting of the left hand at the age of 19 years. He visited our hospital 4 years after the onset of the disease. His past medical history was unremarkable. He played football during junior high school and high school. On neurological examination, weakness and atrophies were confined to the bilateral upper extremities. Ulnar-side dominant atrophies in the forearms and in the intrinsic muscles of both hands. Postural hand tremor was observed, but sensation was intact. Tendon reflexes on the upper and lower extremities were almost normal, and Babinski sign was absent. Routine laboratory data were mostly normal. Motor nerve conduction studies of the median and ulnar nerves showed no delay. Cervical T2-weighted MRI disclosed atrophy of the cervical cord, with a maximum at the C6-C7 level, without disc herniation (Figure 2c and 2d). The use of a cervical collar was recommended.

Case 3

A Japanese 47-year-old female developed weakness and wasting of the right hand at the age of 17 years and exhibited gradual progression of the condition. She was diagnosed as having Hirayama disease at the local neurological clinic. The progression of the disease ceased within a few years. She played basketball during junior high school. Her past medical history was unremarkable. Recently, she noticed dysesthesia and weakness of the left hand, and was referred to our hospital 31 years after the onset of weakness in the right hand. Bilateral weakness and atrophies were observed in the forearms and hands, predominantly on the right side (Figure 1b), and she could not extend the fingers of the right hand. She showed dysesthesia on the left hand. Tendon reflexes on the upper and lower extremities were hyperactive, with both Babinski signs. Cranial nerves and bladder function were intact. Fasciculation was not observed. Preoperative laboratory data were mostly normal. T2-weighted MRI showed localized cervical cord atrophy, with a maximum at C6–C7 (Figure 2c), and disclosed the presence of a symmetrical hyperintense signal in the anterior horn ("snake eyes" appearance) in the axial plane (Figure 2f). T1-weighted MRI (Figure 2g) and myelography (Figure 2h) disclosed a disc hernia at the C5/C6 level. She received anterior decompression and fusion at the C5/C6 level.

Discussion

Hirayama disease is a benign lower motor neuron disorder of the young, with male predominance, insidious onset of weakness and atrophy, and slow progression over 3-5 years, followed by a stationary course. The pathological and MRI findings suggest that repeated or sustained neck flexion cause an anterior shift in the cervical dural sac, which is compressed against the posterior margin of the vertebral body [2,3,7]. The compressed cervical cord at the C6 vertebral level, which corresponds to the C7 and C8 cord segments, results in microcirculation disturbances in the anterior horn. There are many reports of the MRI findings of this disease, including localized lower cervical atrophy, asymmetric cord flattening, loss of cervical lordosis, anterior displacement of the dorsal dura on flexion, and intramedullary hyperintensity [8,9]. Based on this hypothesis, the use of a cervical collar is recommended [3,9].

Judging from the onset of age, clinical course, pattern of atrophy (namely, oblique atrophy), and neurological and MRI findings, the three patients were diagnosed as having Hirayama disease. Originally, the disease was thought to affect unilateral distal upper extremities, but bilateral involvement has been reported, ranging from 15% to 61.8%, and asymmetric involvement is a consistent feature in the reported studies [3,4]. According to the long-term follow-up of 44 patients with brachial monomelic amyotrophy, eight patients (18.2%) showed minimal involvement of the contralateral upper limb, with gross asymmetry [4]. The bilateral symmetric form of this disease has been reported rarely [5,6]. Pradhan [5] reported that 11 patients (approximately 10%) among 106 patients with Hirayama disease had bilaterally symmetric involvement, and that nine of them had a history of unilateral onset. The most important characteristics of this type of presentation are severe weakness and wasting; thus, the author concluded that bilaterally symmetric Hirayama disease is a severe form of the classic disease. Jain et al. [6] reported a young male with symmetrical bilateral weakness of the hands and forearm over the last 2 years, and emphasized the pivotal role of MRI in the diagnosis of this condition. Cases 1 and 2 have this form of the disease. Case 2 showed a history of unilateral onset, but exhibited an almost similar involvement in both upper limbs after 4 years. The progression of weakness and wasting observed in Case 2 did not cease at the examination, and the use of a cervical collar was recommended. The condition of this patient warrants a careful follow-up.

Case 3 was female, and it has been reported that females are affected about 3% - 13% in this disease [3]. After attaining a stationary course, none of these patients developed fresh symptoms or signs during the long follow-up, and there was no evidence of the involvement of pyramidal tracts or cranial nerves during the follow-up assessment [4]. However, Case 3 showed dysesthesia, weakness, and wasting in the contralateral side after a long stationary period. She also exhibited pyramidal tract signs, and MRI and myelography disclosed complication with cervical disc hernia. Cervical spinal canal stenosis and cervical disc hernia are popular in middle-aged people and the elderly; thus, we need to differentiate these incidental complications when the patients show worsening after a long stationary period.

References

1. Hirayama K, Toyokura Y, Tsubaki T (1959) Juvenile muscular atrophy of unilateral upper extremity: A new clinical entity. Psychiatr Neurol Jpn 61: 2190-2198.

2. Hirayama K (2000) Juvenile muscular atrophy of distal upper extremity (Hirayama disease). Intern Med 39: 283-290.

3. Hirayama K, Tashiro K (2013) Hirayama disease - half-a-century since its

discovery –diagnosis treatment pathomechanism. (Istodn). Bunkodo, Tokyo. Japan.

4. Gourie-Devi M, Nalini A (2003) Long-term follow-up of 44 patients with brachial monomelic amyotrophy. Acta Neurol Scand 107: 215-220.
5. Pradham S (2009) Bilaterally symmetric form of Hirayama disease. Neurology 72: 2083-2089.
6. 6.Jain S, Yadav S, Gupta S, Gupta R (2013) Bimelic Hirayama disease: clinical dilemma solved by imaging. Epub 2013: 606-894.
7. Hirayama K (2000) Juvenile muscular atrophy of distal upper extremity (Hirayama disease): Focal cervical ischemic pollomyelopathy. Neuropathology 20: S91-S94.
8. Dojobert M, Geffray A, Delpierre C, Chassande B, Larrieu E, et al. (2013) Hirayama disease: Three cases. Diagn Interv Imaging 94: 319-323.
9. Hassan KM, Sahni H, Jha A (2012) Clinical and radiological profile of Hirayama disease: A flexion myelopathy due to tight cervical dural canal amenable to collar therapy. Ann Indian Acad Neurol 15: 106-112.

10

Citation: Okamoto K, Amari M, Shimada H, Takatama M (2015) Bilateral Involvement in Three Patients with Hirayama Disease. J Clin Case Rep 5: 654. doi:10.4172/2165-7920.1000654

NEUROPATHOLOGY

Neuropathology 2015; ••, ••–••

doi:10.1111/neup.12277

Original Article

Hypersialylation is a common feature of neurofibrillary tangles and granulovacuolar degenerations in Alzheimer's disease and tauopathy brains

Shun Nagamine,[1] Tsuneo Yamazaki,[2] Kouki Makioka,[1] Yukio Fujita,[1] Masaki Ikeda,[1] Masamitsu Takatama,[3] Koichi Okamoto,[3] Hideaki Yokoo[4] and Yoshio Ikeda[1]

[1]Department of Neurology, Gunma University Graduate School of Medicine, [2]Department of Rehabilitation, Gunma University Graduate School of Health Sciences, [3]Geriatrics Research Institute and Hospital, and [4]Department of Human Pathology, Gunma University Graduate School of Medicine, Maebashi, Gunma, Japan

Glycosylation is one of the major post-translational modifications of proteins. The status of sialylation of the neuropathological hallmarks of various neurodegenerative disorders was investigated in this study. Here, we report the novel findings that two phosphorylated tau (p-tau)-containing structures associated with Alzheimer's disease (AD), that is, neurofibrillary tangles (NFTs) and granulovacuolar degenerations (GVDs), were hypersialylated. The NFTs, GVDs and dystrophic neurites of senile plaques (SPs) in AD hippocampi were clearly visualized by immunohistochemistry using an anti-sialic acid (SA) antibody. In contrast, the amyloid core of SPs was not sialylated at all. Interestingly, other p-tau-containing structures, that is, globose-type NFTs in progressive supranuclear palsy and Pick bodies and ballooned neurons in frontotemporal lobar degeneration with Pick bodies, were also hypersialylated. Unlike the p-tau-containing structures observed in tauopathies, the hallmarks of other neurodegenerative disorders, such as Lewy bodies in Parkinson's disease, glial cytoplasmic inclusions in multiple system atrophy, Bunina bodies, skein-like inclusions and round inclusions in amyotrophic lateral sclerosis, intranuclear inclusions in neuronal intranuclear inclusion disease and physiological bodies or granules (lipofuscin granules, corpora amylacea and melanin granules), were not immunolabeled by the anti-SA antibody. Because this antibody specifically identified NFTs and GVDs, immunostaining for sialylation represents a useful tool to screen these structures in a diagnostic setting. These results clearly indicate that the pathological hallmarks of various tauopathies are commonly hypersialylated, and that sialylation plays an important role in the process of p-tau accumulation in AD and other tauopathies.

Key words: Alzheimer's disease, granulovacuolar degeneration, hypersialylation, neurofibrillary tangle, tauopathy.

Correspondence: Yoshio Ikeda, MD, PhD, Department of Neurology, Gunma University Graduate School of Medicine, 3-39-22 Showa-machi, Maebashi, Gunma 371-8511, Japan. Email: ikeday@m66@gunma-u.ac.jp

Received 19 June 2015; revised and accepted 20 October 2015.

INTRODUCTION

Tau is a major component of neurofibrillary tangles (NFT), which are one of the neuropathological hallmarks of Alzheimer's disease (AD) brains.[1] Hyperphosphorylation of tau promotes its self-assembly into paired helical filaments (PHFs).[2] In AD brains, tau is aberrantly glycosylated with various oligosaccharides, including N-acetylneuraminic acid (NeuAc), which is a major member of the sialic acid (SA) family.[3–5] In contrast, deglycosylation by glycosidases depresses the phosphorylation of tau.[6] These findings suggest that aberrant glycosylation in AD brains facilitates the hyperphosphorylation of tau, resulting in the formation of NFTs.[5] In support of this hypothesis, some biological changes of SAs and sialyltransferases have been reported in AD patients.[7–10]

With regard to the relationship between sialylation and amyloid β (Aβ) pathology of AD, it has been reported that the β-site amyloid precursor protein (APP) cleaving enzyme 1 (BACE-1) can cleave not only APP but the sialyltransferase ST6Gal-I, thus downregulating its transferase activity.[11] In addition, a genome-wide association study of AD identified that the common variant of CD33, also known as Siglec-3 and a member of the sialic acid-binding immunoglobulin-like lectins, is a genetic risk factor for AD.[12,13] The uptake and clearance of Aβ due to microglias

are found to be inhibited by a transmembrane microglial protein CD33, so that CD33 could be a potential target to develop an anti-AD therapy.

Granulovacuolar degenerations (GVDs) are not always pathogenic, but are regarded as an additional pathological hallmark of AD.[14] As GVDs contain phosphorylated tau (p-tau) and several tau kinases, such as casein kinase 1δ, GVDs are considered to be the site of tau phosphorylation.[15] Considering that aberrant glycosylation facilitates the hyperphosphorylation of tau, it can be hypothesized that the p-tau present in GVDs is also hypersialylated.[4,5] However, an association between GVDs and sialylation has not been reported so far. The present study reports the novel findings that both NFTs and GVDs were hypersialylated in AD brains. In addition, hypersialylation of tau was also confirmed in other pathological structures from tauopathies, such as progressive supranuclear palsy (PSP) and frontotemporal lobar degeneration with Pick bodies (PickD), although other well-known characteristic pathological structures of Parkinson's disease (PD), multiple system atrophy (MSA), amyotrophic lateral sclerosis (ALS) and neuronal intranuclear inclusion disease (NIID) were not hypersialylated. These findings suggest the existence of a common mechanism in which p-tau is hypersialylated not only in AD, but also in other tauopathies, leading to its aggregation and subsequent neurodegeneration.

MATERIALS AND METHODS

Subjects

A total of 28 autopsied brain and spinal cord tissues (from 15 males and 13 females) and one biopsied skin tissue were collected from the Gunma University Hospital and the Geriatrics Research Institute and Hospital. These samples included six cases of AD, three cases of PD, five cases of MSA, six cases of ALS, one case of PSP, one case of PickD and one case of NIID, as well as six control elderly cases who did not have any neurodegenerative diseases. These autopsy and biopsy materials and their demographic findings are described in Table 1. All autopsies and the biopsy were performed in accordance with established procedures, and the specimens were processed after obtaining written informed consent from the patient or the patient's family.

Table 1 Autopsy and biopsy cases and their demographic findings

Case #	Age at death (years)	Sex	Diagnosis	Brain weight (g)	Final cause of death	Post mortem delay (h)
1	65	M	AD	1080	Pneumonia	11
2	81	M	AD	1175	Pulmonary thromboembolism	1
3	79	F	AD	1050	Double cancer (colon and ovarian)	7
4	83	F	AD	1165	AMI	2
5	63	F	AD	1120	DOA	1
6	84	F	AD	1080	Phlegmon	2
7	71	M	PD	1450	Pneumonia	4
8	78	M	PD	1260	Fracture of the left femur	<1
9	88	F	PD	1165	Heart failure caused by OMI	8
10	65	M	MSA	n.a.	n.a.	n.a.
11	66	M	MSA	n.a.	DOA	<1
12	62	F	MSA	1110	Pneumonia	1
13	54	F	MSA	n.a.	n.a.	n.a.
14	57	F	MSA	n.a.	n.a.	n.a.
15	60	M	ALS	1235	Pneumonia	4
16	65	M	ALS	1280	Pneumonia	1
17	62	M	ALS	1300	Pneumonia	n.a.
18	61	M	ALS	1370	Pneumonia	<1
19	69	M	ALS	810	Pneumonia	<1
20	56	F	ALS	1510	DOA	3
21	71	M	PSP	1200	Pneumonia	3
22	73	M	PickD	1070	Pneumonia	2
23	69*	F	NIID	n.a.	n.a.	n.a.
24	83	F	Control	1330	Renal failure	8
25	90	F	Control	915	Cerebral embolism	n.a.
26	84	F	Control	1110	Cerebral infarction	3
27	79	F	Control	1115	Pneumonia	23
28	85	M	Control	890	Pneumonia	n.a.
29	81	M	Control	1355	ARDS	1

M, male; F, female; AD, Alzheimer's disease; PD, Parkinson's disease; MSA, multiple system atrophy; ALS, amyotrophic lateral sclerosis; PSP, progressive supranuclear palsy; PickD, frontotemporal lobar degeneration with Pick bodies; NIID, neuronal intranuclear inclusion disease; Control, non-neurological control; n.a., not available; AMI, acute myocardial infarction; DOA, dead on arrival; OMI, old myocardial infarction; ARDS, adult respiratory distress syndrome; *, age at biopsy.

Patients with AD (average age at death, 75.8 years; two males and four females) were diagnosed as having clinically probable AD according to the clinical diagnostic criteria published by the Consortium to Establish a Registry for AD, and fulfilled the quantitative neuropathological criteria for diagnosing AD according to the National Institute on Aging – Alzheimer's Association guidelines for the neuropathologic assessment of AD; that is, AD Neuropathologic Change scores of A3, B3 and C3.[16–19]

Patients with PD (average age at death, 79.0 years; two males and one female) were clinically diagnosed using the UK PD Society Brain Bank clinical diagnostic criteria, and the diagnosis was confirmed using histopathologic criteria.[20,21] Patients with MSA (average age at death, 76.0 years; two males and three females) were clinically diagnosed using the criteria for definite MSA of the second consensus statement on the diagnosis of MSA.[22] Patients with ALS (average age at death, 62.2 years; five males and one female) clinically fulfilled the diagnostic criteria for clinically definite ALS, clinically probable ALS, or clinically probable laboratory-supported ALS according to the revised El Escorial criteria, and were proven by autopsy examination.[23] One male patient with PSP (71 years at death) showed parkinsonism, and fulfilled the neuropathologic criteria for PSP of the National Institute of Neurological Disorders and Stroke (NINDS).[24] One male patient with PickD (73 years at death) was clinically diagnosed as having dementia and personality change, and fulfilled the neuropathologic diagnostic and nosologic criteria for frontotemporal lobar degeneration.[25]

One female patient with NIID (aged 69 years at the time of skin biopsy) who showed diffuse leukoencephalopathy on cerebral MRI with characteristic high intensities of subcortical U-fibers on diffusion-weighted imaging was pathologically diagnosed via confirmation of the skin biopsy findings of ubiquitin/p62-positive intranuclear inclusions in sweat gland cells and adipocytes.[26,27]

Immunohistochemistry

Five-micrometer-thick sections from formalin-fixed, paraffin-embedded tissues were deparaffinized and immunostained with primary antibodies using the streptavidin-biotin-peroxidase complex (ABC) method (Histofine SAB-PO kit; Nichirei, Tokyo, Japan). The sections were immersed in 0.3% hydrogen peroxide (Doujin Laboratories, Kumamoto, Japan) in methanol for 30 min, to block endogenous peroxidase activity, and autoclaved for 10 min in 10 mmol/L sodium citrate buffer (pH 6.0), for antigen retrieval. Moreover, for staining with the anti-Aβ antibody, the tissues were treated with 70% formic acid for 3 min. All sections were blocked in a solution supplied by the manufacturer for 30 min at room temperature, incubated with the primary antibodies overnight at 4°C, and then incubated with secondary antibodies raised against the animals that were used to produce the primary antibodies. Immunoreactivity was visualized using 0.5 mg/mL of 3,3′-diaminobenzidine tetrachloride (DAB) containing 0.03% hydrogen peroxide.

To examine the colocalization between SA and α-synuclein in MSA and PD brains, double immunohistochemistry was performed.[28] The anti-SA antibody was visualized via the ABC method using DAB as a chromagen, and the anti-α-synuclein antibody was visualized via the ABC method using the VIP Substrate Kit (Vector Laboratories, Burlingame, CA, USA).

Because Bunina bodies, which are a neuropathological hallmark of ALS, can be easily recognized by HE staining, this method was initially used to identify the location of the spinal anterior horn cells containing Bunina bodies. After the HE sections were photographed, cover slips were removed from the slides in xylene, and the specimens were decolorized in alcohol, then restained using the respective immunolabeling.

To confirm specificity of the anti-SA antibody, the antibody was absorbed by sialyllactose sodium salt (S0885; Tokyo Chemical Industry, Tokyo, Japan) that contains an epitope of the NeuAcα2-3 bond recognized by the SA antibody. An aliquot of the SA antibody (0.4 μL) was preincubated at 4°C for 24 h with 38 mg of the sialyllactose sodium salt in a total volume of 200 μL solution containing 1% bovine serum albumin. Another aliquot of the anti-SA antibody was also preincubated without sialyllactose sodium salt in the same way, and served as a control. The preincubated SA antibodies were used for immunohistochemistry as described above.

All sections were counterstained with hematoxylin. The stained slides were evaluated under an Olympus DP72 microscope using the DP2-BSQ software (Olympus, Tokyo, Japan).

Double immunofluorescence

For immunofluorescence (IF), deparaffinization, antigen retrieval, blocking and labeling with the primary antibodies were performed as described above. Subsequently, the slides were incubated with a mixture of secondary antibodies (Alexa Fluor 488-conjugated goat anti-rabbit IgG (Molecular Probes-Invitrogen, Eugene, OR, USA) and Alexa Fluor 568-conjugated goat anti-mouse IgG (Molecular Probes-Invitrogen)) for 2 h. To avoid autofluorescence signals from the specimens, sections were immersed in Sudan Black (Wako Pure Chemical Industries, Osaka, Japan) for 5 min, then rinsed in 70% ethanol. The stained slides were mounted with Vectashield (Vector Laboratories) and evaluated under an FV1000 confocal microscope (Olympus).

Primary antibodies

The primary antibodies used in this study were as follows: rabbit polyclonal anti-α-synuclein antibody raised against amino

acids (aa) 111-131 (1:500, AB5038P; Millipore, Billerica, MA, USA); rabbit polyclonal anti α-synuclein antibody raised against aa 116-131 (1:2000, prepared in-house);[28,29] rabbit polyclonal anti-Aβ antibody raised against the C terminal of Aβ 1-42 (1:200, AB5078P; Millipore); mouse monoclonal anti-Aβ antibody (clone 4G8) raised against aa 17-24 (1:5000, SIG-39220; Signet, Dedham, MA, USA); mouse monoclonal anti-PHF-tau (clone AT8) raised against purified human PHF-tau phosphorylated at Ser202 and Thr205 (AT8 antibody) (1:1000, MN1020; Thermo Fisher Scientific, Waltham, MA, USA); rabbit polyclonal anti-phosphorylated protein kinase-like ER kinase (anti-pPERK) antibody raised against a fragment of pPERK phosphorylated at Thr981 (1:800, sc-32577; Santa Cruz Biotechnology, Dallas, TX, USA); rabbit polyclonal anti-p-tau antibody raised against a synthesized peptide phosphorylated at Ser214 (p-tau Ser214 antibody) (1:400, 44-742G; Invitrogen, Camarillo, CA, USA); rabbit polyclonal anti-phosphorylated trans-activation response DNA-binding protein 43 (pTDP-43) raised against a peptide containing residues 404-414 with Ser409/Ser410 double phosphorylation, which we named "2A" (1:3000 for the ABC method and 1:600 for IF; prepared in-house);[30] mouse monoclonal anti-SA antibody (clone HYB4) raised against IV3NeuAcnLc4Cer, which recognizes a structure of NeuAcα2-3Galβ1-4GlcNAcβ1-3Galβ1-4Glcβ1-1' Cer (1:500 for ABC the method and 1:100 for IF, 011-25171; Wako Pure Chemical Industries);[31] rabbit polyclonal anti-lysosome-associated membrane protein-1 (LAMP1) antibody raised against aa 131-161 (1:500, AP1823a; ABGENT, San Diego, CA, USA); rabbit polyclonal anti-cathepsin D antibody (1:10, PU205-UP; BioGenex, San Ramon, CA, USA); rabbit polyclonal anti-cystatin-C antibody (1:2500, A0451; DAKO, Glostrup, Denmark); rabbit polyclonal anti-p62 antibody raised against aa 120-440 (1:1000, PM045; MBL, Aichi, Japan); and rabbit polyclonal anti-ubiquitin antibody (1:2000, Z0458, DAKO).[32]

RESULTS

NFTs, GVDs and DNs in both AD and control brains were hypersialylated

Staining with the anti-SA antibody, which recognizes sugar chains containing a NeuAcα2-3 bond, led to the clear visualization of granular or filamentous structures in both AD and control brains. In the hippocampus of AD brains, flame-shaped materials (Fig. 1A, 1B) and granule-containing vacuoles in the neuronal cytoplasm (Fig. 1C), as well as clustered swollen structures located outside of neurons (Fig. 1D) were stained with this antibody. The staining pattern was observed as NFTs, GVDs and dystrophic neurites (DNs) of senile plaques (SPs), respectively.[33] These structures labeled by this antibody were also found in the frontal (Fig. 1E-G) and occipital (Fig. 1H-J) cortices, the periaqueductal gray matter of the midbrain (PAG) (Fig. 1K,L), pontine nuclei (Fig. 1M, N), and the medulla (Fig. 1O,P). Immunohistochemistry showed that positive labeling by the anti-SA antibody was most prominent in the cornu ammonis 1 (CA1) area of the hippocampus in AD brains. The AT8 and p-tau Ser214 antibodies raised against p-tau detected NFTs and DNs, but not GVDs, in AD brains (data not shown). With regard to specificity of the anti-SA antibody, preincubation without sialyllactose sodium salt did not reduce the reactivity of the antibody (Fig. 1Q,R). However, the anti SA antibody preincubated with sialyllactose sodium salt totally lost the reactivity for GVDs, NFTs and DNs (Fig. 1S,T), indicating this antibody specifically recognized the NeuAcα2-3 bond.

To examine whether these hypersialylated structures were actually the same as GVDs, NFTs or DNs, double IF analysis was performed. The amyloid core of SPs, which contains Aβ, was not immunostained by the anti-SA antibody (Fig. 2A-F). In contrast, the DNs surrounding the SP core seemed to be labeled by this antibody (Fig. 2A-F). The p-tau-positive DNs (Fig. 2G-I) and NFTs (Fig. 2J-L) were both stained by the anti-SA antibody. The GVDs, which were negative for p-tau (Fig. 2G-L, circle), but positive for pPERK (Fig. 2M-O, circle) or pTDP-43 (Fig. 2P-R, circle), were also stained by an anti-SA antibody.[30,34] To examine whether the granular structures that were positive for the anti-SA antibody were lysosomes, a double IF analysis using lysosome markers (LAMP1 and cathepsin D) was also performed (Fig. 2S-X). These lysosome markers were partially colocalized with the anti-SA antibody, but not to the extent observed for NFTs or GVDs (Fig. 2S-X).[35,36]

Characteristic pathological hallmarks of tauopathies, but not those of other neurodegenerative disorders, were also hypersialylated

The status of sialylation of the characteristic neuropathological hallmarks of neurodegenerative disorders other than AD was also investigated. Lewy bodies (LBs), which are a

Fig. 1 Anti-sialic acid (SA) antibody detected neurofibrillary tangles (NFTs), and granulovacuolar degenerations (GVDs), and dystrophic neurites (DNs) in neurons from various parts of AD brains. In the cornu ammonis 1 (CA1) area of Alzheimer's disease (AD) brains, NFTs were immunostained by the anti-SA antibody (A). The inset showed flame-shaped NFTs (B). GVDs (C) and DNs of senile plaques (D) were also immunostained by the anti-SA antibody. NFTs, GVDs and DNs were also positive for SA in neurons of the frontal (E-G) and occipital (H-J) cortices, the periaqueductal gray matter of the midbrain (K,L), pontine nuclei (M,N) and the medulla (O,P). The anti-SA antibodies were preincubated without (Q and inset R) or with (S and inset T) the sialyllactose sodium salt, and used for immunohistochemistry of the subiculum of an AD brain. Q and R are comparable to S and T of the same AD subject, respectively. Scale bars: A, O and S, 100 μm; B-P, R and T, 10 μm.

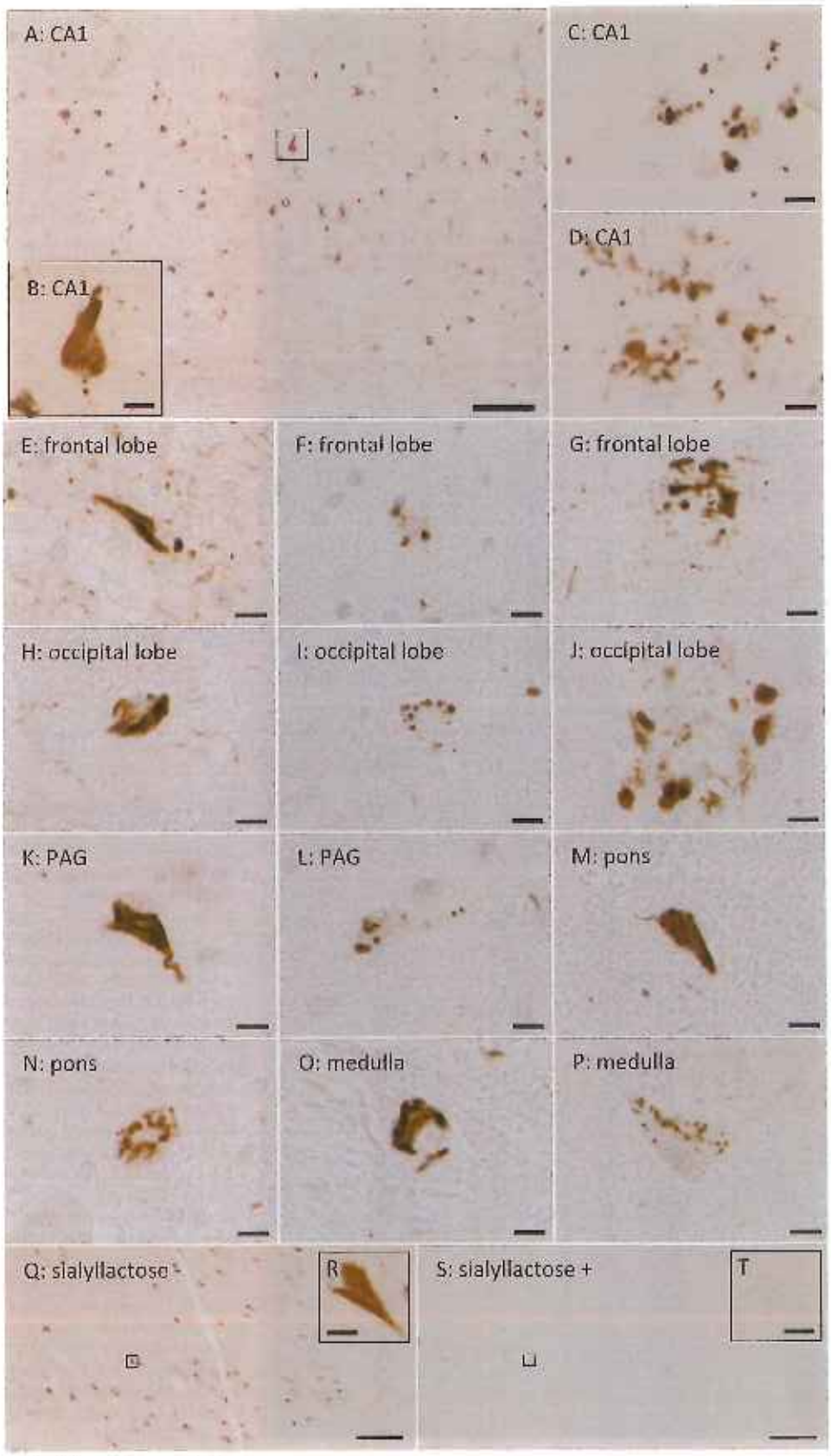

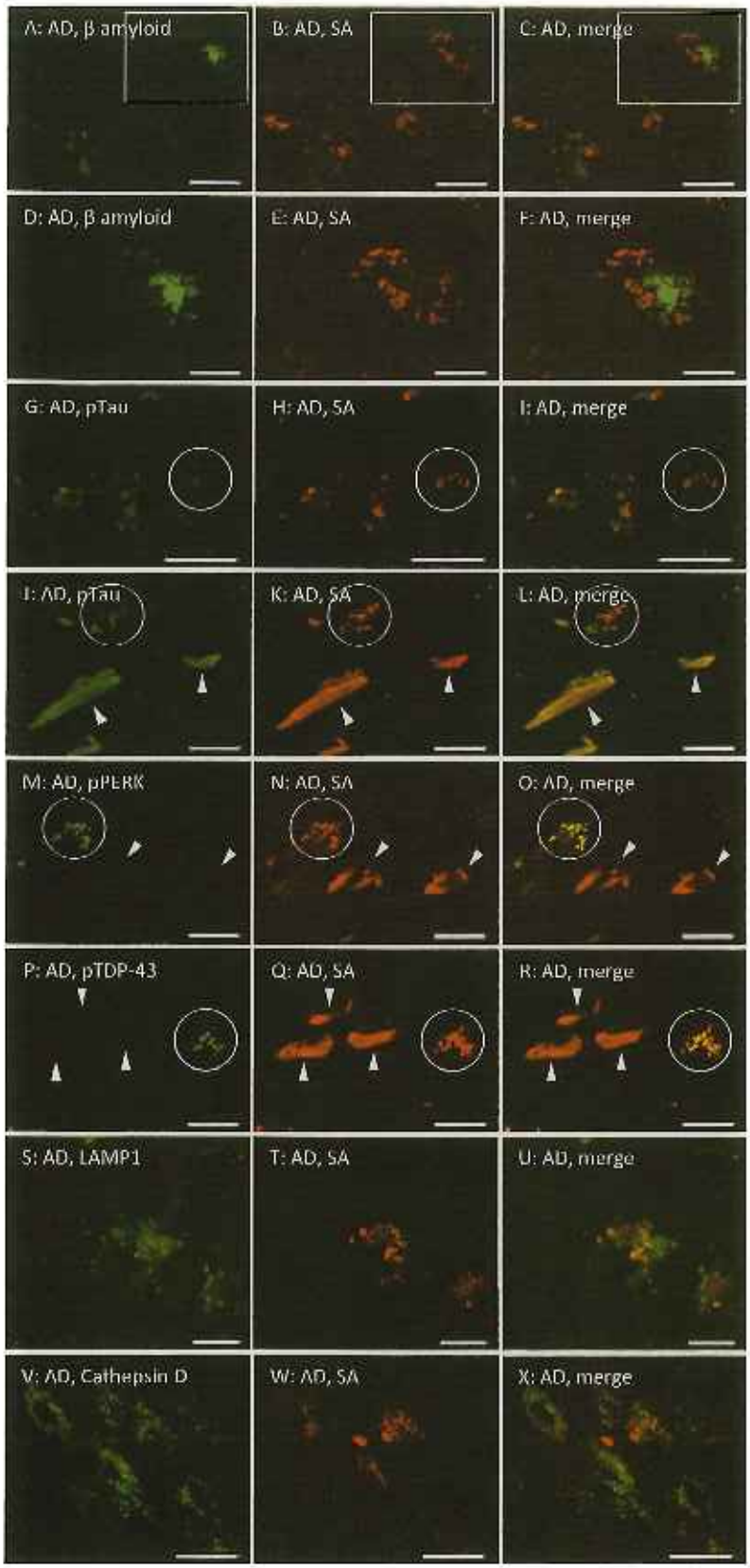

16

Fig. 2 Double immunofluorescence analyses using the anti-sialic acid (SA) antibody in the hippocampus of Alzheimer's disease (AD) brains. The Aβ-positive amyloid core of senile plaques (SPs, rectangle in A, and D) was not stained by the anti-SA antibody (rectangles in B, C, and E, F) in the hippocampus of AD brains. Conversely, the dystrophic neurites (DNs) of SPs were not stained by Aβ (A,D), but were stained by SA (B,C,E,F). The boxed areas in A, B and C are enlarged in D, E and F, respectively. The p-tau-positive DNs (G) and neurofibrillary tangles (NFTs, arrowheads in J) were also labeled by the anti-SA antibody (H,I,K,L, respectively). Granulovacuolar degenerations (GVDs, circles in G-L) were negative for p-tau, but positive for SA. The phosphorylated protein kinase-like ER kinase (pPERK)-positive and phosphorylated trans-activation response DNA-binding protein 43 (pTDP-43)-positive GVDs were colocalized with SA (circles in M-O and P-R, respectively). In contrast, SA-positive NFTs (arrowheads in N and Q) were not positive for pPERK or pTDP-43 (M,O,P,R, respectively). Two lysosome markers, the lysosomal-associated membrane protein-1 (LAMP1) and cathepsin D, were partially colocalized with SA (S-U and V-X, respectively), but not to the extent observed for NFTs or GVDs. Scale bars: A-C, and G-I, 50 μm; D-F, J-O, V-X, 25 μm; S-U, 10 μm.

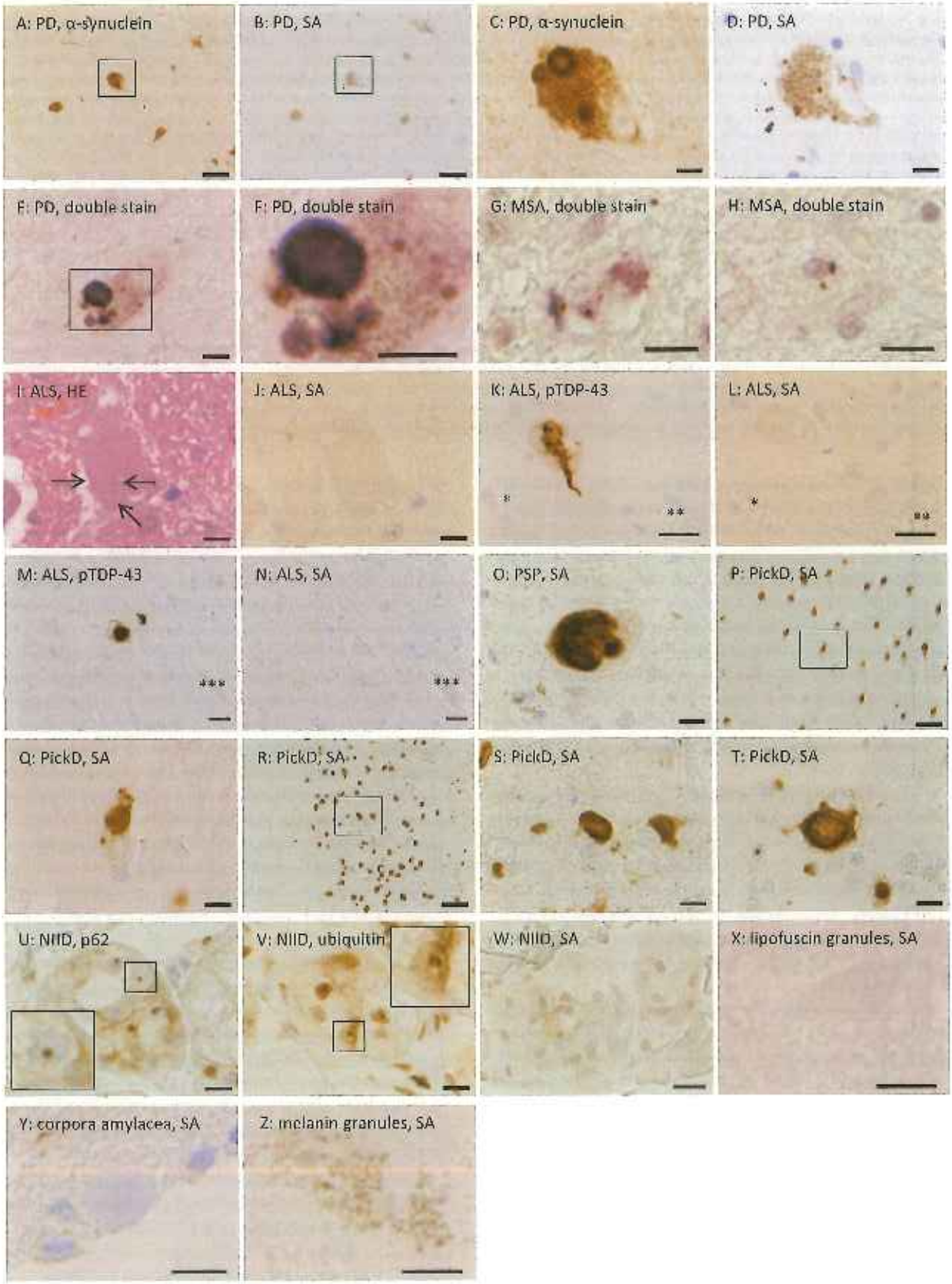

Fig. 3 Sialic acid (SA) immunoreactivity in the pathological hallmarks of various neurodegenerative disorders. A and B are serial sections of the substantia nigra of the same Parkinson's disease (PD) brain. A and B are enlarged in C and D, respectively. The anti-α-synuclein antibody led to the visualization of Lewy bodies (LBs, A,C); however, the same LBs were not labeled by the anti- SA antibody (B,D). However, the smaller punctate structures were labeled by the anti-SA antibody (B,D). Double immunohistochemistry showed that the punctate structures stained by the anti-SA antibody (brown) appeared around LBs were also stained by the anti-α-synuclein antibody (purple) (E and enlarged in F). Some of the brown punctate structures detected in the vacuoles were similar to the appearance of granulovacuolar degenerations (GVDs, E,F). Double immunohistochemistry of the pontine nuclei of multiple system atrophy (MSA) brains using anti-SA (brown) and anti-α-synuclein (purple) antibodies showed that glial cytoplasmic inclusions (GCIs, purple) were not positive for the anti-SA antibody (G). However, the smaller punctate structures were labeled by both the anti-SA (brown) and anti-α-synuclein (purple) antibodies (G,H). HE staining showed the presence of Bunina bodies in the anterior horn cells (arrows in I) in the lumbar spinal cord of amyotrophic lateral sclerosis (ALS). The specimen shown in I was decolorized and restained with the anti-SA antibody, and no positive structures were confirmed in the same anterior horn cell (J). Serial sections of the lumbar cord of a patient with ALS showed that the skein-like inclusions (K) and round inclusions (M) were labeled by the anti-phosphorylated trans-activation response DNA-binding protein 43 antibody (pTDP-43), but not by the anti-SA antibody (K,L and M,N, respectively). Asterisks * and ** in K and L, and *** in M and N indicate the reference vessels that were used to confirm the position of the respective anterior horn cells. The anti-SA antibody labeled the globose-type neurofibrillary tangles (NFTs) in the substantia nigra (SN) neurons of a progressive supranuclear palsy (PSP) brain (O). Pick bodies in neurons from the cornu ammonis 1 (CA1) area (P and enlarged in Q), Pick bodies from the dentate gyrus (R and enlarged in S), and ballooned neurons or Pick cells from the temporal cortex (T) of a brain with frontotemporal lobar degeneration with Pick bodies (PickD). A skin biopsy specimen of a patient with neuronal intranuclear inclusion disease (NIID) showed that the anti-p62 and anti-ubiquitin antibodies labeled intranuclear inclusions in sweat gland cells and adipocytes (U,V and enlarged insets). The anti-SA antibody did not stain these inclusions associated with NIID (W). In the control brains, lipofuscin granules (X) and corpora amylacea (Y) in the CA1 area of the hippocampus, and melanin granules (Z) in the SN of the midbrain were not labeled by the anti-SA antibody. Scale bars: A,B,P,R, 50 μm; C-J,O,Q,S-Z, 10 μm; K-N, 20 μm.

hallmark of PD and contain α-synuclein, were not obviously positive for SA (Fig. 3A-D). However, some punctate materials were labeled by the anti-SA antibody in the same neurons of the substantia nigra (SN) that contained LB and melanin granules (Fig. 3C,D). These findings were reproducibly confirmed in other SN neurons of three PD brains. Double immunohistochemistry showed that the small punctuate structures were stained with the anti-SA antibody (brown), and that LBs were independently stained for α-synuclein (purple) in the same cell (Fig. 3E,F). Moreover, some of the small granular structures were localized within the vacuole, which were similar to the appearance of GVDs (Fig. 3E,F).

In MSA brains, typical glial cytoplasmic inclusions (GCIs), which are a pathological hallmark of MSA and contain α-synuclein, were not obviously labeled by the anti-SA antibody (brown) (Fig. 3G). However, smaller punctate structures were positively labeled by both the anti-SA (brown) and anti-α-synuclein (purple) antibodies (Fig. 3G, H). Some of the smaller punctate structures were localized by the GCIs (Fig. 3G), whereas others were independent of GCIs (Fig. 3H).

The presence of Bunina bodies, which are a pathological hallmark of ALS, was confirmed by HE staining in the lumbar anterior horn cells of patients with ALS (Fig. 3I). The HE-stained slide shown in Figure 3I was decolorized and subsequently restained with the anti-SA antibody. Bunina bodies in the same slide shown in Figure 3I were not labeled by the anti-SA antibody (Fig. 3J). Moreover, other hallmarks of ALS, that is, skein-like inclusions (Fig. 3K) and round inclusions (Fig. 3M) that were positive for pTDP-43 were totally negative for the anti-SA antibody (Fig. 3L,N).

Globose-type NFTs, which are a hallmark of PSP, were detected by the anti-SA antibody in the SN neurons of a PSP midbrain (Fig. 3O). NFTs in the neurons of the putamen, oculomotor nuclei, and PAG were also labeled by the anti-SA antibody in the same PSP subject (data not shown).

Pick bodies, which are a hallmark of PickD, were positive for SA in the neurons of the CA1 area of the hippocampus (Fig. 3P,Q) and of the dentate gyrus (Fig. 3R,S). The smaller granular materials observed within vacuoles, which were similar to the GVDs, were also labeled by the anti-SA antibody (Fig. 3Q). Moreover, staining with this antibody led to the clear visualization of Pick bodies in the neurons of other broad areas, including the temporal cortex, thalamus, putamen, and pallidum (data not shown). In the temporal cortex and putamen, the anti-SA antibody also stained the somata of larger cells, which were reminiscent of ballooned neurons (also known as swollen cells or Pick cells) (Fig. 3T). These ballooned neurons were clearly distinguishable from Pick bodies based on their size and appearance, that is, the ballooned neurons were larger and showed perinuclear staining, and Pick bodies were smaller and round- or oval-shaped (Fig. 3Q,S,T).

The p62/ubiquitin-positive neuronal intranuclear inclusions observed in the sweat gland cells and adipocytes of the skin biopsy tissue from a patient with NIID were not clearly labeled by the anti-SA antibody (Fig. 3U-W). Physiological or nonpathological structures were also analyzed in the control brains. The lipofuscin granules observed in neurons and the corpora amylacea in astrocytes of the CA1 area, and the melanin granules observed in SN neurons were not labeled by the anti-SA antibody (Fig. 3X-Z).

Double IF analyses revealed that the LBs detected in patients with PD were partially colocalized with α-synuclein and SA at the outer edge of LBs; however, the cores of LBs were negative for SA (Fig. 4A-C). The GCIs observed in MSA subjects that were stained with α-synuclein, were

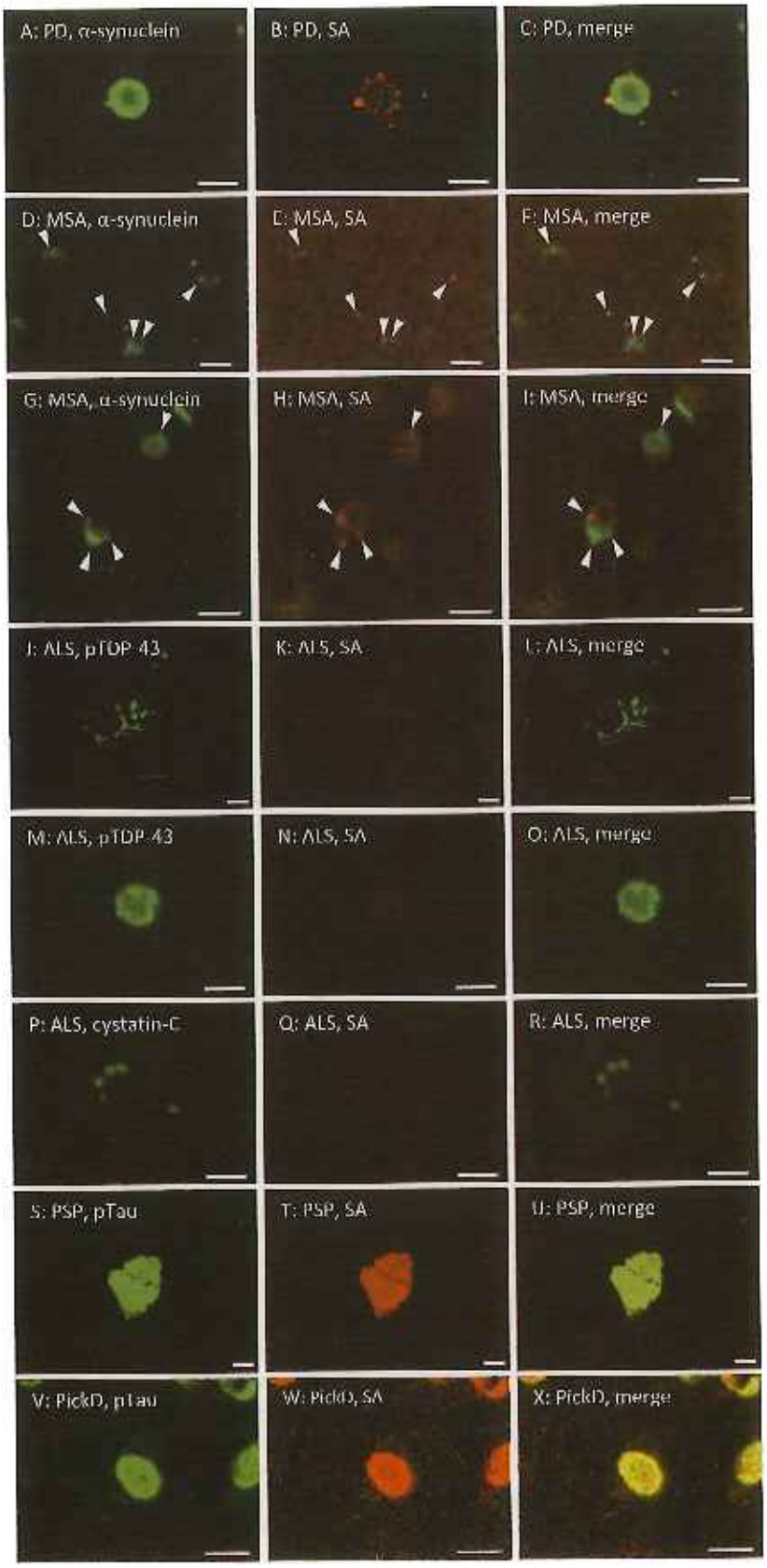

Fig. 4 Double immunofluorescence analyses of the pathological hallmarks of various neurodegenerative disorders using the anti-sialic acid (SA) antibody. In the substantia nigra of a Parkinson's disease (PD) brain, Lewy body cores that were positive for α-synuclein were not immunostained by the anti-SA antibody. However, α-synuclein-positive smaller punctate structures located at the outer edge of the core were colocalized with SA (A-C). In the pontine nuclei of a multiple system atrophy (MSA) brain, glial cytoplasmic inclusions (GCIs) that were positive for α-synuclein were not clearly colocalized with SA; however, smaller punctate structures located nearby or independently of GCIs were colocalized with SA (D-I, arrowheads). In the lumbar anterior horn cells of an amyotrophic lateral sclerosis (ALS) spinal cord, skein-like inclusions and round inclusions that were positive for the phosphorylated trans-activation response DNA-protein 43 (pTDP-43) (J and M, respectively), and Bunina bodies positive for cystatin-C (P) were not colocalized with SA (K and L, N and O, Q and R, respectively). The globose-type neurofibrillary tangles accumulated in the substantia nigra neurons of a progressive supranuclear palsy (PSP) brain were colocalized with p-tau and SA (S-U). Pick bodies in neurons from the cornu ammonis 1 area of a frontotemporal lobar degeneration with Pick bodies (PickD) brain were colocalized with p-tau and SA (V-X). Scale bars: 10 μm.

Table 2 Summary of the status of sialylation of the pathological hallmarks of various neurodegenerative diseases

Disease (no. of cases)	AD ($n=6$)			PD ($n=3$)	MSA ($n=5$)	ALS ($n=6$)			PSP ($n=1$)	PickD ($n=1$)	NIID ($n=1$)
Hallmarks	GVD	NFT	SP	Lewy body	GCI	skein-like inclusion	round inclusion	Bunina body	NFT	Pick body	intranuclear inclusion
Marker proteins	pTDP-43 pPERK etc.	p-tau	Aβ (core) p-tau (DNs)	α-synuclein	α-synuclein	pTDP-43	pTDP-43	cystatin-C	p-tau	p-tau	ubiquitin p62
Status of sialylation	+++	+++	Core - DNs +++	++ (partial)	++ (partial)	-		-	+++	+++	-
Regions examined	Neocortex and brainstem			Substantia nigra	Pontine nucleus	Anterior horn cells of lumbar spinal cord			Substantia nigra	Neocortex	Skin

The status of sialylation was scored by semiquantitative evaluation performed at 200× magnification. +++ severe, ++ moderate, + mild, - none; AD, Alzheimer's disease; PD, Parkinson's disease; MSA, multiple system atrophy; ALS, amyotrophic lateral sclerosis; PSP, progressive supranuclear palsy; PickD, frontotemporal lobar degeneration with Pick bodies; NIID, neuronal intranuclear inclusion disease; GVD, granulovacuolar degeneration; NFT, neurofibrillary tangle; SP, senile plaque; GCI, glial cytoplasmic inclusion; pTDP, phosphorylated TAR DNA-binding protein; pPERK, phosphorylated protein kinase-like ER kinase; p-tau, phosphorylated tau; DNs, dystrophic neurites.

not obviously colocalized with SA (Fig. 4D-I). The smaller punctate structures that were independent of typical GCIs were colocalized with α-synuclein and SA; moreover, some of these structures were located in the proximity of GCIs (Fig. 4D-I, arrowheads). Skein-like inclusions (Fig. 4J-L) and round inclusions (Fig. 4M-O), which were both positive for pTDP-43 and Bunina bodies (Fig. 4P-R), which were positive for cystatin-C, were not obviously colocalized with SA in patients with ALS. The globose-type NFTs, which were positive for p-tau in a PSP brain, were colocalized with SA (Fig. 4S-U). Pick bodies, which were positive for p-tau in a PickD brain, were also colocalized with SA (Fig. 4V-X). The association between the above-mentioned characteristic neuropathological hallmarks of various neurodegenerative disorders and the status of sialylation is summarized in Table 2.

DISCUSSION

The present study clearly showed that prominent hypersialylation of NFTs, GVDs and DNs of SPs is a common pathological feature in AD and other tauopathies.[3,4] Hypersialylation of these structures was confirmed in broad areas, including the CA1 area of the hippocampus, the frontal, temporal and occipital lobes, the PAG of the midbrain, the pons and the medulla of AD brains (Fig. 1). Double IF analyses revealed that, in AD and other tauopathies, p-tau was colocalized with SA (Figs 2G-L and 4S-X). In contrast, the amyloid cores of SPs, which are another important hallmark of AD pathology, did not show colocalization of Aβ and SA (Fig. 2A-F). These results indicate that p-tau, but not Aβ was hypersialylated in AD brains. As physiological or nonpathological structures, such as lipofuscin granules, corpora amylacea and melanin granules, and the characteristic pathological hallmarks of other neurodegenerative disorders, such as PD, MSA, ALS and NIID, were not sialylated at a level detected in AD brains (Figs 3 and 4), hypersialylation of NFTs, GVDs and DNs seems to be a highly specific finding of AD pathogenesis. Interestingly, the disease-specific pathological hallmarks of other tauopathies were also hypersialylated. The globose-type NFTs in a PSP brain and the Pick bodies and ballooned neurons in a PickD brain were also clearly hypersialylated at a level comparable to AD brains (Figs 3O-T and 4S-X). As these pathological hallmarks contained p-tau, p-tau present in the tauopathies may also be hypersialylated.[37,38] These findings indicate that hypersialylation of p-tau is involved in the common pathological processes of AD and other tauopathies. Previous studies have shown that nonphosphorylated tau or p-tau in AD brains, but not normal human tau, are attached by various sugars, such as galactose, glucose, mannose, N-acetylglucosamine (GlcNAc) and NeuAc, via N-linked glycosylation.[1,3] In addition, it has been reported that aberrant glycosylation facilitates hyperphosphorylation of tau, resulting in the formation of NFTs.[1,5,39] Therefore, our results might support the association between hypersialylation and promotion of tau phosphorylation, causing subsequent accumulation of NFTs in AD and other tauopathies.[40]

The LB cores detected in PD brains were not stained with the anti-SA antibody (Figs. 3A-F and 4A-C). Previous reports have shown that a subset of LB cores was stained with an anti-tau antibody in PD and dementia with LBs.[41] According to these findings, it is speculated that tau is not hypersialylated in LB cores, and that the mechanism of tau accumulation in LBs is different from that involved in AD and other tauopathies. α-synuclein may be crucial as a nidus or a seed for tau accumulation at the outer edge of LBs.[42]

In PD and MSA brains, hypersialylated small punctate structures were also confirmed adjacent to the LBs or GCIs (Figs 3A-H and 4A-I). In PD brains, similar structures were

previously reported to contain ER stress-responsive proteins or unfolded protein response (UPR) proteins, such as pPERK and peIF2α, which are involved in the aggregation and accumulation of α-synuclein.[43] Similarly, in MSA brains, small structures were found to contain UPR proteins in oligodendroglia, which were activated at an early stage of MSA neurodegeneration.[46] Moreover, the GVDs were also reported to contain UPR proteins, including pPERK, peIF2α and pIRE1α.[34] The smaller hypersialylated structures detected in PD and MSA brains (Figs 3A-H and 4A-I) suggest that the process of sialylation is closely associated with an activation of the UPR response, because glycosylation pathways can influence ER stress.[45,46]

Lectin is a collective term for the protein family that can bind to sugar chains. The *Maackia amurensis* (MAA) lectin was reported to detect PHF-tau on Western blot, and stains NFTs in the AD brain.[4,47] However, it has not been reported that the GVDs could be detected by lectins.[47] These findings suggest that the anti-SA antibody is able to detect the status of sialylation more sensitively than lectin proteins. Actually the anti-SA antibody was reported to recognize more diverse glycoproteins containing SA residues than the MAA lectin. [31]

In summary, we report the novel findings that the NFTs, GVDs and DNs in AD brains and the characteristic structures in other tauopathies, but not other pathological hallmarks in PD, MSA, ALS and NIID, were hypersialylated. These findings suggest that hypersialylation of tau is commonly associated with the pathogenesis of tauopathies. The UPR-associated smaller structures detected in PD and MSA brains were also hypersialylated, indicating a crucial role of sialylation for the activation of the UPR response. Although previously reported anti-tau antibodies can also detect NFTs, immunoreactivity for GVDs was not always observed by these antibodies.[15,18] Because the anti-SA antibody specifically identified NFTs, GVDs and DNs, immunostaining for sialylation may represent a useful tool to screen these structures in a diagnostic setting. Clarification and a better understanding of the mechanism that leads to the hypersialylation and accumulation of tau will help to develop effective therapies for AD and other tauopathies.

ACKNOWLEDGMENTS

We thank Drs Jun-ichi Satoh and Takaharu Fukasawa for technical advices. This study was supported by Grants-in-Aid for Scientific Research (C) (26461304 to TY and 26461264 to MI) from the Ministry of Education, Culture, Sports, Science and Technology, Japan, as well as Grants-in-Aid from the Research Committee for Ataxic Disease (Mizusawa H), the Ministry of Health, Labour and Welfare, Japan (to YI).

CONFLICT OF INTEREST

Nothing to report.

REFERENCES

1. Lee VM, Balin BJ, Otvos L Jr., Trojanowski JQ. A68: a major subunit of paired helical filaments and derivatized forms of normal Tau. *Science* 1991; **251**: 675–78.
2. Alonso AD, Zaidi T, Novak M, Barra HS, Grundke-Iqbal I, Iqbal K. Interaction of tau isoforms with Alzheimer's disease abnormally hyperphosphorylated tau and in vitro phosphorylation into the disease-like protein. *J Biol Chem* 2001; **276**: 37967–73.
3. Wang JZ, Grundke-Iqbal I, Iqbal K. Glycosylation of microtubule-associated protein tau: an abnormal post-translational modification in Alzheimer's disease. *Nat Med* 1996; **2**: 871–75.
4. Liu F, Zaidi T, Iqbal K, Grundke-Iqbal I, Merkle RK, Gong CX. Role of glycosylation in hyperphosphorylation of tau in Alzheimer's disease. *FEBS Lett* 2002; **512**: 101–06.
5. Gong CX, Liu F, Grundke-Iqbal I, Iqbal K. Post-translational modifications of tau protein in Alzheimer's disease. *J Neural Transm* 2005; **112**: 813–38.
6. Liu F, Iqbal K, Grundke-Iqbal I, Gong CX. Involvement of aberrant glycosylation in phosphorylation of tau by cdk5 and GSK-3beta. *FEBS Lett* 2002; **530**: 209–14.
7. Maguire TM, Gillian AM, O'Mahony D, Coughlan CM, Dennihan A, Breen KC. A decrease in serum sialyltransferase levels in Alzheimer's disease. *Neurobiol Aging* 1994; **15**: 99–102.
8. Maguire TM, Breen KC. A decrease in neural sialyltransferase activity in Alzheimer's disease. *Dementia (Basel, Switzerland)* 1995; **6**: 185–90.
9. Fodero LR, Sáez-Valero J, Barquero MS, Marcos A, McLean CA, Small DH. Wheat germ agglutinin-binding glycoproteins are decreased in Alzheimer's disease cerebrospinal fluid. *J Neurochem* 2001; **79**: 1022–26.
10. Davis G, Baboolal N, Nayak S, McRae A. Sialic acid, homocysteine and CRP: potential markers for dementia. *Neurosci Lett* 2009; **465**: 282–84.
11. Kitazume S, Nakagawa K, Oka R *et al.* In vivo cleavage of alpha2,6-sialyltransferase by Alzheimer beta-secretase. *J Biol Chem* 2005; **280**: 8589–95.
12. Rosenthal SL, Kamboh MI. Late-Onset Alzheimer's Disease Genes and the Potentially Implicated Pathways. *Curr Genet Med Rep* 2014; **2**: 85–101.
13. Hollingworth P, Harold D, Sims R *et al.* Common variants at ABCA7, MS4A6A/MS4A4E, EPHA1, CD33 and CD2AP are associated with Alzheimer's disease. *Nat Genet* 2011; **43**: 429–35.

14. Thal DR, Del Tredici K, Ludolph AC *et al.* Stages of granulovacuolar degeneration: their relation to Alzheimer's disease and chronic stress response. *Acta Neuropathol* 2011; **122**: 577–89.
15. Dickson DW, Ksiezak-Reding H, Davies P, Yen SH. A monoclonal antibody that recognizes a phosphorylated epitope in Alzheimer neurofibrillary tangles, neurofilaments and tau proteins immunostains granulovacuolar degeneration. *Acta Neuropathol* 1987; **73**: 254–58.
16. Morris JC, Heyman A, Mohs RC *et al.* The Consortium to Establish a Registry for Alzheimer's Disease (CERAD). Part I. Clinical and neuropsychological assessment of Alzheimer's disease. *Neurology* 1989; **39**: 1159–65.
17. Braak H, Braak E. Neuropathological stageing of Alzheimer-related changes. *Acta Neuropathol* 1991; **82**: 239–59.
18. Mirra SS, Heyman A, McKeel D *et al.* The Consortium to Establish a Registry for Alzheimer's Disease (CERAD). Part II. Standardization of the neuropathologic assessment of Alzheimer's disease. *Neurology* 1991; **41**: 479–86.
19. Hyman BT, Phelps CH, Beach TG *et al.* National Institute on Aging-Alzheimer's Association guidelines for the neuropathologic assessment of Alzheimer's disease. *Alzheimers Dement* 2012; **8**: 1–13.
20. Hughes AJ, Daniel SE, Kilford L, Lees AJ. Accuracy of clinical diagnosis of idiopathic Parkinson's disease: a clinico-pathological study of 100 cases. *J Neurol Neurosurg Psychiatry* 1992; **55**: 181–84.
21. Gelb DJ, Oliver E, Gilman S, Gelb DJ, Oliver E, Gilman S. Diagnostic Criteria for Parkinson Disease. *Arch Neurol* 1999; **56**: 33.
22. Gilman S, Wenning GK, Low PA *et al.* Second consensus statement on the diagnosis of multiple system atrophy. *Neurology* 2008; **71**: 670–76.
23. Brooks BR, Miller RG, Swash M, Munsat TL, World Federation of Neurology Research Group on Motor Neuron D. El Escorial revisited: revised criteria for the diagnosis of amyotrophic lateral sclerosis. *Amyotroph Lateral Scler Other Motor Neuron Disord* 2000; **1**: 293–99.
24. Hauw JJ, Daniel SE, Dickson D *et al.* Preliminary NINDS neuropathologic criteria for Steele-Richardson-Olszewski syndrome (progressive supranuclear palsy). *Neurology* 1994; **44**: 2015–19.
25. Cairns NJ, Bigio EH, Mackenzie IR *et al.* Neuropathologic diagnostic and nosologic criteria for frontotemporal lobar degeneration: consensus of the Consortium for Frontotemporal Lobar Degeneration. *Acta Neuropathol* 2007; **114**: 5–22.
26. Lindenberg R, Rubinstein LJ, Herman MM, Haydon GB. A light and electron microscopy study of an unusual widespread nuclear inclusion body disease. A possible residuum of an old herpesvirus infection. *Acta Neuropathol* 1968; **10**: 54–73.
27. Takahashi-Fujigasaki J. Neuronal intranuclear hyaline inclusion disease. *Neuropathology* 2003; **23**: 351–59.
28. Fujita Y, Ohama E, Takatama M, Al-Sarraj S, Okamoto K. Fragmentation of Golgi apparatus of nigral neurons with alpha-synuclein-positive inclusions in patients with Parkinson's disease. *Acta Neuropathol* 2006; **112**: 261–65.
29. Wakabayashi K, Hayashi S, Yoshimoto M, Kudo H, Takahashi H. NACP/alpha-synuclein-positive filamentous inclusions in astrocytes and oligodendrocytes of Parkinson's disease brains. *Acta Neuropathol* 2000; **99**: 14–20.
30. Kadokura A, Yamazaki T, Kakuda S *et al.* Phosphorylation-dependent TDP-43 antibody detects intraneuronal dot-like structures showing morphological characters of granulovacuolar degeneration. *Neurosci Lett* 2009; **463**: 87–92.
31. Hidari KI, Yamaguchi M, Ueno F, Abe T, Yoshida K, Suzuki T. Influenza virus utilizes N-linked sialoglycans as receptors in A549 cells. *Biochem Biophys Res Commun* 2013; **436**: 391–99.
32. Ozawa H, Kotani M, Kawashima I, Tai T. Generation of one set of monoclonal antibodies specific for b-pathway ganglio-series gangliosides. *Biochim Biophys Acta* 1992; **1123**: 184–90.
33. Lowe JMS, Hyman BT, Dickson DW. Ageing and dementia. In: Love S, Louis DN, Ellison DW, eds. Greenfield's Neuropathology, vol. 1, 8th edn. London: Edward Arnold Publishers, 2008; 1031–152.
34. Hoozemans JJ, van Haastert ES, Nijholt DA, Rozemuller AJ, Eikelenboom P, Scheper W. The unfolded protein response is activated in pretangle neurons in Alzheimer's disease hippocampus. *Am J Pathol* 2009; **174**: 1241–51.
35. Dunn WA Jr. Studies on the mechanisms of autophagy: maturation of the autophagic vacuole. *J Cell Biol* 1990; **110**: 1935–45.
36. Eskelinen EL, Eskelinen E-L. Rules of LAMP-1 and LAMP-2 in lysosome biogenesis and autophagy. *Mol Aspects Med* 2006; **27**: 495.
37. Murayama S, Mori H, Ihara Y, Tomonaga M. Immunocytochemical and ultrastructural studies of Pick's disease. *Ann Neurol* 1990; **27**: 394–405.
38. Schwab C, DeMaggio AJ, Ghoshal N, Binder LI, Kuret J, McGeer PL. Casein kinase 1 delta is associated with pathological accumulation of tau in several neurodegenerative diseases. *Neurobiol Aging* 2000; **21**: 503–10.
39. Schneider A, Mandelkow E. Tau-based treatment strategies in neurodegenerative diseases. *Neurotherapeutics* 2008; **5**: 443–57.

40. Lagalwar S, Berry RW, Binder LI. Relation of hippocampal phospho-SAPK/JNK granules in Alzheimer's disease and tauopathies to granulovacuolar degeneration bodies. *Acta Neuropathol* 2007; **113**: 63–73.
41. Arima K, Hirai S, Sunohara N *et al.* Cellular colocalization of phosphorylated tau- and NACP/alpha-synuclein-epitopes in lewy bodies in sporadic Parkinson's disease and in dementia with Lewy bodies. *Brain Res* 1999; **843**: 53–61.
42. Ishizawa T, Mattila P, Davies P, Wang D, Dickson DW. Colocalization of tau and alpha-synuclein epitopes in Lewy bodies. *J Neuropathol Exp Neurol* 2003; **62**: 389–97.
43. Hoozemans JJ, van Haastert ES, Eikelenboom P, de Vos RA, Rozemuller JM, Scheper W. Activation of the unfolded protein response in Parkinson's disease. *Biochem Biophys Res Commun* 2007; **354**: 707–11.
44. Makioka K, Yamazaki T, Fujita Y, Takatama M, Nakazato Y, Okamoto K. Involvement of endoplasmic reticulum stress defined by activated unfolded protein response in multiple system atrophy. *J Neurol Sci* 2010; **297**: 60–65.
45. Ruddock LW, Molinari M. N-glycan processing in ER quality control. *J Cell Sci* 2006; **119**: 4373–80.
46. Xi H, Kurtoglu M, Liu H *et al.* 2-Deoxy-D-glucose activates autophagy via endoplasmic reticulum stress rather than ATP depletion. *Cancer Chemother Pharmacol* 2011; **67**: 899–910.
47. Guevara J, Espinosa B, Zenteno E *et al.* Altered glycosylation pattern of proteins in Alzheimer disease. *J Neuropathol Exp Neurol* 1998; **57**: 905–14.
48. Joachim CL, Morris JH, Selkoe DJ, Kosik KS. Tau epitopes are incorporated into a range of lesions in Alzheimer's disease. *J Neuropathol Exp Neurol* 1987; **46**: 611–22.

INTERNAL MEDICINE

□ CASE REPORT □

Anti-MuSK Antibody-positive Myasthenia Gravis Mimicking Amyotrophic Lateral Sclerosis

Natsumi Furuta[1], Kunihiko Ishizawa[1], Makoto Shibata[2], Setsuki Tsukagoshi[1], Shun Nagamine[1], Kouki Makioka[1], Yukio Fujita[1], Masaki Ikeda[1], Shunsuke Yoshimura[3], Masakatsu Motomura[2,3], Koichi Okamoto[4] and Yoshio Ikeda[1]

Abstract

We herein investigated the clinical features of three patients with anti-muscle-specific tyrosine kinase (MuSK) antibody-positive myasthenia gravis (MG), which was initially difficult to distinguish from amyotrophic lateral sclerosis (ALS). The patients exhibited dropped head syndrome or dysphagia as initial symptoms. Although their clinical findings were compatible with the revised El Escorial Criteria for ALS, their progression appeared to be more rapid than that of ALS. Both the edrophonium and repetitive nerve stimulation tests yielded negative results, and diurnal fluctuation was not confirmed. The patients were ultimately diagnosed with anti-MuSK antibody-positive MG. We therefore recommend the measurement of anti-MuSK antibodies when encountering such cases.

Key words: muscle-specific tyrosine kinase (MuSK), anti-MuSK antibody, amyotrophic lateral sclerosis (ALS), myasthenia gravis (MG), plasmapheresis

(Intern Med 54: 2497-2501, 2015)
(DOI: 10.2169/internalmedicine.54.4645)

24

Introduction

Amyotrophic lateral sclerosis (ALS) is characterized by signs and symptoms caused by the degeneration of the upper and lower motor neurons, which leads to the progressive weakness of the bulbar, limb, thoracic, and abdominal muscles (1, 2). Almost half of all ALS patients will die within 3 years of symptom onset, primarily because of respiratory failure (3, 4). A misdiagnosis of ALS, instead of other neurological disorders which can be treated, should be avoided.

Approximately 5-8% of the total number of patients with myasthenia gravis (MG) has antibodies against the muscle-specific tyrosine kinase (MuSK) receptor (5). The patients with anti-MuSK antibody-positive myasthenia gravis (MuSK-MG) exhibit a distinct clinical phenotype and may differ from "typical" MG associated with antibodies against the acetylcholine receptor (AChR) (5, 6). The diagnosis of MuSK-MG is often challenging because of its atypical presentation, with little or no diurnal fluctuation of the myasthenic symptoms, poor response to the edrophonium test, and negative results in the electrodiagnostic studies, including repetitive nerve stimulation (RNS). Bulbar weakness or dropped head syndrome, which is commonly found in both the patients with MuSK-MG and motor neuron disease (MND), may hamper the differential diagnosis of this condition (6).

We herein report three cases ultimately diagnosed as MuSK-MG and whose clinical findings were compatible with the revised El Escorial Criteria for ALS (7).

Case Reports

Case 1

A 73-year-old Japanese woman presented with dropped

[1]Department of Neurology, Gunma University Graduate School of Medicine, Japan, [2]Department of Neurology and Strokology, Nagasaki University Hospital, Japan, [3]Medical Engineering Course, Nagasaki Institute of Applied Science, Japan and [4]Department of Neurology, Geriatrics Research Institute, Japan

Received for publication December 3, 2014; Accepted for publication February 11, 2015

Correspondence to Dr. Yoshio Ikeda, ikeday006@gunma-u.ac.jp

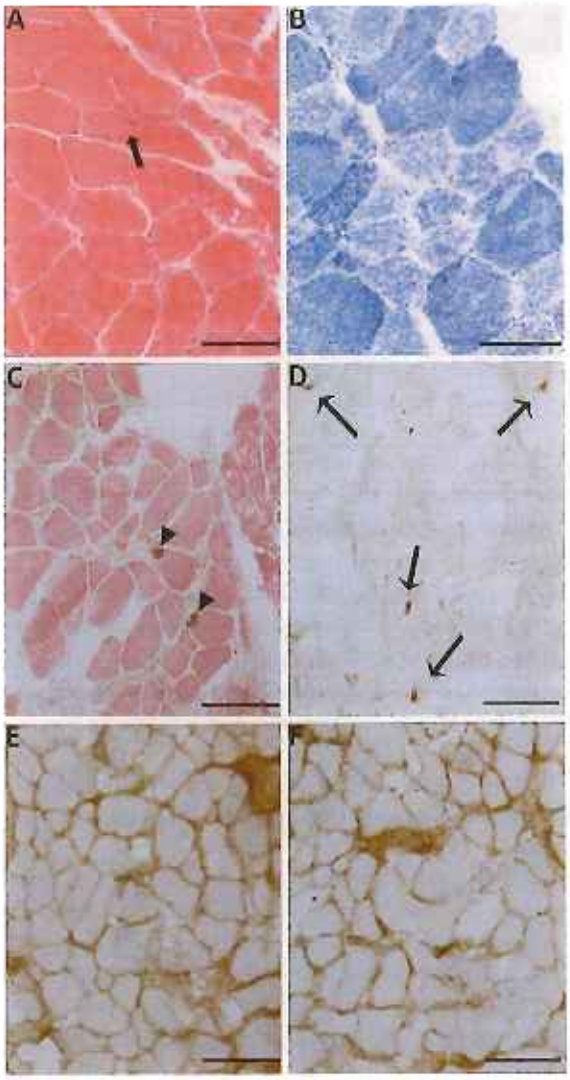

Figure. A histological analysis of a muscle biopsy specimen from case 1. (A) Hematoxylin and Eosin staining showed mild variability of the fiber diameter and infrequent small angulated fibers (arrow). (B) Nicotinamide adenine dinucleotide tetrazolium reductase staining showed a mosaic distribution of types 1 and 2 muscle fibers and no fiber-type grouping. (C) Cholinesterase staining using thiocholine revealed an almost normal distribution and amount of motor end-plates (arrowheads). (D) Acetylcholine receptor (AChR) staining using peroxidase-labeled alpha-bungarotoxin revealed that the AChR density was not visibly decreased (arrows). (E) Complement component 3 (C3) staining using peroxidase-labeled anti-C3 antibodies and (F) immunoglobulin G (IgG) staining using peroxidase-labeled Protein A showed no immune complex depositions (C3 and IgG) at the motor end-plates. Bar, 100 μm.

head syndrome in March 2005. Two months later, she was admitted to our hospital because of the progressive weakness of neck extensor muscles, dysarthria, and dysphagia. She had a history of cervical spondylosis, hypertension, and hypercholesterolemia. A neurological examination disclosed weakness in the neck extensor, orbicularis oculi, orbicularis oris, and deltoid muscles, with grade 4 manual muscle testing (MMT). Fasciculations were observed in the facial, bilateral biceps brachii, triceps brachii, and quadriceps femoris muscles. There was no evidence of muscle atrophy. Her tendon reflexes were all normal. The Babinski reflex was present bilaterally. Her neurological findings were compatible with the revised El Escorial Criteria for possible ALS (7), although her pyramidal tract signs could have resulted from cervical spondylosis. She did not report a diurnal fluctuation of the motor symptoms. The edrophonium test did not improve her muscle weakness, and RNS at 3 Hz in the right abductor digiti minimi and trapezius muscles did not show decremental responses. The results of the nerve conduction studies (NCS) performed at the bilateral median, ulnar, tibial, peroneal, and sural nerves were all normal. Needle electromyography (EMG) disclosed fasciculation potentials at rest in the bilateral biceps brachii, first dorsal interossei, and quadriceps femoris muscles. Her anti-AChR antibody titer was within the normal range. Chest computed tomography (CT) revealed a normal appearance of the anterior mediastinum, without either any obvious thymoma or thymic hyperplasia.

Seven months later, she developed diplopia, bilateral blepharoptosis, and dyspnea. Repeated RNS at 3 Hz revealed a 10% decrement in the left trapezius muscles. The anti-MuSK antibody titer, as evaluated by a radioimmunoassay, showed a pathological elevation to 10.53 nmol/L (normal level, <0.05 nmol/L). Her forced vital capacity (FVC) was 28.6%, and her quantitative myasthenia gravis (QMG) score was 19. A muscle biopsy was performed at the left biceps brachii muscles. Hematoxylin and Eosin staining showed a mild variability of the fiber diameter and infrequent small angulated fibers (Figure A). Nicotinamide adenine dinucleotide tetrazolium reductase staining showed mosaic distribution of types 1 and 2 muscle fibers and no fiber-type grouping (Figure B). Cholinesterase staining using thiocholine revealed an almost normal distribution and amount of end-plates (Figure C), and AChR staining using peroxidase-labeled alpha-bungarotoxin (Figure D) showed that the AChR density was not obviously decreased. Complement component 3 (C3) staining using peroxidase-labeled anti-C3 antibodies (Figure E) and immunoglobulin G (IgG) staining using peroxidase-labeled Protein A (Figure F) revealed an absence of immune complex depositions (C3 and IgG) at the motor end-plates. These findings were consistent with the histopathological characteristics of MuSK-MG (8, 9). According to the abovementioned findings, a diagnosis of MuSK-MG was established.

The patient was treated with oral prednisolone, which was increased up to 25 mg daily for 4 weeks, and thereafter was tapered to 22.5 mg daily. She also received seven courses of double filtration plasmapheresis. The patient showed a remarkable improvement after treatment, with an FVC of 74.7% and a QMG score of 5.

Nine years after the onset of the disease, the patient

showed no exacerbation of the symptoms with a maintenance therapy of prednisolone (8 mg daily) and tacrolimus hydrate (2 mg daily).

Case 2

A 62-year-old Japanese woman presented with dysphagia in January 2013. She had no remarkable medical history. Six months later, she was admitted to our hospital due to the development of dysphagia, dysarthria, and dyspnea. She had rapidly lost weight over the previous year (6 kg in 1 year). A neurological examination disclosed weakness in the orbicularis oculi and oris muscles, with grade 4 MMT. There was no evidence of limb weakness. Her tendon reflexes were generally hyperactive, and her jaw reflex was brisk. Muscle atrophy and fasciculations were not observed. The Babinski reflex was absent. Her neurological findings were compatible with the revised El Escorial Criteria for possible ALS (7). She did not report a diurnal fluctuation of the motor symptoms. The edrophonium test and RNS in the right abductor digiti minimi showed negative results. The NCS and EMG findings were normal. Her anti-AChR antibody titer was within the normal range. Furthermore, no thymic abnormalities on chest CT were observed. Although her FVC was normal (102.5%), an arterial blood gas (ABG) analysis on room air showed hypoxemia [partial pressure of oxygen (PaO_2), 63.9 mmHg] and hypercapnia [partial pressure of carbon dioxide ($PaCO_2$), 51.2 mmHg]. Her QMG score was 5. The anti-MuSK antibody titer elevated to 23.0 nmol/L (normal, <0.01 nmol/L). According to these findings, the patient was diagnosed with MuSK-MG.

The patient was treated with oral prednisolone, which was increased up to 20 mg daily for 4 weeks, and thereafter was tapered to 17.5 mg daily. She also received three courses of simple plasma exchange. An ABG analysis on room air revealed an improvement, with a PaO_2 of 88.9 mmHg and a $PaCO_2$ of 47.5 mmHg. The patient also exhibited an improved QMG score of 3.

One year after the onset of the disease, the patient showed no exacerbation of the symptoms with a maintenance therapy of prednisolone (15 mg daily).

Case 3

A 63-year-old Japanese woman presented with dropped head syndrome in April 2013. She had medical histories of autoimmune hepatitis, hypertension, and hypercholesterolemia. Two months later, she was admitted to our hospital with complaints of weakness of the neck extensor muscles, dysphagia, dysarthria, and dyspnea. She had rapidly lost weight over the previous year (10 kg in 1 year). A neurological examination disclosed bilateral blepharoptosis, weakness of the orbicularis oculi and deltoid muscles with grade 4 MMT, atrophy of the tongue, and hyperactive tendon reflexes in the upper extremities. There was no evidence of any muscle atrophy in the limbs. Fasciculations were observed in the left first dorsal interossei muscle. The Babinski reflex was absent. Her neurological findings were compatible with the revised El Escorial Criteria for possible ALS (7). She did not report a diurnal fluctuation of the motor symptoms. The edrophonium test and RNS in the right abductor digiti minimi and thenar muscles showed negative results. The NCS findings were normal. The EMG showed fasciculation potentials at rest in the left first dorsal interossei muscle. Her anti-AChR antibody titer was within the normal range. There was no thymic abnormality on chest CT. Her FVC was 55.6%, and her QMG score was 13. The anti-MuSK antibody titer elevated to 18.0 nmol/L (normal, <0.01 nmol/L). According to these findings, the patient was diagnosed with MuSK-MG.

The patient was treated with oral prednisolone, which was increased up to 25 mg daily for 4 weeks, and then tapered to 22.5 mg daily. She also received three courses of simple plasma exchange. The patient showed a remarkable improvement after therapy, with an FVC of 63.6% and a QMG score of 6.

One year after the onset of the disease, the patient showed no exacerbation of the symptoms with a maintenance therapy of prednisolone (15 mg daily).

Discussion

In this report, we described three cases of MuSK-MG that were difficult to distinguish clinically from bulbar-onset ALS.

All three patients were female and exhibited an onset of weakness at over 60 years of age. Their neurological findings were all compatible with the revised El Escorial Criteria for possible ALS; however, the progression of their disease appeared to be more rapid than that of ALS. Although all three patients had weakness in the eyelid closure, facial weakness is not classically considered to be a characteristic early symptom of ALS; rather, it is a more common feature of MG (10). Cases 2 and 3 had substantial weight loss, which was potentially caused by dysphagia associated with the disease.

The mild neurogenic changes observed on a muscle biopsy in case 1 may have been caused by her complication of cervical spondylosis or by MuSK-MG itself. The lack of a diurnal fluctuation of the myasthenic symptoms, a positive response to the edrophonium test, and decremental responses of RNS observed in the three cases made it difficult to prioritize MuSK-MG as the most probable candidate diagnosis. A combination therapy of plasmapheresis and high-dose prednisolone was effective in all three cases (Table).

In a previous report, decremental responses of RNS in the orbicularis oculi muscles were more useful than those in the limb muscles of MuSK-MG patients (11). However, decremental responses of RNS can also occur in the denervated muscles of ALS patients (12); therefore, anti-MuSK antibodies must be evaluated for the establishment of an accurate diagnosis.

There appear to be three distinct clinical phenotypes of MuSK-MG: (i) a form with generalized muscle weakness;

Table. Clinical Summary of Three Patients with Anti-MuSK Antibody-positive MG Mimicking ALS.

	Case 1	Case 2	Case 3
Age at onset	73	62	63
Sex	female	female	female
Initial symptom	dropped head	dysphagia	dropped head
Fasciculation	positive	none	positive
Onset-to-admission time (months)	2	6	2
Revised El Escorial Criteria for ALS	possible	possible	possible
Daily fluctuation	negative	negative	negative
Edrophonium test	negative	negative	negative
Repetitive nerve stimulation	decrement	normal	normal
Anti-MuSK antibody level (nmol/L)	10.53 (<0.05)	23.0 (<0.01)	18.0 (<0.01)
Apheresis therapy	DFPP	PE	PE
Initial prednisolone (mg/day)	25	20	25
Improvement of the QMG score	19→5	5→3	13→6
Complication	cervical spondylosis	none	autoimmune hepatitis

MuSK: muscle-specific tyrosine kinase, MG: myasthenia gravis, ALS: amyotrophic lateral sclerosis, DFPP: double filtration plasmapheresis, PE: plasma exchange, QMG: quantitative myasthenia gravis

(ii) a more focal form with neck, shoulder, and respiratory muscle weakness; and (iii) a severe form with prevalent bulbar weakness and frequent respiratory crises (13). It is likely that patient-specific differences regarding the susceptibility of the muscles (e.g., the extent of MuSK expression) are one of the explanations of the phenotypic variability observed in this disease (13). The present cases seem to correspond to type (ii) MuSK-MG, whereas bulbar weakness and dropped head syndrome are reminiscent of bulbar-onset ALS.

The MuSK protein, which is located at the postsynaptic membrane, anchors the C-terminal portion of collagen Q (ColQ), which binds acetylcholinesterase (AChE) at the N terminal (14, 15). AChE stabilization depends on its binding to ColQ (16). The anti-MuSK antibodies interfere with the MuSK-ColQ binding and reduce the AChE activity at the neuromuscular junction, resulting in an increased synaptic acetylcholine concentration (15). As a result, the MuSK antibodies may produce peripheral nerve hyperexcitability, which can cause muscular fasciculation activities (17). In cases 1 and 3 reported in the present study, fasciculations were constantly confirmed in the widespread areas. The generalized presence of fasciculations in these MuSK-MG patients further raised the possibility of a diagnosis of ALS.

As uncharacteristic clinical findings may be associated with negative results in the pharmacological and electrodiagnostic testing, the diagnosis of MuSK-MG may be overlooked or considerably delayed (6). The present cases suggest that MuSK-MG patients can be misdiagnosed as having a bulbar- or proximal-onset type of ALS. Thus, the evaluation of MuSK antibodies plays an important role in the establishment of an accurate and rapid diagnosis, as well as in the decision of a therapeutic strategy.

The authors state that they have no Conflict of Interest (COI).

Financial Support

This study was supported in part by Grants-in-Aid for Scientific Research (C) 24591263 (to Y.I.) from the Ministry of Education, Culture, Sports, Science and Technology, Japan.

Acknowledgement

We thank Kiyoe Ohta (Clinical Research Center, Utano National Hospital) for measuring the anti-MuSK antibodies.

References

1. Eisen A. Amyotrophic lateral sclerosis. Intern Med **34**: 824-832, 1995.
2. Andersen PM, Abrahams S, Borasio GD, et al. EFNS guidelines on the clinical management of amyotrophic lateral sclerosis (MALS)-revised report of an EFNS task force. Eur J Neurol **19**: 360-375, 2012.
3. Ringel SP, Murphy JR, Alderson MK, et al. The natural history of amyotrophic lateral sclerosis. Neurology **43**: 1316-1322, 1993.
4. Czaplinski A, Yen AA, Appel SH. Amyotrophic lateral sclerosis: early predictors of prolonged survival. J Neurol **253**: 1428-1436, 2006.
5. El-Salem K, Yassin A, Al-Hayk K, Yahya S, Al-Shnrafat D, Dahbour SS. Diagnosis and therapy of myasthenia gravis with antibodies to muscle-specific kinase. Curr Treat Options Neurol **16**: 283, 2014.
6. Evoli A, Padua L. Diagnosis and therapy of myasthenia gravis with antibodies to muscle-specific kinase. Autoimmun Rev **12**: 931-935, 2013.
7. Brooks BR, Miller RG, Swash M, Munsat TL. El Escorial revisited: revised criteria for the diagnosis of amyotrophic lateral sclerosis. Amyotroph Lateral Scler Other Motor Neuron Disord **1**: 293-299, 2000.
8. Martignago S, Fania M, Albertini E, Pegoraro E, Angelini C. Muscle histopathology in myasthenia gravis with antibodies against MuSK and AChR. Neuropathol Appl Neurobiol **35**: 103-110, 2009.
9. Shiraishi H, Motomura M, Yoshimura T, et al. Acetylcholine receptors loss and postsynaptic damage in MuSK antibody-positive myasthenia gravis. Ann Neurol **57**: 289-293, 2005.

10. Rowin J. Approach to the patient with suspected myasthenia gravis or ALS: a clinician's guide. Continuum Lifelong Learning Neurol 15: 13-34, 2009.
11. Oh SJ, Hatanaka Y, Hemmi S, et al. Repetitive nerve stimulation of facial muscles in MuSK antibody-positive myasthenia gravis. Muscle Nerve 33: 500-504, 2006.
12. Henderson RD, Daube JR. Decrement in surface-recorded motor unit potentials in amyotrophic lateral sclerosis. Neurology 63: 1670-1674, 2004.
13. Koneczny I, Cossins J, Vincent A. The role of muscle-specific tyrosine kinase (MuSK) and mystery of MuSK myasthenia gravis. J Anat 224: 29-35, 2014.
14. Evoli A, Lindstrom J. Myasthenia gravis with antibodies to MuSK: another step toward solving mystery? Neurology 77: 1783-1784, 2011.
15. Kawakami Y, Ito M, Hirayama M, et al. Anti-MuSK autoantibodies block binding of collagen Q to MuSK. Neurology 77: 1819-1826, 2011.
16. Cartaud A, Strochlic L, Guerra M, et al. MuSK is required for anchoring acetylcholinesterase at the neuromuscular junction. J Cell Biol 165: 505-515, 2004.
17. Simon NG, Reddel SW, Kiernan MC, Layzer R. Muscle-specific kinase antibodies: a novel cause of peripheral nerve hyperexcitability? Muscle Nerve 48: 819-823, 2013.

28

Journal of the Neurological Sciences 358 (2015) 512–514

Contents lists available at ScienceDirect

Journal of the Neurological Sciences

journal homepage: www.elsevier.com/locate/jns

Letter to the Editor

Ectopic germinoma involving multiple midline and paramedian structures outside the pineal gland or hypophyseal region of the brain prior to tumor development

Keywords:
Germinoma
Internal capsule
Medulla oblongata
Corpus callosum
Neuromyelitis optica
Hypersomnia

Dear Editor

A previously healthy 29-year-old Japanese male presented with a two-month history of hypersomnia, which had gradually developed and deteriorated and he could not continue his job as a system engineer. On admission, no other neurological deficits were observed. There were no symptoms indicative of diabetes insipidus, such as polyuria/nocturia or polydipsia. Brain MRI showed multiple T1-iso- or -hypo-intensities, and T2-hyperintensity lesions without contrast enhancement in the dorsal medulla (Fig. 1A), genu of the right internal capsule (Fig. 1B), and corpus callosum (Fig. 1C), and no tumors including the pineal gland (Fig. 1E). CSF analysis showed normal results for the cytology, as well as protein and orexin concentrations, while the IgG index was elevated to 0.91 and oligoclonal IgG bands were positive. Anti-nuclear, anti-SS-A, and anti-SS-B antibodies in the serum were negative, and whole spinal MRI showed no abnormality. There was no evidence of viral infection, sarcoidosis, malignant lymphoma, anti-phospholipid antibody syndrome, or Beçhet disease. Full overnight polysomnography revealed central sleep apnea episodes. Hypersomnia as a presenting symptom and the lesion distributions in the brain appeared similar to those reported in neuromyelitis optica (NMO) [1]; however, serum NMO-IgG was negative. He was tentatively considered to have inflammatory brain disease (IBD), especially primary progressive multiple sclerosis, and subjected to high-dose steroid therapy (methylprednisolone 1 g × 3), but with no clinical improvement. Brain MRI after two cycles of the therapy revealed a new lesion in the left cerebellar white matter adjacent to the fourth ventricle (Fig. 1D), and nystagmus and orthostatic hypotension developed. Then, he received 5 courses of plasma exchange; however, dysphagia and intractable hiccups developed. A third round of high-dose steroid therapy was performed with amelioration of the intractable hiccups, while the other symptoms persisted. After commencing oral prednisolone (PSL)(60 mg, daily), no additional symptoms were observed. Eight months after the onset, while taking 15 mg of PSL a day, a pineal tumor (Fig. 1G) was found incidentally on the follow-up brain MRI, and lesions of the dorsal medulla appeared enlarged with contrast enhancement (Fig. 1H). Human chorionic gonadotropin-β subunit (β-hCG) was measurable in both the serum (9.9 ng/mL) and CSF (0.6 ng/mL), and serum alpha-fetoprotein (AFP) levels were normal. Cryopreserved serum samples obtained on admission and two months after admission revealed unmeasurable β-hCG (<0.1 ng/mL) (Fig. 1E, F). Ultrasonography of the testis and whole-body FDG-PET/CT showed no abnormality. Histologic examination of the tumor yielded a diagnosis of germinoma with lymphocytic and plasmacytic infiltrations (Fig. 1I). Although there was no evidence of spinal dissemination, the patient underwent an irradiation of the craniospinal axis (40 Gy to the whole brain, 30 Gy to the whole spine), based on the observation by a radiologist in our hospital that he had Gd-enhancing lesions in the dorsal medulla, close to the spinal cord. After radiotherapy, the pineal tumor disappeared, while the non-enhanced lesions remained with T1-hypo and T2-hyperintensities. A clinical follow-up 4 years later revealed no additional symptoms.

Extragonadal germ cell tumors have been documented to arise in midline locations, most commonly in the anterior mediastinum, retroperitoneum, and the pineal gland or suprasellar regions of the brain [2]. Intracranial germinomas (IGs) comprise 1.3% of all primary intracranial brain tumors in adolescents and young adults, and, among them, only 5–10% develop in other brain regions, which are known as ectopic germinomas (EGs) [3]. IGs may result from the mismigration of embryonic cells into the neural plate area and so the midline of the embryonic disk has been reported to be a site of germ cell tumor origin [4]. Therefore, these tumors may originate from any midline or paramedian structure of the brain. EGs in the basal ganglia or thalamus are the most common [3], but so far, there have been only a few EGs reported in the corpus callosum [5], medulla oblongata [6], and cerebellum [7], all of which showed no other lesion locations simultaneously. Accordingly, our patient is unique in terms of the multiplicity of lesions along with midline and paramedian structures in the brain outside the pineal or hypophysial area, suggesting a novel clinicophenotype of EGs.

The initial presentation of our case was highly suggestive of IBD, especially multiple sclerosis (MS); however, a pineal tumor eventually developed. IGs mimicking IBD were previously reported in only two cases, one mimicking chronic progressive MS [8], and the other, optic neuritis [9]. The patient mimicking MS [8] showed slow progressive numbness of the right extremities; however, craniospinal MRI had shown no pathology for three years until a pineal tumor developed. This observation is in contrast to that of our patient, who had already developed multiple intracranial lesions before a pineal tumor appeared. Thus, the clinical profiles of IGs mimicking IBD may vary, and the further studies are required to delineat such atypical cases. The pathophysiology of IGs masquerading as IBD remains unclear, but one hypothesis is that the leptomeningeal dissemination of germinoma cells precedes

http://dx.doi.org/10.1016/j.jns.2015.09.369
0022-510X/

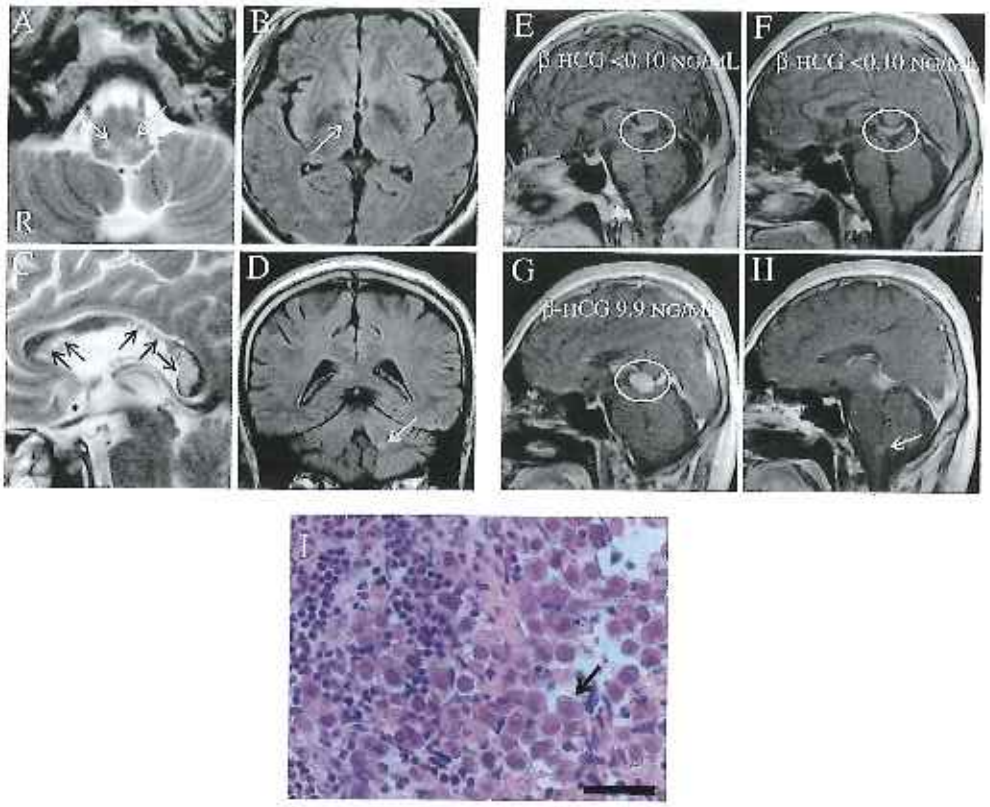

Fig. 1. Multiple hyperintensity lesions are present in the dorsal portion of the medulla (A, white arrows, axial view), genu of the right internal capsule (B, white arrow, axial view), and corpus callosum (C, black arrows, sagittal view) on magnetic resonance images (MRI) (A, C: T2-weighted images, TR, 4400 ms; TE, 79.5 ms. B: FLAIR image, TR, 9202 ms; TE, 107 ms). Later, a hyperintensity lesion developed in the left cerebellar white matter adjacent to the fourth ventricle (D, white arrow, coronal view of FLAIR image). E–H indicate longitudinal changes of MRI (sagittal views of gadolinium-enhanced T1-weighted images, TR, 730.3 ms; TE, 10.0 ms) and human chorionic gonadotropin-β subunit (β-hCG). E: On admission. F: Two months after admission. G, H: Eight months after admission when a pineal tumor was found incidentally, and a gadolinium-enhanced lesion was seen in the dorsal medulla (H, white arrow). Beta-hCG was unmeasurable in the patient's serum until a pineal tumor became evident (compare G with E and F). Each white circle in E–G depicts a pineal region. The panel I shows a histological appearance of germinoma. The tumor cells have a large nucleus, prominent nucleoli, and clear cytoplasm (bold black arrow) accompanied by mononuclear cell infiltrations (two cell pattern). Immunohistochemical staining (not shown) revealed that the tumor cells were positive for c-kit, oct-4, and D2-40, partially positive for placental alkaline phosphatase, and negative for human chorionic gonadotropin, S-100, and glial fibrillary acidic protein. Most of the infiltrating mononuclear cells were positive for CD3 (T cell), and few were CD20 (B cell)- and CD138 (plasma cell)-positive. Hematoxylin and eosin staining. R: right. Bar = 20 μm.

tumor development, and that non-specific inflammatory reactions in tumor tissues may generate intrathecal IgG [8]. To better distinguish such atypical IGs from IBD, Tao et al. reported the role of MRI and tumor markers in the CSF, and found that an increased level of β-hCG in the CSF preceded MRI abnormalities [10]. Indeed, regarding the serum, our patient showed no β-hCG elevation until a pineal tumor became recognizable on brain MRI (Fig. 1). Van Battum et al. [2] postulated that in the case of multiple intracranial midline tumors with normal or slightly elevated values of β-hCG and normal values of AFP in both the serum and CSF, the only possible diagnosis is a germinoma, and, in such a situation, no histological confirmation was required to start low-dose radiotherapy. Since germinomas are curable in the majority of cases when treated early, these observations should be examined further.

In conclusion, we report a case that highlights the importance of considering IGs when patients show multiple midline or paramedian lesion localizations outside the pineal or hypophysial area, and the outcome does not agree with the classical clinical presentation of IBD.

Conflict of interest

All authors declare that this case report involves no conflicts of interest.

Acknowledgments

This work was partially supported by a Grant-in-Aid for Scientific Research (C) (No. 25461317) from the Ministry of Education, Science, Sports, Culture and Technology of Japan to S. Hayashi.

References

[1] D.M. Wingerchuk, B. Banwell, J.L. Bennett, et al., International consensus diagnostic criteria for neuromyelitis optica spectrum disorders, Neurology 85 (2015) 1–13.
[2] P. Van Battum, M.S.P. Huijberts, A.C. Heijckmann, et al., Intracranial multiple midline germinomas: is histological verification crucial for therapy? Neth. J. Med. 65 (2007) 386–389.
[3] D.I. Kim, P.H. Yoon, Y.H. Ryu, et al., MRI of germinomas arising from the basal ganglia and thalamus, Neuroradiology 40 (1998) 507–511.
[4] K. Sano, Pathogenesis of intracranial germ cell tumors reconsidered, J. Neurosurg. 90 (1999) 258–264.
[5] H. Yonezawa, Y. Shinsato, S. Obara, et al., Germinoma with syncytiotrophoblastic giant cells arising in the corpus callosum, Neurol. Med. Chir. (Tokyo) 50 (2010) 588–591.
[6] S. Okuno, M. Hisanaga, S. Ohtoku, et al., Germinoma with granulomatous reaction arising from the corona radiata: case report and review of articles, No shinkei Geka 20 (1992) 775–780.
[7] H. Nakase, H. Ohnishi, H. Touho, et al., Cerebellar primary germ-cell tumor in a young boy, Brain Dev. 16 (1994) 396–398.
[8] T. Birnbaum, H. Pellkofer, U. Buettner, Intracranial germinoma clinically mimicking chronic progressive multiple sclerosis, J. Neurol. 255 (2008) 775–776.
[9] P. Krolak-Salmon, G. Androdias, J. Honnorat, et al., Beware of optic neuritis, Lancet Neurol. 1 (2002) 516–517.

[10] Y. Tao, D. Lian, Z. Hui-juan, P. Hui, J. Zi-meng, Value of brain magnetic resonance imaging and tumor markers in the diagnosis and treatment of intracranial germinoma in children, Zhongguo Yi Xue Ke Xue Yuan Xue Bao 33 (2011) 111–115.

Shintaro Hayashi
Department of Neurology, Gunma University Graduate School of Medicine, 3-39-15, Showa-machi, Maebashi, Gunma 371-8511, Japan
Department of Neurology, Tokyo Metropolitan Neurological Hospital, 2-6-1 Musashidai, Fuchu, Tokyo 183-0042, Japan
Corresponding author at: Department of Neurology, Tokyo Metropolitan Neurological Hospital, 2-6-1 Musashidai, Fuchu, Tokyo 183-0042, Japan.
E-mail address: shintaro@neuro.med.kyushu-u.ac.jp.

Koichi Okamoto
Geriatrics Research Institute and Hospital, 3-26-8 Otomo-machi, Maebashi, Gunma 371-0847, Japan

28 July 2015

資　料

在宅筋萎縮性側索硬化症療養者の急変時対応に関する認識と実態

大谷　忠広[1]，牛久保美津子[2]，川尻　洋美[3]，中川　裕[1]，飯山　苗恵[4]，岡本　幸市[5]

1　群馬県前橋市昭和町3-39-15　群馬大学医学部附属病院
2　群馬県前橋市昭和町3-39-22　群馬大学大学院保健学研究科
3　群馬県前橋市朝倉町3-39-15　群馬県難病相談支援センター
4　群馬県前橋市上沖町323-1　群馬県立県民健康科学大学
5　群馬県前橋市大友町3-26-8　老年病研究所

要　旨

目　的：筋萎縮性側索硬化症（ALS）の病状は進行予測が難しく，在宅療養中に急変して緊急入院となることがある．そのため，急変時の対応を整備する必要がある．本研究目的は，在宅ALS療養者の急変時対応の認識と実態を明らかにすることである．

方　法：A大学病院神経内科でALSの診断を受け2011～2013年の間に外来受診歴がある患者とALS患者会関係者5名を含めた計77名．郵送法による質問票調査を実施した．倫理的配慮は，群馬大学医学部疫学研究に関する倫理審査会にて承認を得た．

結　果：回収は42件（回収率55%）で，有効回答41件を分析した．急変経験者は17名，未経験者は24名であった．自宅での急変に備えて，事前に医療の対応方法に関する意思表明は「必要はない」「わからない」は，経験者6名，未経験者9名．理由は，「まだ大丈夫だと思っている」，「症状が軽いから」などであった．急変時に最初にする連絡先は，「決まっていない」が，急変経験者0名，未経験者10名であった．急変経験者17名の急変の回数は，1回が11名，2回が2名，3回以上が2名であった．

結　論：急変未経験者は，急変経験者に比べ急変時対応の認識が希薄で対応方法が未整備であることが明らかとなった．早期から急変時の対応方法について患者教育をする必要がある．

文献情報

キーワード：
筋萎縮性側索硬化症，
在宅療養，
急変時対応，
意思表示，チーム医療

投稿履歴：
受付　平成26年11月20日
修正　平成26年12月3日
採択　平成26年12月4日

論文別刷請求先：
大谷忠広
〒371-8511　群馬県前橋市昭和町3-39-15
群馬大学医学部附属病院
電話：027-220-8751
E-mail: t.ohtani@gunma-u.ac.jp

はじめに

筋萎縮性側索硬化症（以下，ALS）は，徐々に悪化進行あるいは寛解と悪化を繰り返しながら慢性的に経過することを特徴とする．また，治療法がいまだ確立されていないため，診断後の多くの患者は，疾患をかかえたまま在宅療養生活を送る．さらに，特定疾患医療受給者は増加していることから，在宅ALS療養者はますます増えることが予想される．ALSの病状の進行は発症タイプにより異なり，速度も個別性が高いため，進行予測が困難である．[1] これらのことから，緊急受診件数もまた増えていくことが予想される．在宅ALS療養者が安心して療養生活を送るためには，病状急変時の緊急受診体制を整えることは非常に重要である．

在宅における病状急変時に，早急かつ適切な対応を行うためには，事前に緊急時の対処方法・連絡体制について，往診や訪問看護師ら地域支援者と，受け入れ先の病院スタッフが，療養者と家族とともに話し合い，その内容を関係者間で情報共有することが重要である．しかし，現状ではいまだそのような体制は十分にできているとは言い難い．こ

のような緊急受診体制を整備するためには，まずは現状と問題点を把握する必要があるが，それを明らかにした調査研究はみられない．

国内における緊急受診状況の調査研究は，救急搬送患者を対象としたものが多数報告されている．そのうち，在宅神経難病療養者を対象とした報告は，緊急受診の網羅的な調査研究が2件のみで，1病院からの実態を明らかにしたものであった[2,3]．本研究の目的は，在宅ALS療養者の緊急受診体制を整備するための資料を得るため，在宅ALS療養者の緊急入院・緊急受診の認識と実態を明らかにすることとした．

方法

1．研究対象者

A大学病院神経内科でALSの診断を受け2011～2013年の間に外来受診歴がある患者のうち，病名が未告知の患者と死亡者は除外した．これにALS患者会関係者5名を含めた計77名とした．

2．調査方法

郵送法による無記名式質問票調査を2013年12月～2014年1月に実施した．質問票は，修士号以上の学位を有する神経難病に携わる看護師4名と医師2名が文献を参考にして協議して作成したものを，患者3名にプレテストを実施したうえで使用した．質問項目は，患者基礎情報，急変時対応の認知度，急変の有無，急変経験者に対する急変時の対応状況についてであり，回答方法は選択式と自由記載式とした．個人のプライバシーの保護のために無記名とした．

3．用語の定義

「病状の急変」とは，予想しなかった病状の悪化があり，療養者と家族だけでは対応しきれない状態とした．

4．倫理的配慮

群馬大学医学部疫学研究に関する倫理審査委員会にて承認を得た（承認番号25-50）．調査票の表紙に，本調査の目的，プライバシーの保護，協力しなくても不利益はないこと，調査票の回収をもって，同意とみなすなどの説明を記載した．

結果

回収は42名（回収率55%）であったが，うち1名はALS以外の診断であったことから除外し，分析対象は41名とした．急変経験あり群（急変経験群）は17名，急変経験なし群（急変未経験群）は24名であった．以下，この2群間の比較検討を行った．

1．対象者概要（表1）

年齢は，急変経験群では急変未経験群より，65歳以上がやや多かった．療養場所は，急変経験群は自宅が7名（41%）と入院中が8名（48%）と約半数ずつであったが，急変未経験群は自宅が22名（92%）であった．呼吸管理は，急変経験群では気管切開と気管切開下陽圧換気（TPPV）が8名（47%），急変未経験群では何もなしが16名（67%），非侵襲的陽圧換気（NPPV）が5名（21%）であった．診断からの期間は，急変経験群では，6年以上が6名（35%）を占めていた一方で，0～1年以内の4名（24%）が急変を経験していた．急変未経験群では，0～1年以内が12名（50%）であったが，診断から6年以上経過していても急変経験がない人が2名（8%）いた．回答者は，配偶者が23名（56%）と最も多く，患者本人が11名（27%），子どもが5名（12%）であった（複数回答）．

2．緊急時の準備に対する認識と意思表示（表2）

自宅で病状の急変があった場合に備えて，事前に医療の対応方法に関する意思表明をしておく必要性について，「必要がある」との回答は21名（急変経験群9名，急変未経験群12名）であった．「必要はない」，あるいは「わからない」との回答は，13名（急変経験群4名，急変未経験群9名）であった．理由は，「症状は両脚のみであるから」，「まだ大丈夫だと思っている」，「症状が軽いから」，「なんとかなると信じているから」，「ALSではないから」などがあった．また，急変時の呼吸の処置に対する意思表明については（急変経験群からTPPV療養中の7名を除外），「考えていない」は9名（急変未経験群9名），「考えているが迷っている」は8名（急変経験群3名，急変未経験群5名）であった．症状が急変した際に最初にする連絡先について（急変経験群から，長期入院中の者4名を除外），「決まっている」と24名（急変経験群10名，急変未経験群14名）が回答していた．しかし，「決まっていない」は10名が回答したが，全員が急変未経験群であった．

3．急変経験者による実態と認識（表3）

緊急で病院に受診・入院した経験は，1回が8名，2回が3名，3回が1名，7回が1名であった．受診先選択の理由は，「ずっとかかっていた病院だから」が11名で最も多かったが，「ずっとかかっていた病院が受け入れ拒否」が1名，「ずっとかかっていた病院ではないが話し合いで決めていた緊急搬送先」が3名であった．急変時に最初に連絡した人については，訪問看護師が6名，地域主治医が5名であり，119番が4名であった．緊急受診をしたときの症状は，呼吸苦・呼吸減弱が13名（76%），痰が切れなくなったが3名（18%）であり，呼吸関連が94%を占めていた．

119番をした4名の詳細は，1名は他市に住む娘宅で急変，1名は1回目が119番であったが，2回目は訪問看護師に連絡していた．1名は1回目が訪問看護師であったが，2

表1　対象者概要　　(n=41)

		急変経験 あり (n=17) 人数	%	なし (n=24) 人数	%	合計 人数	%
年齢	40-65歳未満	7	41%	13	54%	20	49%
	65歳以上	10	59%	11	46%	21	51%
性別	男性	9	53%	13	54%	22	54%
	女性	8	47%	11	46%	19	46%
療養場所	自宅	7	41%	22	92%	29	71%
	入院中 (退院予定あり)	4	24%	0	0%	4	10%
	長期入院中	4	24%	0	0%	4	10%
	その他	0	0%	0	0%	0	0%
	無記入	2	12%	2	8%	4	10%
調査時点での呼吸管理	何もなし	4	24%	16	67%	20	49%
	NPPV	2	12%	5	21%	7	17%
	気管切開	1	6%	0	0%	1	2%
	TPPV	7	41%	1	4%	8	20%
	酸素吸入	1	6%	1	4%	2	5%
	不明・無記入	2	12%	1	4%	3	7%
調査時点での栄養管理	経口	2	12%	19	79%	21	51%
	胃瘻	5	29%	2	8%	7	17%
	鼻腔栄養	5	29%	0	0%	5	12%
	経口と胃瘻の併用	2	12%	3	13%	5	12%
	その他・無記入	3	18%	0	0%	3	7%
初発症状	球麻痺型	3	18%	9	38%	12	29%
	上肢型	9	53%	9	38%	18	44%
	下肢型	2	12%	5	21%	7	17%
	無記入	3	18%	1	4%	4	10%
発症～調査時点	0-1年以内	3	18%	4	17%	7	17%
	2-5年以内	5	29%	18	75%	23	56%
	6年以上	8	47%	0	0%	8	20%
	不明	1	6%	2	8%	3	7%
診断～調査時点	0-1年以内	4	24%	12	50%	16	39%
	2-5年以内	7	41%	10	42%	17	41%
	6年以上	6	35%	2	8%	8	20%
回答者 (複数回答)	患者本人	2	12%	9	38%	11	27%
	配偶者	12	71%	11	46%	23	56%
	子ども	1	6%	4	17%	5	12%
	その他	4	24%	1	4%	5	12%

表2　緊急時の準備に対する認識と意思表示　　(n=41)

	急変経験 あり (n=17) 人数	%	なし (n=24) 人数	%	合計 人数	%
緊急時医療処置の意思表明をしておく必要はあるか						
必要がある	9	53%	12	50%	21	51%
必要はない	1	6%	3	13%	4	10%
わからない	3	18%	6	25%	9	22%
無記入	4	24%	3	13%	7	17%
呼吸の処置に対する意思※1						
考えていない	0	0%	9	38%	9	26%
考えているが迷っている	3	30%	5	21%	8	24%
人工呼吸器を装着する	1	10%	4	17%	5	14%
酸素吸入のみ	0	0%	0	0%	0	0%
その他	2	20%	4	17%	6	18%
無記入	4	40%	2	8%	6	18%
急変時の最初の連絡先※2						
決まっている	10	77%	14	58%	24	65%
決まっていない	0	0%	10	42%	10	27%
無記入	3	23%	0	0%	3	8%

※1　急変経験あり群より，気管切開下陽圧換気 (TPPV) 者の7名は除外
※2　急変経験あり群より，長期入院中 (退院見込みなし) 4名は除外

表3　急変経験者による実態と認識　(n=17)

		人数	%
緊急で病院に受診・入院した経験	1回	8	47%
	2回	3	18%
	3回	1	6%
	7回	1	6%
	無記入	4	24%
入院先選択の理由			
ずっとかかっていた病院だから		11	65%
ずっとかかっていた病院が受け入れ拒否		1	6%
話し合いで決めていた緊急搬送先		3	18%
救急隊におまかせ		1	6%
無記入		1	6%
急変時に最初に連絡した人 (複数回答)			
地域主治医		5	29%
訪問看護師		6	35%
病院の主治医		0	0%
119番		4	24%
ケアマネジャー		1	6%
家族や親族		1	6%
その他		2	12%
無記入		3	18%
緊急受診をしたときの症状 (複数回答)			
呼吸苦・呼吸減弱		13	76%
痰が切れなくなった		3	18%
発熱		6	35%
窒息		1	6%
胃瘻のトラブル		1	6%
意識消失		0	0%
誤嚥性肺炎		1	6%
下痢・褥瘡悪化		1	6%

同月は119番であった．もう1名は看護師である娘の判断で119番にて娘の病院に緊急搬送となったなど，さまざまな状況が明らかになった．また，自由記載においては，力量のない訪問看護師の一人対応に不安であったとの回答があった．

4．急変経験群による急変時対応についての要望

「緊急時にすぐ入院できる病院を確保して欲しい」が7件あった．ほかに「急変時にいつでも対応できる往診医」「往診医や受け入れ病院には，これまでかかっていた病院と連絡をとって欲しい」という連携に関する意見が3件あった．

考察

在宅ALS療養者の病状の急変時には，いつでもすみやかに医療者と連絡がとれ，受診の必要があれば，受け入れ先がすぐ決まることが重要である．さらに，自分のことをよく知っている医療機関に受診できることは，緊急時の精神的動揺がある中，本人にとっても家族にとっても安心できる．緊急時であっても，受け入れ先との切れ目のない医療やケアの提供が課題である．ALS療養者の急変対応に関する認識と院内・地域医療機関の連携体制の状況を明らかにすることは，切れ目のない医療やケアを提供する体制を構築する上での基礎データとして特に重要と考える．

1．急変経験群と急変未経験群における急変時対応の認識

急変経験群は，9名 (53%) が「緊急時医療処置の意思表明をしておく必要がある」と回答し，全員が何かしら急変時の呼吸処置に対する意思を検討し，10名 (77%) が急変時の最初の連絡先が決まっていた．これにより，急変経験者は自身の経験を踏まえ緊急時の対応についての認識が高まり，対応方法が整備されていることが明らかとなった．しかし，急変未経験群では，「緊急時医療処置の意思表明をしておく必要がある」について急変経験群9名 (53%) と，ほぼ同じ割合で12名 (50%) が回答している．しかし，急変未経験群では急変時の呼吸処置に対する意思を「考えていない」とする回答が9名 (38%) に上り，急変時の最初の連絡先が「決まっている」が14名 (58%) に留まった．このことから，急変経験群と比較して急変未経験群は急変時対応について認識が希薄なことが明らかとなった．

また，今対象者のうち29名 (71%) が自宅で療養生活を送っており，20名 (49%) が呼吸管理を何も行っていないことから，今後，介護を行う家族が急変時の発見や初期対応を行う可能性が高いことが予想される．本研究対象者は「呼吸苦や呼吸減弱」，「痰が切れなくなった」などの呼吸器症状により緊急受診をしており，先行研究においても呼吸不全による急変が最も多かった[5]．このことから，家族が予測しなかったALS療養者の呼吸器症状による急変に直面した際に，苦しむALS療養者を目の前にして呼吸苦の処置全てについて意思決定を行うことは非常に困難である．

それを回避するためにALS療養者の意思決定については，家族と十分に話し合い，納得した決断をしてもらうために呼吸障害がなくコミュニケーションが十分に図れる早期から始めるべきとの指摘[6]がされ，アドバンスドケアプランニングや事前意思確認書が導入されている．

支援チームは，定期的に病状の説明と意思決定について確認を行う必要がある．しかし，ALS療養者は病状に対する理解不足や必要性はわかっていても，悪い予後は考えたくないという思いも同時に持っている[7]ことから，「症状は両腕だけだから」「まだ大丈夫」などと楽観的な予測を立てていたり，急変などを経験していない状況で医療処置の意思表明をチーム支援者から求められても実感がないため意思決定を先延ばしにしている状況がある[7]．

さらに，意思決定についての話し合いのタイミングも，病状を受け入れられない状況や実感がわかない状況では，療養者と支援者間の認識のズレが生じるばかりで効果的ではない[8]．それでも確実に呼吸障害は進行していくため，チーム支援者はALS療養者や家族の心情を理解しながら急変時の対応に関する意思決定を確認するタイミングを早めに見計らい，急変時の対応方法について患者教育を行う

必要がある．

A病院では，2012年から事前意思確認書を導入した意思決定支援をはかっている[10]が，病状が急速に進行している患者への支援は難しい．診断まもない患者であってもいつ急変するかわからない状況があるため，特にA病院から遠方に居住している患者の場合には，最低でも，急変時の最初の連絡先や受診先の確保，起こりうる症状について家族や地域支援者への知識提供や対応方法を指導する必要がある．

2．救急対応と院内・地域医療機関間の連携体制整備

緊急受診したALS療養者は1～7回の急変を経験していた．その際の入院先の選択の理由では，「ずっとかかっていた病院だから」が11名（65%）で最も多かったが，「ずっとかかっていたにも関わらず受け入れを拒否された」対象者が1名（6%）いた．しかし，「話し合いで決めておいた緊急搬送先」に3名（17%）が入院できていた．これは，急変時の症状や状況によっては「ずっとかかっていた病院」と言う理由だけでは緊急入院ができない状況があることを示唆している．また，急変時に最初に連絡した人は訪問看護師が6名（35%），地域主治医が5名（29%）とほぼ同数であった．急変時に最初に連絡する人が決まっていることで，家族が急変の場面に遭遇しても症状や対処方法について専門家へ相談して助言をもらうことができていたのではないかと考えられる．

しかし，一方で119番に直接依頼したALS療養者も4名（24%）いた．早期からチーム支援体制が構築されていると緊急時対応が適切に行われ，在宅医療を継続できており，各受療期に応じた適切な支援が円滑にできるとされている．[11] チーム支援体制が構築され，ALS療養者や家族の意思決定が共有されていれば「ずっとかかっている病院」や「話し合いで決めていた緊急搬送先」において，ALS療養者の状態や急変時の医療処置に関する意思決定の内容について把握されている可能性が高くなる．それにより，緊急の受診であってもALS療養者や家族の意思に反する不必要な医療処置が施される可能性や，緊急時に意思決定を行わざるを得なかった家族の不全感を軽減させられることが予想される．ALS療養者が明確な意思表示を行っていなければ，それ以外の病院へ緊急搬送で対応された場合，救命が優先され意思に反した医療処置が施される可能性が高まる．

その対策としては，急変時に統一した対応が取れるように支援チーム内で緊急時の連絡先の確認や医療処置についての希望を示した事前意思確認書などを活用した対応が求められる．ALS療養者や家族とチーム支援者が事前指示書を用いて意思決定を行う過程において，病状の理解が深まり，予後の漠然とした不安が具体化されるなど，疾病の受容に影響を及ぼすことができたとされている．[7] このことからも，緊急時の対応について，院内外の支援チームによる緊急時の対応を決めておく必要性が改めて認識された．

今後の課題としては，本調査の急変経験者は，救命された患者のみであるため，今後は救命がかなわなかった症例に関する調査が必要と考える．

謝辞

質問票調査にご協力をいただきましたALS療養者とご家族様に感謝申し上げます．

本研究の要旨は，第2回日本難病医療ネットワーク学会（2014年11月，鹿児島市）にて発表した．

引用文献

1. 「筋萎縮性側索硬化症診療ガイドライン」作成委員会：1. 疫学，病型，経過・予後，病因・病態．筋萎縮性側索硬化症診療ガイドライン2013．東京：南江堂，2013; 2-21.
2. 中川　裕．在宅筋萎縮性側索硬化症療養者の緊急入院における状況と支援課題．日本難病看護学会誌　2014; 19(1): 41.
3. 小川雅文．在宅療養神経難病進行例の問題点　特に緊急入院が必要な事例についての検討．厚生労働科学研究費補助金　難治性疾患克服事業重要難病患者の地域医療体制の構築に関する研究班　平成19年度総括・分担研究報告書．2008; 23-24.
4. 牛久保美津子，飯田苗恵，大谷忠広．在宅ALS療養者の人工呼吸器をめぐる意思決定支援のあり方に関する看護研究．Kitakanto Med J　2008; 58: 209-216.
5. 松田千春，飯田苗恵，小倉朗子ら．筋萎縮性側索硬化症（ALS）療養者の人工呼吸器装着の意思決定過程の分析．日本難病看護学会誌　2011; 15(3): 185-198.
6. 荻野美恵子，荻野　裕，坂井文彦．「緊急時の対処方法ガイド」（事前指示書）導入後の評価．臨床神経　2005; 45(12): 45.
7. 荻野美恵子．神経難病の事前指定書　北里大学東病院の取り組み．難病と在宅ケア　2004; 10(2): 15-18.
8. 橋爪希子，山本巳幸，内山　剛ら．ALS患者さんへの事前意思決定確認書の運用と課題．難病と在宅ケア　2007; 13(1): 57-61.
9. 牛久保美津子．ALS療養者における人工呼吸器非装着の選択にいたった意思決定状況　訪問看護師の振り返りによる一．難病と在宅ケア　2008; 14(1): 43-46.
10. 塚越政貴，古田夏海，牛久保美津子ら．筋萎縮性側索硬化症療養者への事前意思確認書の導入状況と課題．Kitakanto Med J　2013; 63: 333.
11. 高久順子，飯田苗恵，佐々木栄子ら．保健所保健師によるALS療養者への診断確定期からの支援．日本難病看護学会誌　2007; 12(2): 172-177.

Preparations and Realities Regarding Physical Emergency Among in-home Amyotrophic Lateral Sclerosis Patients

Tadahiro Ohtani[1], Mitsuko Ushikubo[2], Hiromi Kawajiri[3], Hiroshi Nakagawa[1], Mitsue Iida[4] and Koichi Okamoto[5]

1 Gunma University Hospital, 3-39-15 Showa-machi, Maebashi, Gunma 371-8511, Japan
2 Gunma University Graduate School of Health Sciences, 3-39-22 Showa-machi, Maebashi, Gunma 371-8514, Japan
3 Gunma Prefectural Support Center for Intractable Diseases, 3-39-15 Showa-machi, Maebashi, Gunma 371-8511, Japan
4 Gunma Prefectural College of Health and Sciences, 323-1 Kamioki-machi, Maebashi, Gunma 371-0052, Japan
5 Geriatrics Research Institute, 3-26-8 Ohtomo-machi, Maebashi, Gunma 371-0847, Japan

Purpose: The purpose of this study was to clarify the preparations and realities regarding emergency on physical condition among in-home amyotrophic lateral sclerosis (ALS) patients for effective countermeasure.
Methods: The participants were 72 patients with ALS who were treated at University Hospital A between 2011 and 2013, and 5 people involved with an ALS patient association. A questionnaire survey was conducted by mail. The study was approved by the University Ethics Committee.
Results: Out of 77 participants, 42 responded (55% response rate), of which 41 responses were valid. Seventeen patients had experienced an emergency sudden change in their conditions, and 24 had no such experience. Nine patients who had not had such an experience selected either "*Not necessary*" or "*Not sure*" when asked about their advanced directives. Reasons for these responses were "*I'm fine at the moment*" and "*My symptoms are mild*". First contact at emergency was listed as "*Not decided*" by none who had experienced physical emergency and 10 patients who had not. The number of emergency episode was 1 in 11 patients, 2 in 2 patients, and 3 or more episodes in 2 patients.
Conclusions: The study findings showed that patients who had not experienced an emergency in their ALS were less aware and less prepared for their emergency than their counterparts with such an experience. The findings suggest the need for better education on early preparations for emergency in ALS symptoms.

Key words:
amyotrophic lateral sclerosis,
home care,
emergency hospitalization,
advanced directive,
interdisciplinary care

パーキンソン病の診断と治療

岡本幸市

はじめに

パーキンソン病は，1817年にジェイムス・パーキンソンがAn Essay of the Shaking Palsyというタイトルで記載したことに始まるが，ローマ法王，ヒトラー，モハメド・アリなど多くの有名人が罹患しており，非常にポピュラーな病気である．本邦では約12～13万人が罹患しており，中高年で発症することが多い．男女差はなく，40歳以下の発症例は「若年性パーキンソン病」と呼ばれる．

パーキンソン病とは

パーキンソン病は，中脳黒質のドパミン神経細胞の変性を主体とする原因不明の神経変性疾患である（図１）．黒質から線条体（尾状核と被殻）へ神経突起が伸びているが，線条体のドパミン量が20％程度まで減少すると発病すると言われている．病理学的には黒質の神経細胞の脱落とLewy小体（図１）の形成が特徴的である．大半は孤発性であるが，約５％は家族性に発症する．原因は不明であるが，図２に示すような機序が想定されている．発症には遺伝的素因と環境因子が関与していると想定されているが，40歳以下での発症例では遺伝的素因の関与が大きく，遺伝子異常も次々に報告されている．

パーキンソン病の病理の進展と，初期病変部位は？

パーキンソン病の病理学的マーカーはLewy小体（図１）であるが，Lewy小体の主な構成成分はα-シヌクレイン（α-synuclein）からなる．多数の剖検例での抗α-シヌクレイン抗体を用いた免疫組織学的検討では，Lewy小体は，延髄迷走神経背側核や嗅球に最初にみられ，次第に，橋被蓋，中脳黒質，扁桃核，大脳皮質などへ波及していくことが明らかになった[1]．中脳黒質に病変が及んだ段階でパーキンソン病の症状がみられるようになる．パーキンソン病の病理は中脳黒質以外に広範囲に病変がみられ，Parkinson's complexとも呼ばれるようになっている[2]．

パーキンソン病の病理がどこから始まるかはまだ不明であるが，図３に示すように末梢の自律神経系（腸管，心臓）や嗅球も初期病変部位として考えられている．すなわち，パーキンソン病を引き起こす外的要因が外界と接する腸管や嗅球から吸収される可能性が指摘されている．

パーキンソン病の症状

パーキンソン病には図４に示すように，運動症状と非運動症状がある．すなわち，運動症状，抑うつ，認知機能低下，睡眠障害，嗅覚障害，自律神経障害，便秘など多彩な症状を呈する．運動症状には左右差があることが特徴的である．症状は徐々に進行するが，重症度分類は図５のヤール分類が使用されている．特定疾患として申請可能なのはヤール３度以上でかつ生活機能障害度が２度以上である．

パーキンソン病の運動症状に先行する非運

公益財団法人老年病研究所

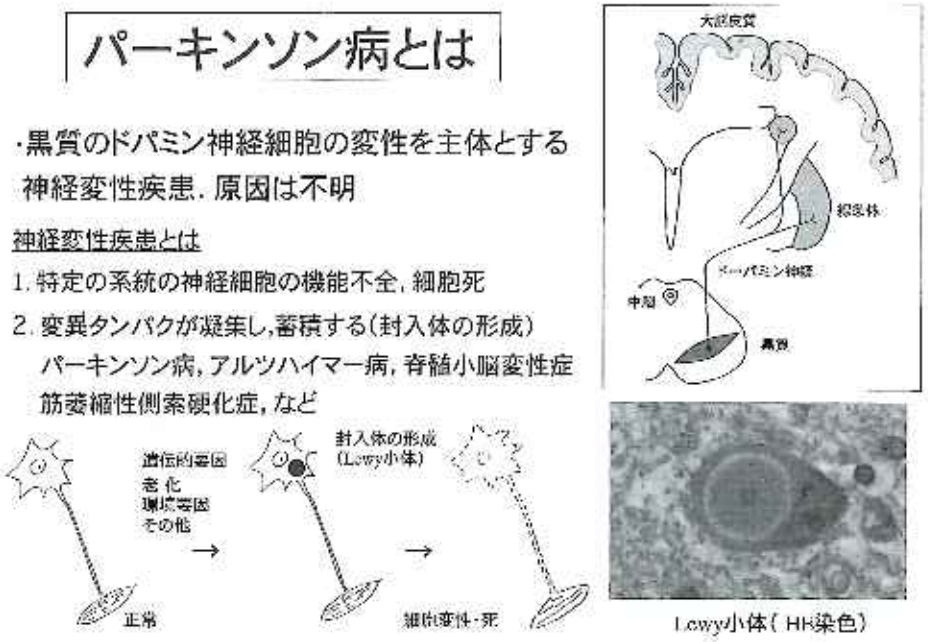

図1

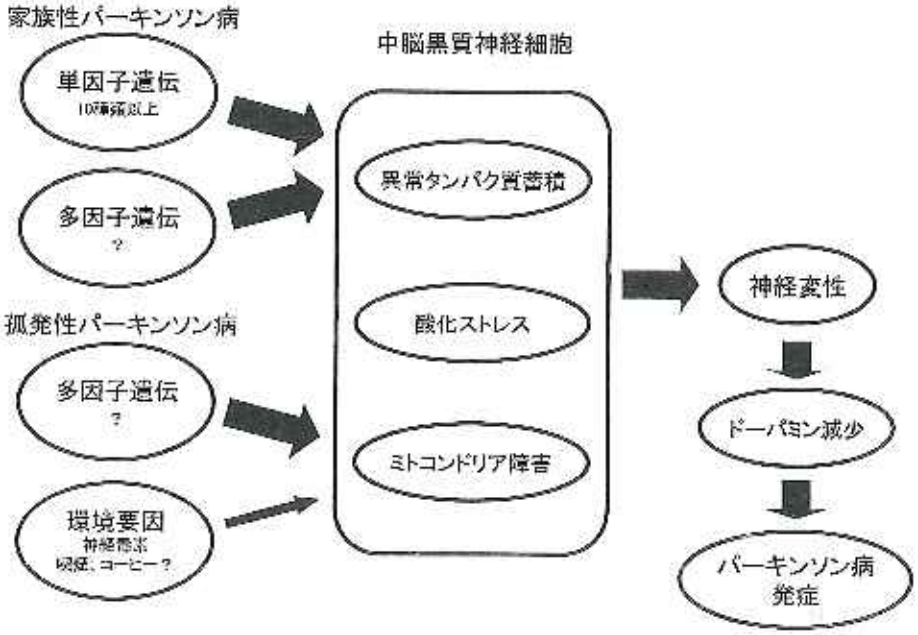

図2

動症状として，1）嗅覚低下，2）自律神経障害（とくに便秘），3）睡眠障害（レム期行動異常症）などが指摘されている．レム期行動異常症とは，睡眠のレム期に夢の内容に反応して異常行動が出現する睡眠障害である．また，パーキンソン病の病前性格としては，几帳面で正直な人に多い印象がある．

診断

パーキンソン病の診断の要点は以下の4点である．

1．パーキンソニズムがある．パーキンソニ

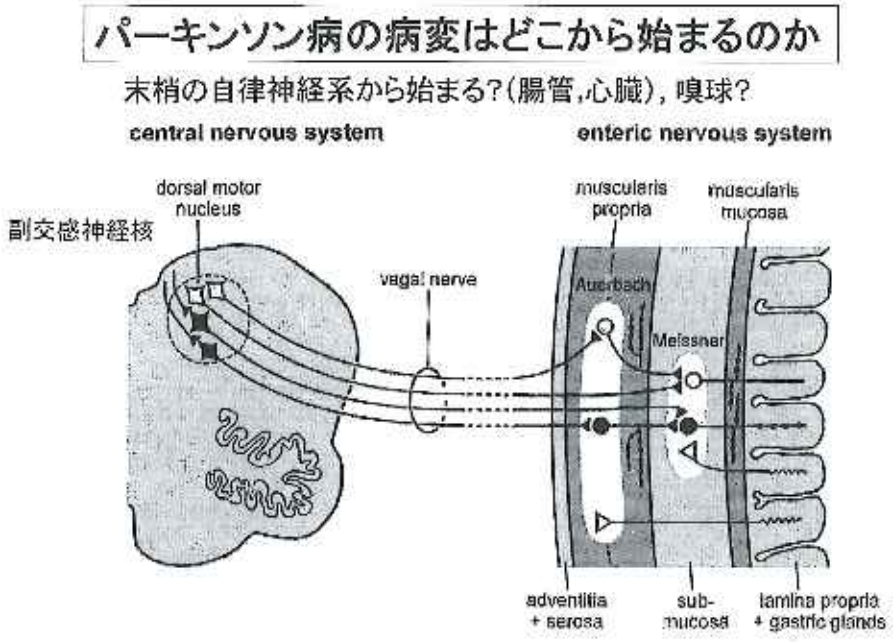

図 3

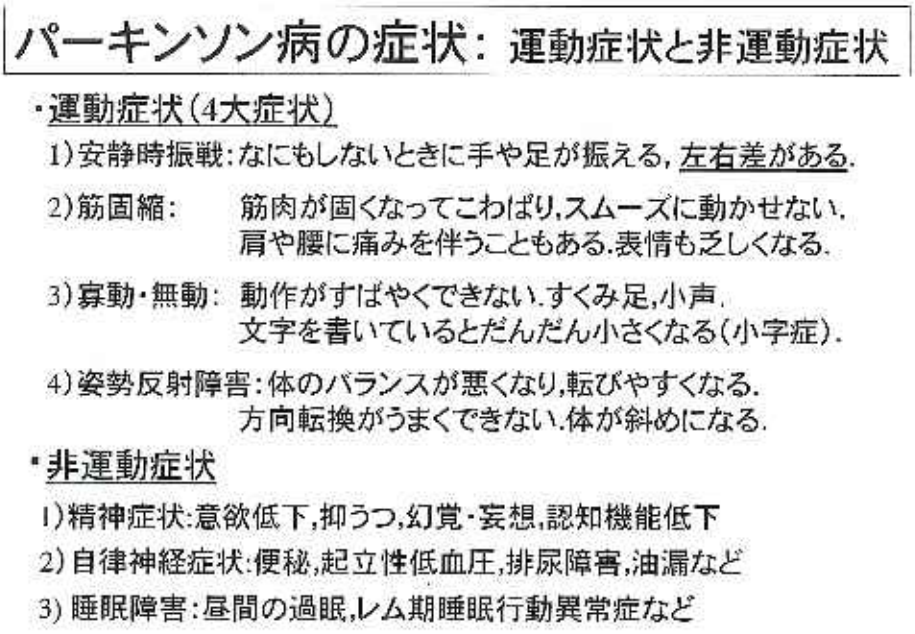

図 4

ズムの定義は次の1), 2)のいずれかに該当する場合：1) 左右差のある4－6 Hzの安静時振戦, 2) 歯車様筋固縮, 動作緩慢, 姿勢反射障害（すくみ足, 加速現象, 突進現象）のうちの2つ以上が存在.

2．脳CTやMRIで特徴的異常（パーキンソニズムの原因となるような所見）がない.

3．パーキンソニズムを起こすような薬物・毒物への暴露がない.

4．抗パーキンソン病薬でパーキンソニズムが改善する.

鑑別診断

パーキンソニズムを起こす疾患は多い．主な疾患の鑑別のポイントを図６に示す．パーキンソン病では初期から易転倒性を示すことはない．薬剤で多いのはメトクロプラミド（プリンペラン）とスルピリド（ドグマチール）であり，これらを服用中は動作緩慢などの出現に注意する必要がある．

Lewy小体型認知症は，パーキンソン病と同一線上にある疾患であり，大脳皮質に広範にLewy小体がみられる．注意や明晰さの著明な変化を伴う認知機能の変動，構築され具体的内容の繰り返される幻視体験，特発性パーキンソニズムが特徴的であり，日常診療で診る例が増加している印象がある．

検査

脳CTやMRIにはパーキンソン病に特徴的

ヤール重症度分類

1度：体の一側，軽い

2度：両側，日常生活に不自由なし

3度：姿勢反射障害，すくみ足

4度：日常生活に一部介助が必要

5度：1人で起立，歩行ができない

生活機能障害度

1度：日常生活，通院に制限なし

2度：日常生活，通院に部分的介助が必要

3度：日常生活に全面的介助が必要

図５

鑑別診断のポイント

■パーキンソン症候群がみられるか

安静時振戦

固縮，動作緩慢，姿勢反射障害のうち少なくとも2つ

■パーキンソン病か，二次性パーキンソン症候群か

1）安静時振戦（+）　→ 大半がパーキンソン病

2）抗ドパミン薬を服用中　→ 薬剤性パーキンソニズム

3）下半身に目立つ歩行障害　→ 血管性パーキンソニズム

4）自律神経症状，小脳症状　→ 多系統萎縮症

5）上方視障害，易転倒性　→ 進行性核上性麻痺

6）運動失行，著明な左右差　→ 大脳皮質基底核変性症

図６

な所見はなく，鑑別診断のために必ず行っている．MIBG心筋スペクトも鑑別が難しい場合に行っている．MIBG（メタヨードベンジルグアニジン）とはノルアドレナリンの生理的アナログであり，交感神経終末でノルアドレナリンと同様の摂取，貯蔵，放出が行われる．^{123}IMIBG心筋スペクトは心臓の節後性交感神経機能の評価のために行われており，各種心疾患に伴う局所交感神経障害，糖尿病に伴う心自律神経障害，Lewy小体病（パーキンソン病，Lewy小体型認知症，純粋自律神経不全症）で低下する．静脈注射15－30分後（早期像）と3－4時間後（後期像）に心・縦隔比（H／M比）を求める．正常は早期像，後期像ともに2.0以上である．洗い出し率washout rateは正常は20%以下，40－50%以上は明らかに異常である．図7に実例を示すが，低下がないといってもパーキンソン病を否定できるわけではない．

最近パーキンソン症候群とLewy小体型認知症の診断薬としてダットスキャンが認可になった．黒質線条体神経の終末部に存在するドパミントランスポーターを可視化するものでドパミン神経の変性・脱落をスペクトで評価するものである．進行性核上性麻痺や多系統萎縮症でも線条体での取り込みが低下し，パーキンソン病との鑑別にはまだ難がある検査である．

治療

パーキンソン病の治療は不足しているドパミンを補い，症状を緩和する「補充療法」が基本である．患者の症状，年齢，職業，希望などを加味し，副作用を少なくしながら，有意義な生活を送れるようにきめ細かく薬物調整を行う．しかしながら徐々に進行し，運動合併症（薬効の減弱，症状の日内変動，ジスキネジアなど），幻覚や認知症などがみられるようになり，治療に難渋するようになる．

抗パーキンソン病薬はL-ドパ製剤とドパミンアゴニスト（ドパミン受容体刺激薬）が主体である．ドパミン受容体刺激薬には麦角系製剤と非麦角系製剤がある．麦角系製剤であるペルマックスとカバサールは心弁膜肥厚が

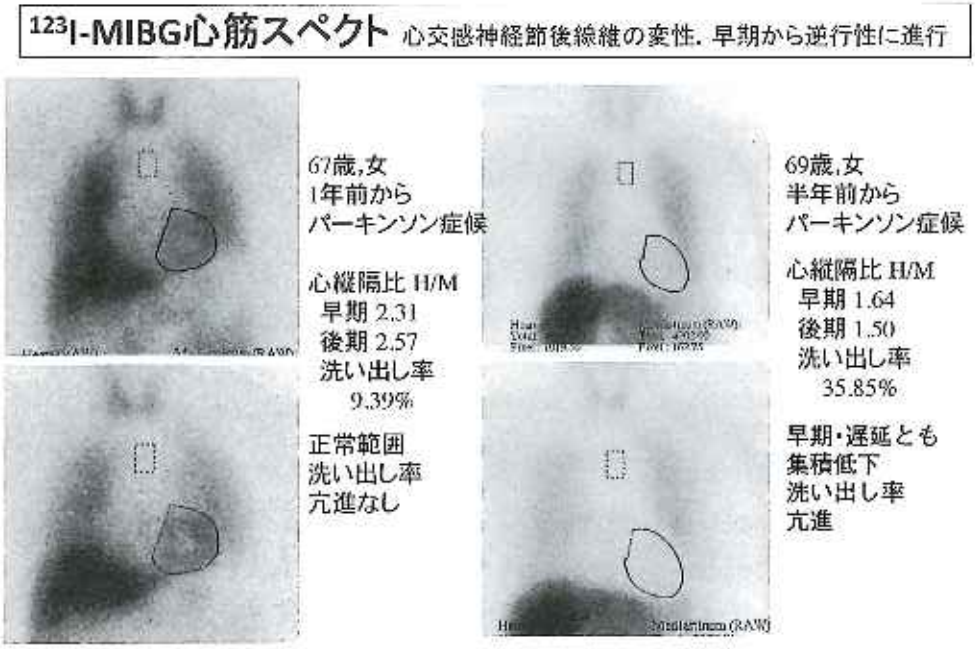

図7

誘発されることが指摘されてから使用頻度は減少している．最近では朝１回の投与でよい非麦角系製剤の徐放錠（ミラペックスLA，レキップCR）や，１日１枚でよい貼付薬（ニュープロパッチ）が多く用いられるようになっている．

2011年のパーキンソン病治療ガイドライン[3]では，70歳以上の高齢者や，認知機能障害・精神症状の合併のある患者ではL-ドパ製剤で治療を開始することが推奨されている．70歳未満で当面の症状を優先させる特別な事情がない場合には，運動合併症の発現を遅らせるためにドパミンアゴニストでの治療開始が推奨されている．しかしながら，ドパミンアゴニストは，１）高価，２）効果発現までに時間がかかる，３）単剤では効果が不十分，４）突発性睡眠や浮腫などの副作用がある，さらにL-ドパ製剤でも少量投与なら運動合併症の発現頻度は多くないことなどから，実際には年齢に関係なく，まずL-ドパ製剤で開始し，なるだけ300mg/日以下で維持する．効果が不十分なら少量のドパミンアゴニストやFP錠などを併用している場合が多い．

ドパミンアゴニストの副作用としては，１）消化器症状は服用開始時に多いので少量からの漸増，２）急激な姿勢異常（首下がり，腰曲がり，側屈など），３）麦角系では心弁膜症（実際にはまれ），４）非麦角系では突発性睡眠，５）Dopamine dysregulation syndrome（衝動制御障害）：病的賭博，買い物依存症，過食，過剰な性欲など，６）反復常同行動：１つのことに熱中する，などである．その他の抗パーキンソン病薬については図８に示す．2014年12月にはL-ドパ／カルビドパ／コムタンの３剤の合剤が使用可能になる予定である．

定位脳手術

2000年から深部電気刺激療法Deep Brain Stimulation（DBS）が保険適応になり，主に視床下核電気刺療法が行われている．高頻度での電気刺激で神経細胞の活動を停止させ症状の改善をもたらす．適応は，１）70歳以下，２）認知症がない，３）症状の変動

その他の抗パーキンソン病薬

1)抗コリン薬(アーテン):振えにはよいが,高齢者ではあまり用いない
2)塩酸アマンタジン(シンメトレル):全般的な症状の改善
3)ドプス:すくみ足によいとされるが,あまり効果はない.
4)FP錠:中枢でのドパミンの代謝を抑制.L-ドパを30%増量したのと同等
5)コムタン:末梢でのL-ドパの分解を阻害し,L-ドパの血中半減期を延長
6)トレリーフ:抗てんかん薬,我が国で開発された.
　　症状の日内変動(ウエアリング・オフ現象)の改善効果
7)ノウリアスト:アデノシンA_{2A}受容体拮抗薬
　　症状の日内変動(ウエアリング・オフ現象)の改善効果
8)アポカイン(皮下注射):即効性で作用時間が短い.
9)スタレボ（2014年12月から発売）
　　L-ドパ/カルビドパ/コムタンの3剤の合剤

図８

(wearing-off現象) とジスキネジアがあり，薬物でのコントロールに難渋している，4) L-ドパに反応するなどである．

非薬物療法・生活指導

非薬物療法や生活指導も大事である．廃用症候群の予防と転倒の予防も必要である．明るく，前向きに生活することが大事で，「病気になっても病人にならない」ように指導する．初期にはいままで通りの生活をしてもらい，運動は時間を決めて行うように指導する．ポイントは，1) 筋力をつける (とくに腸腰筋)，2) よい姿勢を保つ，3) 動作にリズムをつける，4) 方向転換は大回りに，5) すくみ足があるときには片方の足を後ろに引いて，その足を前に踏み出すようにする，などである．

抗パーキンソン薬は急に止めないことも大事である．急に中断すると悪性症候群 (高熱・発汗・意識障害・筋固縮・血清CK値の著明な高値) の発生の危険性がある．

おわりに

パーキンソン病は全身病であることの再認識が必要である．運動障害以外に，自律神経症状 (便秘，起立性低血圧)，精神症状 (睡眠障害，幻覚，認知症など) にも注目し，全身管理が必要である．自治医大で試験的に行われている遺伝子治療も有効なようであり，京都大学でのiPS細胞を用いた臨床治験も2015年には始まろうとしており，パーキンソン病の治療がさらに発展することに期待したい．

文献

1) Braak H et al. Stages in the development of Parkinson's disease-related pathology. Cell Tissue Res 318:121-34, 2004.
2) Langston JW. The Parkinson's complex: parkinsonism is just the tip of the iceberg. Ann Neurol 59:591-6, 2006.
3) パーキンソン病治療ガイドライン2011．日本神経学会監修，医学書院，2011.

重度の嚥下障害によりリハビリテーションに難渋したWallenberg症候群の1例

公益財団法人老年病研究所附属病院　神経内科
酒井保治郎　　甘利雅邦

公益財団法人老年病研究所附属病院　リハビリテーション科
神宮俊哉　　丹下弥生

要　旨

症例は40歳代，女性．2012年10月下旬，頭痛で発症した．右の椎骨動脈の解離性動脈瘤破裂によるくも膜下出血で，コイル塞栓術が施行されたが，術後，脳梗塞による右のWallenberg症候群と診断された．水頭症を併発し，脳室腹腔シャントを行った．2013年1月上旬，リハビリテーションのため当院に転院となった．意識は清明で，FIMは運動39，認知20であった．めまいを訴え，右のホルネル徴候，左方視で注視方向性眼振，下顎反射陽性，咽頭反射が右で消失，左で低下，嚥下障害，右の上下肢の失調，左上下肢の温度覚，痛覚の消失などを認めた．誤嚥時の反射がほとんどなく，唾液が気管に大量に流入するので，食事は経管，気管カニューレはカフ付きであった．嚥下造影検査では気管，食道に同等に入り，食道入口部の拡大訓練を行い，自分で管を食道まで入れ，経管栄養食が可能となった．唾液などの気道への流入が減少し，スピーチカニューレに交換したが，誤嚥性肺炎を起こし，元のカニューレに戻した．リハビリテーションを継続したが，食事の経口摂取はできなかった．2014年2月初めに，喉頭挙上術，両側輪状咽頭筋切断，右被裂軟骨内転術を行い，5月には後屈60度，下顎突出位で全粥が可能になり，スピーチカニューレとなった．歩行は杖で監視歩行であった．発症から約1年半の経過で，経口摂取が可能となった稀な1例である．

症　例

患　者：40歳代，女性

主　訴：めまい，嚥下障害，歩行障害

既往歴：高血圧を指摘されていたが，治療歴はない

家族歴：特記すべきことはない

現病歴：2012年10月下旬，前日からあった頭痛が増悪し，近医に救急搬送された．その救急車内で四肢の強直性けいれんと右への共同偏視が出現した．頭部CTでくも膜下出血があり，その原因は右の椎骨動脈の解離性動脈瘤破裂で，コイル塞栓術が施行された．術後，右の延髄背外側（Wallenberg症候群），右の小脳半球の内側に梗塞巣を生じた．2日後に気管切開，その後，肺炎，敗血症を起こした．12月10日に水頭症で，脳室腹腔シャントを行った．2012年1月上旬，嚥下障害，歩行障害のリハビリテーションのため当院の回復期病棟に転院となった．

入院時現症：

（一般身体所見）　身長158cm，体重52.7kg，血圧110/75mmHg，脈拍98/分，体温37.1℃で胸腹部には異常はなかった．経鼻胃管が挿入され，気管切開されて，カフ付きカニューレが入っていたが，酸素の吸入はなかった．

（神経学的所見）　意識は清明で，めまいを訴え，右のホルネル徴候，左方視で水平注視方向性眼振，右顔面で軽度痛覚低下，下顎反射陽性，咽頭反射が右で消失，左で低下，カーテン徴候は陰性，嚥下障害，左上下肢の温度覚，痛覚の消失を認めた．麻痺はなく，Babinski 徴候は陰性であったが，右で指鼻試験，踵膝試験は拙劣で，閉眼で増強し，右の上下肢の失調がめだった．起立保持はできなかった．長谷川式簡易知的機能評価スケールは29点であった．

画像ならびに検査所見：転院時の頭部 MRI（Flair 画像）では，右の延髄背外側に脳梗塞による高信号域を認めた（図１）．血算，検尿には異常を認めなかった．一般生化学的検査ではアルブミン3.5 g/dl と低下，CRP 1.56であったが，他には異常を認めなかった．短潜時体性感覚誘発電位では左正中神経では正常であったが，右正中神経では N_{13} 潜時までは正常であったが，N_{20} は出現しなかった（図２）．

経　過：入院当初の FIM は運動39，認知20で，訓練室と病棟間の道順を憶えることができなかった．約２週間して，ようやく道順を迷うことがなくなった．口腔内の唾液が多く，嚥下自体は可能だが，多くが気道に流入し，咳き込みなどの咳反射はほとんど見られなかった．唾液と痰の量が多く，気管カニューレの内壁には痰がこびりつき，カフ付きカニューレをおおむね週に１回交換した．間接的嚥下練習に加え，食道入口部開大を目的に，頸部突出位で空気のバルーン飲み嚥下練習を

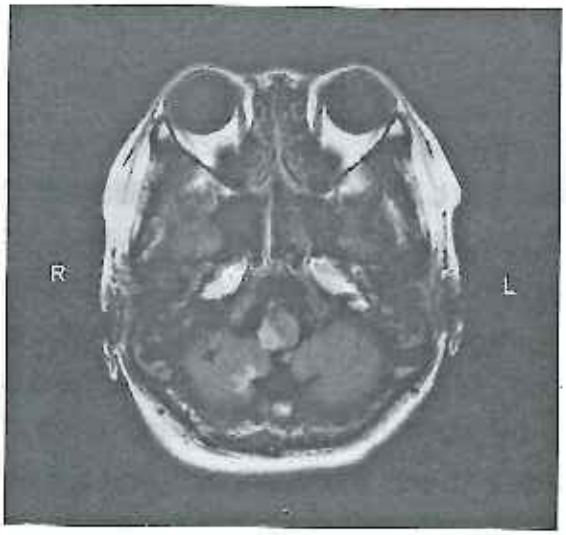

図１　転院時の頭部 MRI（Flair 画像）
右の延髄背外側部，小脳内側に脳梗塞による高信号域を認める

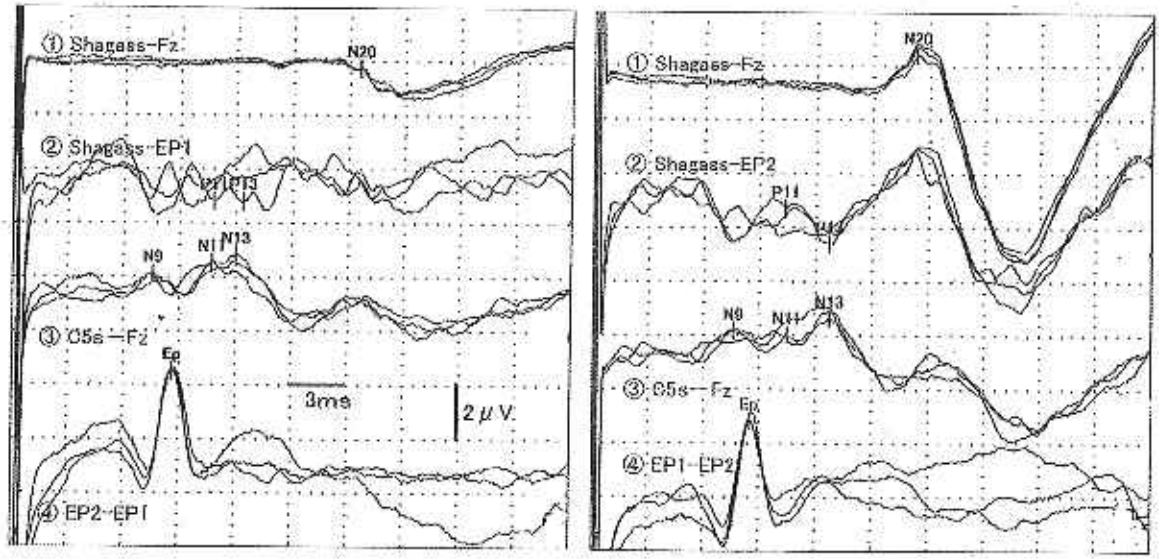

右正中神経　　左正中神経

図２　短潜時体性感覚誘発電位（正中神経刺激）
右正中神経では N_{13} 潜時までは正常であるが，N_{20} は出現しない．左正中神経では正常である

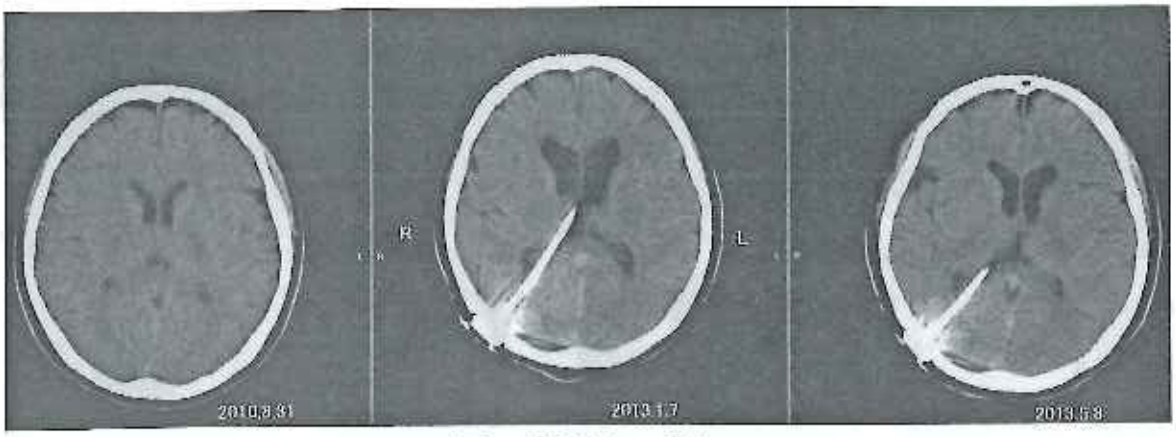

図3　頭部CTの比較
脳室腹腔シャントから約1ヶ月経過していたが，入院時はまだ脳室は拡大している．
5月には脳室拡大はかなり軽快しているが，発症前の状態には戻っていない

続けたが，誤嚥性肺炎は起こさなかった．

今回のくも膜下出血を起こす2年以上前に，当院で頭部CTを撮っていたので，そのCTと入院時，その約4ヶ月後の頭部CT画像を示した（図3）．脳室腹腔シャント後であったが，入院時はまだ脳室は拡大し，5月には脳室拡大はかなり軽快したが，発症前の画像と比較すると脳室は拡大していた．

一方，運動失調については，2月中旬には車椅子への移乗が可能となり，トイレ動作が自立した．それに伴い，日中は車椅子座位で居ることが多くなり，口腔内唾液の量は減少し，ゼリーの嚥下練習を開始した．スライスゼリーを飲み込み後，空気のバルーン飲みを複数回行い，その後クリアして，20-30ml摂取できたが，終了時にはカニューレのサイドチューブから数mlの誤嚥物が引けた．嚥下造影検査（VF）を行ったところ，食道入口部の輪状咽頭筋全体の弛緩が悪かった．しかし気管への垂れ込みもあるが，食道へも入ることを確認した．

そのため空気のバルーン飲み訓練とゼリーの摂取訓練を続けることとした．さらに経鼻胃管をファインコンフィーディングチューブSをE7からE5に変更（チューブの外形を4.5mmから3.5mmに）したところ，口腔内の唾液貯留が明らかに減少し，ゼリーの摂取時間も速く，50mlを約15分で可能となった．ミキサー食も試したが，誤嚥が多く，E5チューブを挿入したままでゼリー摂取を続けることとした．入院約2ヶ月後から，昼のみ胃管を抜去してゼリー食を続けた．この頃，まだめまい，眼振は続き，右半身の運動失調も強かったが，筋力の回復，易疲労性の減少もあり，歩行器歩行が少し可能となった．ゼリーは20分かけて，70mlまで可能となったが，37.5℃に発熱し，右下肺野に誤嚥性肺炎を起こした．抗生剤などで加療を行うと共に，ゼリー摂取は一時中止した．さらに抗生剤で薬疹を生じ，抗生剤を変更した．その後，肺炎は治癒したが，気管カニューレのサイドチューブから誤嚥物が引け，また誤嚥性肺炎を再発するリスクが高く，経口摂取を断念した．FIMの認知項目が32に改善したこともあり，間歇的口腔食道経管栄養法（Intermittent Oro Esophageal Tube Feeding, OE法）を試すこととした．本法は食事の時だけ胃管を食道まで飲み込み，先端を食道に留置して，食事を注入し，それが終われば抜去する食事法である．朝夕は経管栄養のままで，昼のみ歯列から31cmまで（胸椎のTh7の高さに相当）飲み込み，経管栄養を注入した．咽頭反射がほとんどないこともあり，1週間で自分で飲み込み，深さの調整もできるようになった．やがて，食事

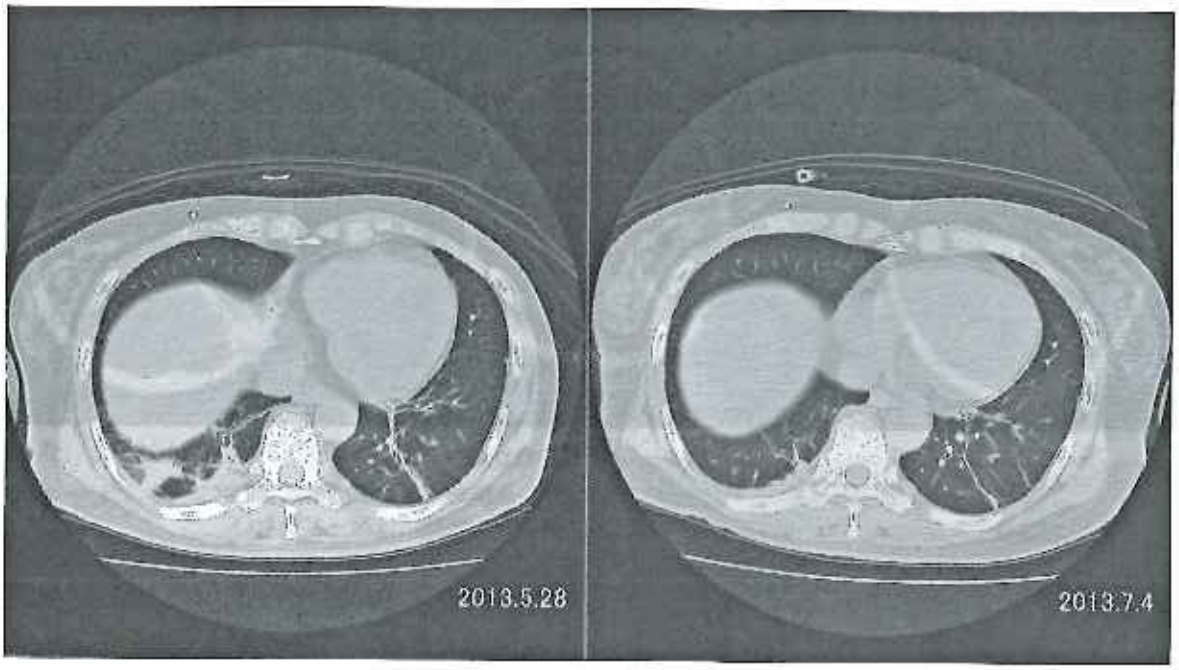

図4　嚥性肺炎の経過（2回目）
今回も右の下肺野に誤嚥性肺炎も起こしている．緑膿菌が検出されたが，抗生剤による加療により，約1ヶ月後には治癒している．なお，左肺の線状陰影は転院前に起こした肺炎による無気肺の陰影と思われる

量を調整も含め，自分で注入できるようになり，3食ともOE法で摂取可能となった．食事の味を味わうことはできないが，4月下旬には必要量の食事摂取が自立し，自宅復帰への一つの障害は解決できた．

次の課題は気管カニューレ抜去と発声であった．胃管が間歇的になったこともあり痰や唾液量も減少し，カニューレ交換は2週間毎となった．カフ付きスピーチカニューレ(高研#3264)に交換したところ，軽い嗄声はあったが，十分な声量の発語があった．しかしカニューレの内径が狭くなることもあってか，呼吸困難を訴え，サイズなどの調整を行ったが，カフ付きスピーチカニューレに対する不安を強く訴え，元の気管カニューレに戻した．唾液など分泌物の気管への流入量を測定した．カニューレのカフ上部に貯留する分泌物量を側管を通して引ける吸引量として3回測定したところ，1日で順次58ml，46ml，65ml（平均56ml）で1回目と3回目とで42日経過していたが，減少は見られなかった．プチルスコポラミン軟膏を耳朶下部から下顎に塗布したところ，順次33ml，51ml，43ml（平均42ml）で約75%に減少した．唾液量は1日で約1,000 1,500ml[1]であるので，この量は約3－4%にすぎないが，気道圧の上昇や，カニューレ交換時などに肺に流入すると誤嚥性肺炎のリスクが高いと思われた．プチルスコポラミン軟膏を続けたが，5月下旬に発熱し，二度目の肺炎を起こした(図4)．痰が緑色調であり，起炎菌として複数回緑膿菌が検出され，抗生剤加療を続けたが治療に約1ヶ月余りを要した．

その後も分泌物の気道への流入量は30mlほどあり，手術を考えたが，定期的耳鼻科受診ではまだ手術は困難との返事であった．しかし7月中旬には，左方視で注視方向性眼振はあるが，歩行は四点杖にて15mから20m監視歩行ができるようになり，その後は肺炎もなく，気管カニューレ留置での自宅復帰を望める状況となった．訪問による自宅の改修指導を行い，食事はOE法による自己摂取，気管カ

ニューレは往診による医師の交換と訪問看護による管理，送迎付きデイケアサービスの2回／週の利用，定期的耳鼻科通院の準備を行い，8月25日に自宅退院となった．退院時の最終FIMは運動76，認知34で，介護保険は要介護4を取得した．自宅での生活では，肺炎を起こすことなく，デイケアなど順調に利用することができた．2014年2月初めになり，S病院耳鼻科で喉頭挙上術，両側輪状咽頭筋切断，右披裂軟骨内転術を行い，5月には後屈60度，下顎突出位で全粥が可能になり，スピーチカニューレとなった．歩行は四点杖で監視歩行であった．発症から約1年半の経過で，本来の経口摂取を獲得し，発声も可能となった．なお食事は，椅子に座って，少し後屈の姿勢で，主食は少し柔らかめのごはん，野菜はそのままで，ジュースなどの飲み物はとろみを付けて摂取している（水はまだ耳鼻科で許可されていない）．退院後は一度も肺炎は起こしていない．

考　　察

本例は音声による会話，食事の経口摂取，歩行の獲得までに発症から約1年半を要し，基本的ADLの獲得に難渋した症例であった．歩行もまだ杖による監視歩行レベルである．Wallenberg症候群の嚥下障害は，開口障害などの口腔期障害を認めることもあるが，主に咽頭期障害をきたす．咽頭障害として，重症例では健側の輪状咽頭筋の障害もときに見られ，この異常はpassage pattern abnormality (PPA) として知られている[2]．本例は咽頭反射が右で消失，左で低下し，カーテン徴候も陰性であり，VFの所見も合わせて，PPA陽性で重症例と考えられる．バルーンブジー法やバルーン飲み訓練で食事が獲得できないときは，筋へのボツリヌス毒素注入[3]や手術療法[4]が選択される．われわれはボツリヌス毒素注入は経験がなく，約3ヶ月毎に繰り返す必要があり，断念した．そのため手術療法を検討したが，本人，家族は不安も強く，まだリハビリテーションに期待する気持ちが強く，一方，通院していた耳鼻科からも手術ではなく，経過観察を推奨された．限られた入院リハビリテーションの期間のなかで自宅復帰を考えると，OE法による食事摂取は必然の方法であったと考えられる．自宅退院後，徐々に患者みずから手術を希望するようになり，手術を受け，現在のADLを獲得した．今後，経過観察し気管切開部を閉鎖する予定となっている．以上，本例がリハビリテーションに難渋した最大の原因はこの重篤な嚥下障害にあると考えるが，他にもいくつかの原因が考えられる．

Wallenberg症候群の原因として，多くは脳梗塞であるが，本例はくも膜下出血に原因があり，水頭症も併発し，転院当初は認知機能や意欲が低下していたことも関係している．さらに体性感覚誘発電位の異常も一因と考えられる．体性感覚誘発電位は深部覚の異常と相関する．右の正中神経ではN_{13}潜時は正常であったが，N_{20}は出現しなかった．N_{13}は楔状束核で出現する電位であるので，毛帯交差を経て内側毛帯から第一次感覚野へ至るルートのどこかの障害を意味するものと思われる．病巣から考えて，右の椎骨動脈から分岐する動脈の貫流異常で，右の楔状束核からの神経線維が毛帯交差に至る直前で障害された可能性が高いと考えられる．まだ監視歩行レベルであるのは，本来の右の下小脳脚の障害による小脳性運動失調に加えて，右の深部覚障害による感覚性（脊髄性）失調を伴っている可能性が考えられる．

文　　献

1）大地陸男．生理学テキスト（第6版．東京：文光堂；2010．p.385．
2）巨島文子．延髄外側梗塞（wallenberg症

候群）による嚥下障害．臨床神経　2011；51：1069-1071．
3）Porter RF, Gyawadi CP. Botulinum toxin injection in dysphagiasyndromes with preserved esophageal peristalsis and incomplete lower esophageal sphincter relaxation. Neurogastroenterol Motil 2011；23：139-144.
4）安達明幸，梅崎俊郎，杉本俊彦ら．輪状咽頭筋切断術が奏功した Wallenberg 症候群の1例．耳鼻　1996；42：995-999．

50